PULSE COMPRESSION APPLIED TO THE DETECTION OF F.S.K. AND P.S.K. SIGNALS

by

WASIM WADIE SALIM JIBRAIL

A thesis submitted to the
University of Aston in Birmingham
for the degree of
DOCTOR OF PHILOSOPHY

September 1980

PULSE COMPRESSION APPLIED TO THE DETECTION OF F.S.K. AND P.S.K. SIGNALS

by

WASIM WADIE SALIM JIBRAIL, BSc, MSc

submitted for the
Degree of Doctor of Philosophy
at
The University of Aston in Birmingham
1980

Summary

The matched filter detector is well known as the optimum detector for use in communication, as well as in radar systems for signals corrupted by Additive White Gaussian Noise (A.W.G.N.).

Non-coherent F.S.K. and differentially coherent P.S.K. (D.P.S.K.) detection schemes, which employ a new approach in realizing the matched filter processor, are investigated. The new approach utilizes pulse compression techniques, well known in radar systems, to facilitate the implementation of the matched filter in the form of the Pulse Compressor Matched Filter (P.C.M.F.). Both detection schemes feature a mixer - P.C.M.F. Compound as their predetector processor. The Compound is utilized to convert F.S.K. modulation into pulse position modulation, and P.S.K. modulation into pulse polarity modulation. The mechanisms of both detection schemes are studied through examining the properties of the Autocorrelation function (A.C.F.) at the output of the P.C.M.F.. The effects produced by time delay, and carrier interference on the output A.C.F. are determined.

Work related to the F.S.K. detection scheme is mostly confined to verifying its validity, whereas the D.P.S.K. detection scheme has not been reported before. Consequently, an experimental system was constructed, which utilized combined hardware and software, and operated under the supervision of a microprocessor system. The experimental system was used to develop error-rate models for both detection schemes under investigation.

Performances of both F.S.K. and D.P.S.K. detection schemes were established in the presence of A.W.G.N., practical imperfections, time delay, and carrier interference. The results highlight the candidacy of both detection schemes for use in the field of digital data communication and, in particular, the D.P.S.K. detection scheme, which performed very close to optimum in a background of A.W.G.N..

Keywords

FREQUENCY SHIFT KEYING (F.S.K.), PHASE SHIFT KEYING (P.S.K.), DIGITAL COMMUNICATIONS, CHIRP, PULSE COMPRESSION

ACKNOWLEDGEMENTS

The author wishes to thank his supervisor, Dr. R.L. Brewster, for his constant guideness throughout this work. Thanks are also due to Professor J.E. Flood in his capacity as Head of Department and Director of research for the Telecommunications Group.

Special thanks to colleagues Dr. M.S. El-Alem, Mr. P. Cadman, and C.Y. Linn for the fruitful discussion that took place in different stages of this work. Thanks are also due to technicians of the Department of Electrical and Electronic Engineering, who, in one way or another, helped to bring this work to its final conclusion.

Special thanks to Miss N.P. Freeman for her patience in typing the manuscript.

Finally, the author wishes to thank the University of Technology in Baghdad, Iraq, for providing the necessary financial support to carry out this work.

LIST OF CONTENTS

CHAPTER ONE

INTRODUCTION

1. INTRODUCTION

Digital communication is the technology dealing with the generation, propagation, and processing of discrete information in the form of a data signal. The functional elements of the communication system are the transmitter, the channel, and the receiver. The transmitter couples the digital data in the form of a data signal to the channel. The channel is the medium, wherein the signal is contaminated by noise, and distorted. The receiver performs a detection process on the signal to extract the data transmitted from a background of noise.

The key operations performed on the digital data by the transmitter, and receiver are modulation and demodulation (i.e. detection) respectively. The modulator impresses the digital data either upon a carrier phase, frequency, or amplitude to generate a data signal in the form of phase shift keying (P.S.K.), frequency shift keying (F.S.K.) or Amplitude shift keying (A.S.K.) respectively. The receiver performs a detection process on the received data signals, first by extracting the signals from a noise background, and secondly by resolving different signals to recover the digital data transmitted.

The performance measure of the receiver is the probability of making the wrong decision on the received data signal (i.e. the probability of making an error P_e). Hence the goodness of the receiver is identified by its (P_e), which also provides a good measure of the capability of the receiver in extracting signals masked by noise.

Decreasing (P_e) from the receiver point of view is one way of improving the performance of the digital communication system. Moreover, the importance of (P_e) as a performance measure stems from its direct relationship with the signal-to-noise ratio (SNR) parameter. The processor which maximises the (SNR), and hence minimizes the probability of error (P_e), (i.e. optimizes the detection process) when detecting the output data signal of an additive white Gaussian noise (A.W.G.N.) channel is known as the "Matched filter" processor [1].

F.S.K. and P.S.K. are the most attractive, practical and widely used data signals for digital data transmission over channels whose performance is limited by A.W.G.N. These factors, together with the advent of large scale integration (LSI), automation, and the computer revolution, have stimulated the search for more efficient detection schemes for both types of data signal with the object of achieving the performance of the ideal matched filter detector. The optimum coherent detector (coherent detection requires a reference signal perfectly matched in both frequency and phase to the received carrier) for a pair of F.S.K. signals consists of two matched filters followed by integrate-and-dump filters [2] - [4]. A non-coherent detector (non-coherent detection does not require a phase reference) for the same pair of signals consists of two matched filters followed by envelope detectors and a comparator [2] - [5]. P.S.K. signals are preferred

for digital data transmission rather than F.S.K. signals, when bandwidth utilization is required. Moreover, coherent P.S.K. out performs coherent F.S.K. by 3 dB less SNR at the same probability of error (P_e). However, a reference signal of the same phase and frequency as the carrier may be difficult to establish in practice. In this event non-coherent detection for F.S.K. signals is preferred, or another form of P.S.K. signal may be employed, whereby the binary bit is conveyed in the relative phase of the carrier by using differential encoding at the transmitter. At the receiver a differential detector is employed to store one data signal, and compare it with the one received before. The detection of differential P.S.K. (D.P.S.K) signals in A.W.G.N. makes use of the matched filtering process by employing an integrate-and-dump filter in addition to its differential detector [2] - [5]. Therefore, non-coherent F.S.K. and D.P.S.K. detection schemes make use of the matched-filtering process to optimize their detection capabilities.

Due to practical difficulties in implementing matched filters [2], [5], other detection techniques are employed to detect F.S.K. signals. Frequency discriminators, phase-locked loops, and integrate-and-dump filters [6] - [10] are used as F.S.K. detectors to approach in practice the performance of the ideal matched filter detector. However, a detection scheme for PAM-FM signals corrupted by A.W.G.N. was suggested by (Darlington, S.), [11] which employed pulse compression techniques used in radar systems [13] - [15].

This has led to a new approach for detecting F.S.K. signals which is described later [12]. The new approach hinges on two operations at the receiver, to make the matched filtering process more readily realizable using only one matched filter for a pair of F.S.K. signals. The first operation converts the received F.S.K. signal into a new signal, while the second operation transmits the new signal through a pulse compression filter. The new signal is chosen to be a linear - FM (or chirp) signal.

Comprehensive investigations into the feasibility, utility, and practical performance in A.W.G.N. interference and other interfering signals of the F.S.K. detection scheme by pulse compression were required, since the reported work about this scheme has so far been mostly confined to its validity. Moreover, it was found that the same approach could be utilized to optimally process a pair of D.P.S.K. signals corrupted by A.W.G.N. This has not been reported before. To carry out experimental investigations (e.g. performances in different types of channels, practical imperfections, and unavoidable systems distortions), into both detection schemes, a flexible experimental system for each seemed to be of great advantage.

The next section describes the pulse compression concept of radar systems with emphasis on the practicability of the pulse compressor matched filter, and its utilization of several new technologies. Chapter 2 examines the mechanism

of both detection schemes, highlighting their detection capabilities in the presence of A.W.G.N, some possible practical imperfections, time delay, and carrier interference. To avoid inconvenient interruptions, derivations of the auto-correlation functions at the output of the pulse compressor, for a pair of F.S.K. and P.S.K. signals received, in the presence of carrier interference and, in the presence of time delay, are carried out in full in Appendix A, Appendix B, and Appendix C respectively. This chapter also underlies some of the reasoning in the present work. In Chapter 3, two experimental error-rate models are developed untilizing hardware, and software techniques for both detection schemes under investigation. In addition, a random phase carrier interference model is also implemented. Flowcharts are provided for the software used. In Chapter 4, both models are operated, under the supervision of the TMS-9900 microprocessor system, to perform error-rate measurements. Error-rate results are discussed, and compared whenever possible with published results for conventional detection systems. Chapter 5 includes the conclusions, and some suggestions for further work.

1.1 PULSE COMPRESSION (1), (13)-(16)

Pulse compression techniques of radar systemswere originally used to enchance the resolution of the radar receiver when processing returns from adjacent targets, and also to overcome the problem of limited peak power

of the radar transmitter. This was achieved by utilizing a family of compressible signals which enjoy a large time-bandwidth product. A member of this family is the linear-FM (or chirp) signal. This is a finite duration signal, which may sweep linearily upwards or downwards in frequency over a limited bandwidth. A chirp signal is said to have a positive frequency/time relationship (i.e. slope), or a negative slope respectively, when sweeping upwards, or downwards in frequency. Pulse compression is accomplished by utilizing a pulse compressor filter to speed up the higher frequencies relative to the lower frequencies in a chirp signal while preserving its energy. When a chirp signal is processed by its matched filter, the output resembles that of shorter duration pulse of amplitude value (determined by the time-bandwidth product) usually well above the noise threshold at a predetermined instant of time. In this way the matched filter forms the basis of the pulse compressor matched filter (P.C.M.F.)

A matched filter is a linear time-invariant filter defined either by its impulse response, or frequency response. The impulse response is the time-reversed replica (suitably delayed) of the signal to which it is matched. Moreover, since the impulse response and the frequency response of a filter are a Fourier transform pair, the matched filter frequency response forms the complex conjugate of the signal frequency spectrum.

The output of the P.C.M.F. is found by correlating

(i.e. Multiplying) the spectrum of the signal with the frequency response of the filter. However, since correlation in the frequency domain corresponds to convolution in the time domain, and vice versa, the output of the P.C.M.F. is found by convolving the input signal with the impulse response of the filter. Hence for a given signal M(t), and impulse response h(t), the output of the P.C.M.F. may be expressed as

$$g(t) = k \int_{-\infty}^{\infty} M(t)\ h(t-\tau)\ d\tau \qquad (1)$$

where k is the amplitude scaling factor

τ is an arbitrary time delay

1.1.1 Practicability of the P.C.M.F.

The P.C.M.F. is a storage and summing device which accumulates the received signal energy in a given interval, integrates it, and outputs it in a short burst. The basic configuration of the P.C.M.F. takes the form of a transversal filter [17]. This filter comprises separated delay elements, tapped at their outputs with weighting resistors. The outputs of these resistors are summed together to resemble the output of the filter. The conductance values of the weighting resistors are identified as the impulse response of the transversal filter. The filter is made to perform the matched filtering process on a given signal by constructing its time reversed replica on the weighting resistors. The transversal filter is used for pulse compression in radar

systems [14], [15], [18], whereas in communication it was first suggested by (Winkler, M.R.) [19] and later used for compressing chirp data signals [20], [21], [22].

The main technologies at present available for implementing the P.C.M.F. are charge coupled devices (CCD), digital electronics (i.e. microprocessors), and surface acoustic wave (SAW) devices [23], [24], [25]. However, each has its own area of application, which is mainly governed by the received signal bandwidth due for processing. Digital, and CCD are suitable for bandwidths of less than 100 KHz, and in the range of 1 KHz to 20 MHz, respectively; while for bandwidths in excess of 50 MHz, SAW technology is the proper choice. However, digital and CCD technologies, being of the silicon technology family, are readily interfaced with the necessary digital processing circuits in most digital communication systems. Generally CCD and digital P.C.M.F.'s are suitable for baseband operations, whereas SAW P.C.M.F.'s are suitable for passband operations.

Investigations into programmable, and microprocessor controlled P.C.M.F.'s using CCD have been carried out [26] - [28]. These have the advantage of being flexible regarding their impulse response implementation, which may be stored in a read-only memory (ROM), or calculated by a microprocessor, and changed as required by reprogramming the ROM, or the microprocessor. However, the experimental system in the present work required an even more flexible, and experimental P.C.M.F. This was achieved by implementing the P.C.M.F.

in software to facilitate the impulse response implementation, and consequently eased the deliberate insertion for investigation purposes of new parameters which cause deviations of the P.C.M.F. from its ideal performance.

CHAPTER TWO

F.S.K. AND P.S.K. DETECTION BY CHIRP MODULATION AND COMPRESSION

2. F.S.K. AND P.S.K. DETECTION BY CHIPP MODULATION AND COMPRESSION

Both detection schemes under consideration incorporate a mixer-P.C.M.F. compound (shown in Fig. 1) to act as the optimum predetector processor by which two linear operations (where supposition theorem is applicable) are performed on the received F.S.K., or P.S.K. data signal. The mixer essentially Multiplies (Modulates) the received data signal by a locally generated chirp signal. Multiplication of two unrelated signals produces a signal whose spectrum is the convolution of the spectra of both signals. Thus, if the received signal is narrow-band compared with the locally generated chirp signal, the product signal will have nearly the same spectrum as that of the chirp signal. The P.C.M.F. is then required to be matched to the new chirp signal generated rather than to the original received data signal.

It will be shown that the mixer-P.C.M.F. compound exhibits the capability of maximizing the SNR. However, its processing capability is dictated by non-ideal behaviour, which might occur in practice. These factors, together with its near-optimum capability for processing F.S.K. signals, and optimum capability for processing P.S.K. signals, will be demonstrated by examining the output of the PC.M.F. in each of these two cases. For mathematical convenience signals are expressed in complex form, whereas results are given in real form

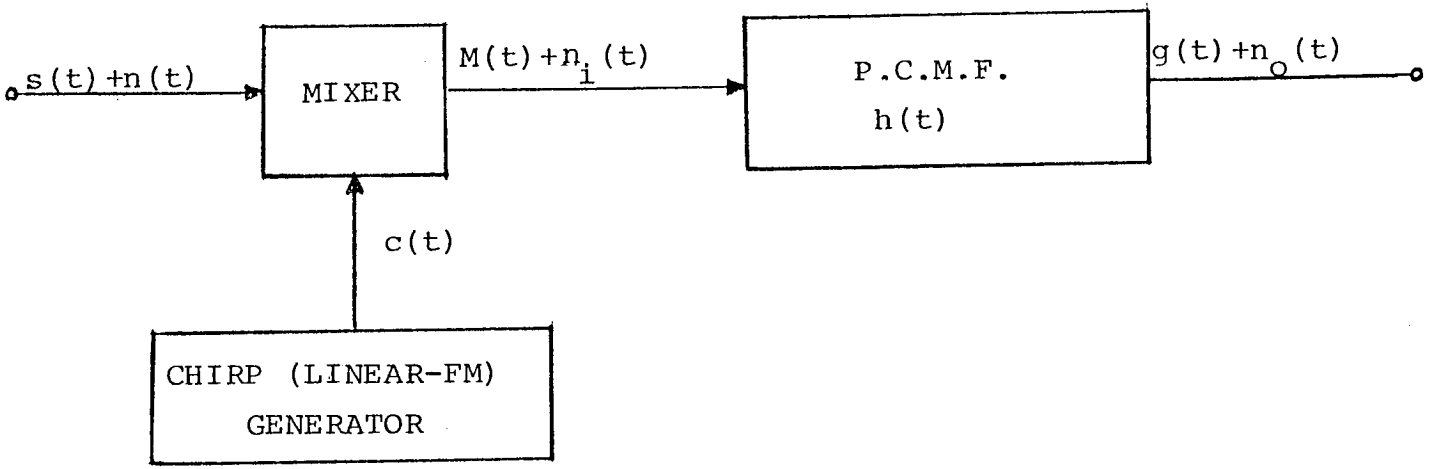

FIG. 1

THE MIXER-P.C.M.F. COMPOUND

throughout this chapter. A locally generated chirp signal of angular centre frequency (ω_o), duration (T), bandwidth (B), slope (μ), and instantaneous angular frequency ($\omega_{inst.}$) may be expressed as

$$C(t) = \exp.j\ (\omega_o t + \frac{1}{2}\mu t^2),\ |t| \leq \frac{T}{2} \qquad (2.1)$$

where

$$\mu = 2\pi\frac{B}{T}$$

$$\omega_{inst.} = \omega_o + \mu t$$

The output of the mixer may be expressed as follows

$$M(t) = [S(t)][C(t)]^* \qquad (2.2)$$

where $[C(t)]^*$ is the complex conjugate of C(t)

S(t) is the received data signal.

Since the mixer-P.C.M.F. compound is a linear system, it is possible to carry out the analyses of signal and noise separately.

2.1 THE OUTPUT AUTOCORRELATION FUNCTION OF THE P.C.M.F.

The mechanism of the mixer-P.C.M.F. compound and its response to a received data signal is best studied by examining the Autocorrelation Function (A.C.F.), and its properties at the output of the P.C.M.F. Consider the chirp signal of (2.1) to be present at the input of the P.C.M.F.. Matching is achieved by storing a chirp signal of opposite slope, and at the same centre frequency to that of the input chirp signal in the P.C.M.F. to act as its impulse response.

Thus, the impulse response of the P.C.M.F. may be expressed as

$$h(t) = \exp.j(\omega_o t - \frac{1}{2}\mu t^2), \quad |t| \leq \frac{T}{2} \qquad (2.3)$$

The A.C.F. of the P.C.M.F. using the convolution integral of (1) yields the following[16],[29].

$$g(t) = \sqrt{BT}(1-\frac{|t|}{T})\,\mathrm{Sinc}\pi\left[Bt(1-\frac{|t|}{T})\right]\cos\omega_o t, \quad |t| \leq T \qquad (2.4)$$

$\sqrt{BT}$ is the processing gain due to pulse compression, $(1-\frac{|t|}{T})$ is the envelope of the A.C.F., $\mathrm{Sinc}\pi\left[Bt(1-\frac{|t|}{T})\right]$ is the matched filter A.C.F., and $\cos\omega_o t$ is the high frequency component at the centre frequency of the P.C.M.F.. $|g(t)|$ is illustrated in Fig.2 with $\sqrt{BT}$ normalized to unity, representing the ideal A.C.F. of a P.C.M.F., which is perfectly matched to a rectangular-envelope chirp signal. However, the behaviour of the A.C.F. is essentially attributable to the following parameters of the input chirp signal to the P.C.M.F.

(i) Centre Frequency

The matched filter A.C.F. has its peak value at zero time shift when the P.C.M.F. and its input chirp signal are centred at the same frequency. A shift in the centre frequency of the input chirp (known as the doppler shift effect in radar systems)[16]

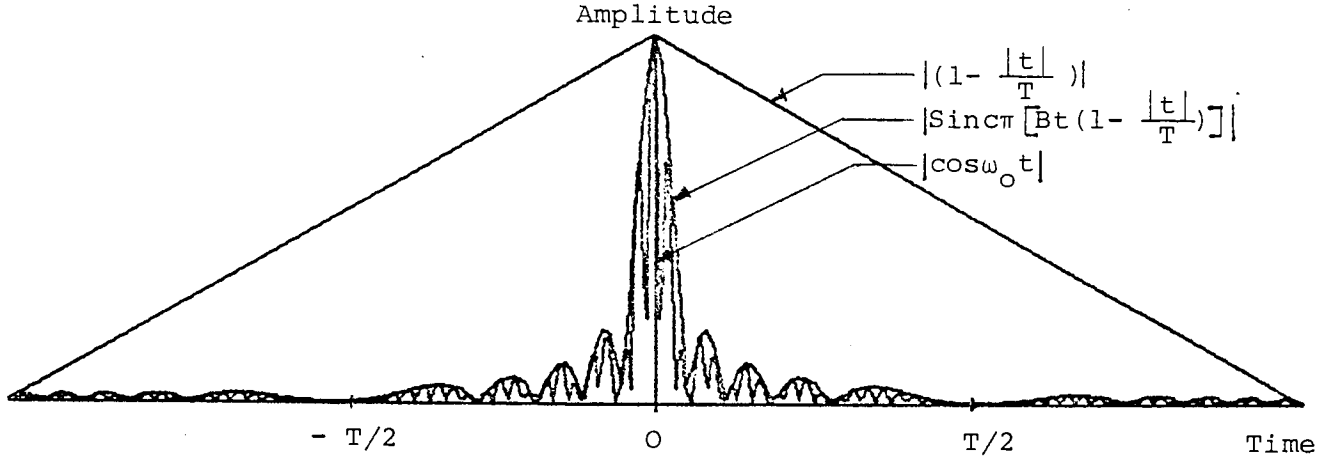

FIG. 2

THE OUTPUT AUTOCORRELATION FUNCTION OF THE P.C.M.F.

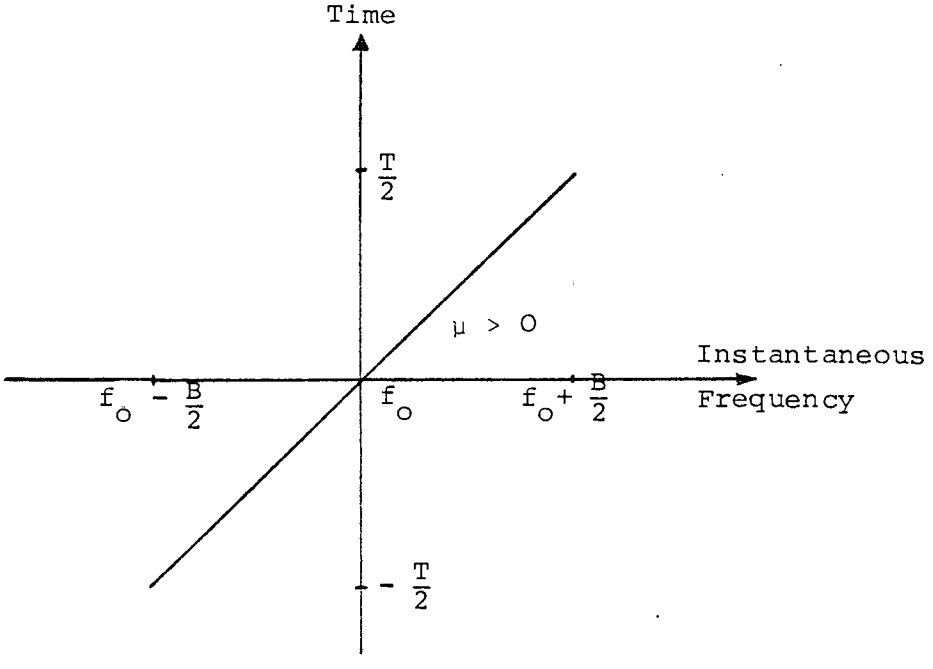

FIG. 3

THE LINEAR-FM LAW

would correspond to a time shift of the A.C.F. peak at the output of the P.C.M.F.. This property of the A.C.F. will be utilized in the following section to detect F.S.K. data signals.

(ii) Initial Phase

The initial phase of the input chirp signal may be used to control the polarity of the A.C.F.. This property has been utilized to detect P.S.K. and D.P.S.K. chirp data signals employed for digital data transmission[30],[31], and it will be utilized later in this work to detect D.P.S.K. data signals.

(iii) The Envelope

Rectangular, and amplitude modulated envelopes of the input chirp signal to the P.C.M.F. introduce, respectively, high sidelobes, or two similar sidelobes (known as paired echoes), usually flanking around the main lobe of the matched filter A.C.F.[14],[16]. Both kinds of envelopes are sources of distortion by which the A.C.F. is deviated from the state of perfect match, thus deteriorating the P.C.M.F. performance, and hence the system that utilizes it. To reduce the effects of such distortions either time, or frequency weighting of the P.C.M.F. impulse response may be used.

(iv) The Slope

This parameter plays an important role in affecting

the behaviour of the A.C.F.. The perfect match state, together with pulse compression, are achieved when the slope of the input chirp signal is equal in magnitude, but opposite in direction, to that of the impulse response of the P.C.M.F. Pulse dispersion, the dual of pulse compression, may be achieved by reversing the slope of the input chirp signal. Slope reversal chirps have been employed for digital data transmission utilizing this property of the A.C.F.[21]. However, a deviation in the slope magnitude of the input chirp signal deviates the A.C.F. from its ideal properties causing the so called "slope mismatch".

(v) Instantaneous Frequency

The frequency/time relationship of the input chirp signal to the P.C.M.F. is linear (follows the linear-FM law, Fig. 3) for the perfect match state. However, non-linearities in the phase are likely to develop due to generation and/or processing of the chirp signal, causing a distorted A.C.F. at the output of the P.C.M.F.

(vi) Time-Bandwidth Product

The time-bandwidth product of the input chirp signal specifies the processing gain due to pulse compression, as well as the degree of complexity of the P.C.M.F.. The higher the time-bandwidth product, the narrower

the A.C.F., and the larger the number of delay elements required in the P.C.M.F. to accommodate the required impulse response chirp signal[14].

2.1.1 Implementation of the F.S.K. Detection Scheme

Consider an F.S.K. signal present at the input of the mixer-P.C.M.F. compound of (Fig. 1) which may be expressed in terms of its angular centre fequency (ω_a), bandwidth (F), and constant amplitude (A) as follows

$$S(t) = A \exp.j(\omega_a t + \pi RFt), \quad |t| \leq \frac{T}{2} \qquad (2.5)$$

where R = +1 for a space, and -1 for a mark

$\omega_a = 2\pi fa.$

The modulation index (h) may be defined as

$$h = (fs - fm)T = FT \qquad (2.6)$$

where

fs is the space frequency

fm is the mark frequency

T is the period of one bit.

Each F.S.K. signal is converted into a chirp signal at the mixer output by beating it with the locally generated chirp of (2.1) which is generated periodically, and in sychronism, with the received F.S.K. signal. Thus, by making use of (2.2), the output of the mixer is given by

$$M(t) = A \exp.j(\omega_c t + \pi RFt - \frac{1}{2}\mu t^2), \quad |t| \leq \frac{T}{2} \qquad (2.7)$$

where $\omega_c = \omega_a - \omega_o$

which shows that the mixer output comprises two negative slope chirp signals of bandwidth (B), duration (T) and centre frequencies $(fc + \frac{F}{2})$, and $(fc - \frac{F}{2})$ respectively depending whether the F.S.K. signal is conveying a mark, or a space. Hence, through the process of conversion, the F.S.K. signal shifts the centre frequency of the local chirp, generating two doppler shifted chirps. This implies that the required P.C.M.F. to detect and compress both signals must be of the following impulse response

$$h(t) = \exp.j(\omega_c t + \frac{1}{2}\mu t^2), \qquad |t| \leq \frac{T}{2} \qquad (2.8)$$

Substituting from (2.7), and (2.8) in (1), the output A.C.F. of the P.C.M.F. (derived in Appendix A) is given by

$$g(t) = A\sqrt{BT}\ (1-\frac{|t|}{T}),\mathrm{Sinc}\pi(Bt+\frac{Rh}{2})\ (1-\frac{|t|}{T})\ \mathrm{Cos}(\omega_c t+\frac{\pi Rh}{2T}t), |t| \leq T \qquad (2.9)$$

which indicates that the envelope of the matched filter A.C.F. peaks at two different times depending on whether a mark, or a space is received. These times are found (by equating the argument of Sinc (.) to zero) to be

$$ts = -\frac{h}{2B}\ , \text{ for a space received}$$
$$tm = \frac{h}{2B}\ , \text{ for a mark received} \qquad (2.10)$$

which implies, together with (2.9), that the envelope of the matched filter comprises the vital information conveyed by the F.S.K. data signal in terms of its position on the time-axis. Thus, chirp modulation followed by pulse compression converts F.S.K. modulation into pulse position modulation. The position of the envelope depends mainly on the F.S.K. modulation index and the bandwidth of the system, while its magnitude is dictated by the envelope of the A.C.F.. Fig.4 illustrates (2.9) without the high frequency component, for two integer modulation indices. This detection scheme may be utilized to detect higher modulation index F.S.K. (i.e. wideband F.S.K.), as well as low modulation index F.S.K. However, in order to create the doppler shift effect through the waveform conversion process, the F.S.K. spectrum must contain the two spectral lines representing the two tones transmitted (i.e. mark and space frequencies). For a non-integer modulation index, the F.S.K. spectrum does not contain spectral lines at the mark and space frequencies[32),(33)].

Fig. 5 illustrates the overall schematic of the receiver which employs in addition to the mixer-P.C.M.F. compound, an envelope detector, a threshold detector and decision circuits by which the recovered mark and space signals are sampled at the two different times given by (2.10). A scheme for recovering the received binary bit utilizing digital signal processing at the output of the threshold detector is used as an alternative to the analogue processing of the signal at the output of the P.C.M.F.[(12)]. The receiver's instrumentation

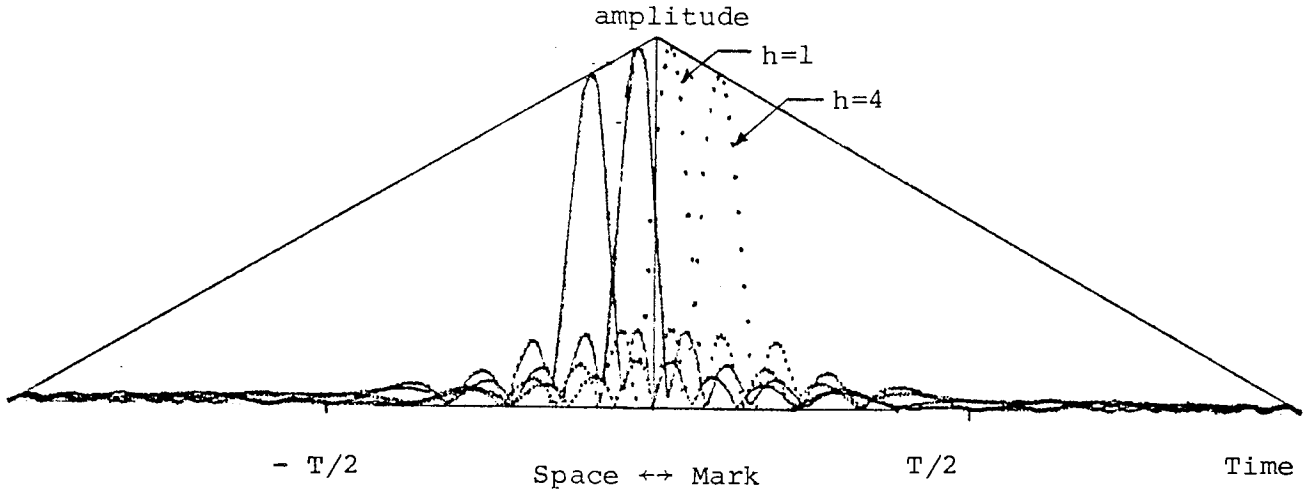

FIG. 4

ENVELOPES OF MARK AND SPACE SIGNALS AT THE OUTPUT OF P.C.M.F. FOR DIFFERENT VALUES OF MODULATION INDEX

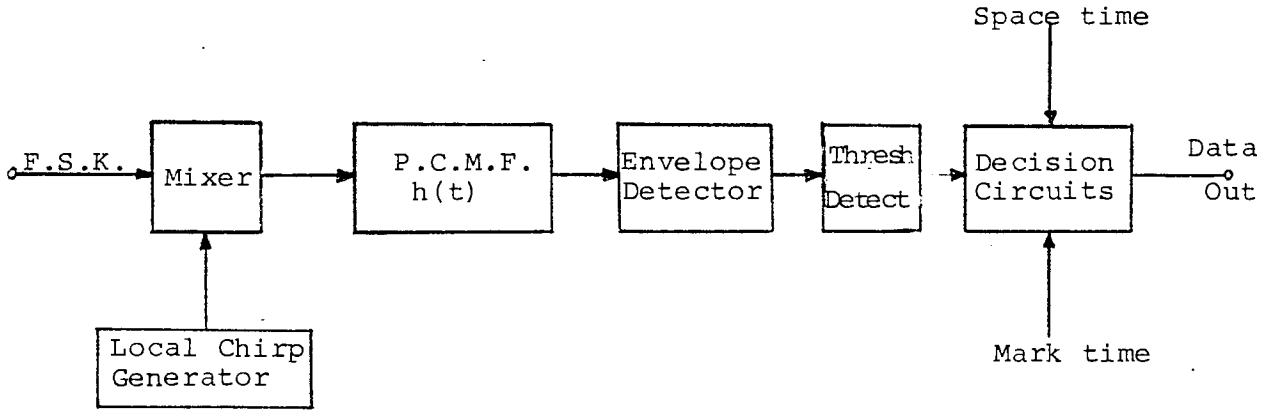

FIG. 5

OVERALL SCHEMATIC OF THE F.S.K. RECEIVER

utilizes both hardware, and software techniques, as will be described in Chapter 4.

2.1.2 Implementation of the D.P.S.K. Detection Scheme

A P.S.K. or D.P.S.K. signal whereby respectively digital data, or differentially coded digital data are conveyed by reversing the phase (ϕ_i) of a constant angular frequency (ω_b) carrier, and constant amplitude (G) may be expressed as

$$S_i(t) = G \exp.j(\omega_b t + \phi_i), \quad |t| \leq \frac{T}{2} \qquad (2.11)$$

where $i = \begin{cases} 1 \text{ for } \phi_1 = \pi \\ 2 \text{ for } \phi_2 = 0 \end{cases}$

Consider $S_i(t)$ to be present at the input of the mixer-P.C.M.F. compound of (Fig. 1). The output of the mixer, using (2.1) and (2.2) is given by

$$M(t) = G \exp.j(\omega_p t + \phi_i - \frac{1}{2}\mu t^2), \quad |t| \leq \frac{T}{2} \qquad (2.12)$$

where $\omega_p = \omega_b - \omega_o$

This relation indicates that the mixing process transfers the phase (ϕ_i) from the input data signal to the chirp signal at the mixer output. The format of the generated chirp signal is essentially the same as that of P.S.K. and D.P.S.K. chirp data signals employed for digital data transmission[30],[31]. Thus, the required

P.C.M.F. to detect and compress the new chirp signal is of the following impulse response

$$h(t) = \exp.j(\omega_p t + \frac{1}{2}\mu t^2) \quad , \quad |t| \leq \frac{T}{2} \qquad (2.13)$$

substituting from (2.12) and (2.13) in (1), the output A.C.F. of the P.C.M.F. (derived in Appendix A) is given by

$$g(t) = G\sqrt{BT}\,(1-\frac{|t|}{T})\,\mathrm{Sinc}\pi Bt(1-\frac{|t|}{T})\,\mathrm{Cos}(\omega_p t+\phi_i)\,, \quad |t| \leq T \qquad (2.14)$$

which indicates that the polarity of the output A.C.F. of the P.C.M.F. depends on the value of the phase angle (ϕ_i) (i.e. $\phi_1 = \pi$ gives a negative output, while $\phi_2 = 0$ gives a positive output), while the envelope of the matched filter is positioned at zero time shift. This implies that the perfect match state of the P.C.M.F. with its input chirp signal (i.e. optimum processing) may be achieved if the following conditions are maintained.

(i) The phase angle (ϕ_i) is faithfully transferred by virtue of the mixing process from the input P.S.K. or D.P.S.K. signal to the chirp signal at the output of the mixer.

(ii) The centre frequencies of the P.C.M.F. and its input chirp signal are the same, (i.e. the absence of doppler shift).

Fig. 6 shows the envelope of the output A.C.F. for

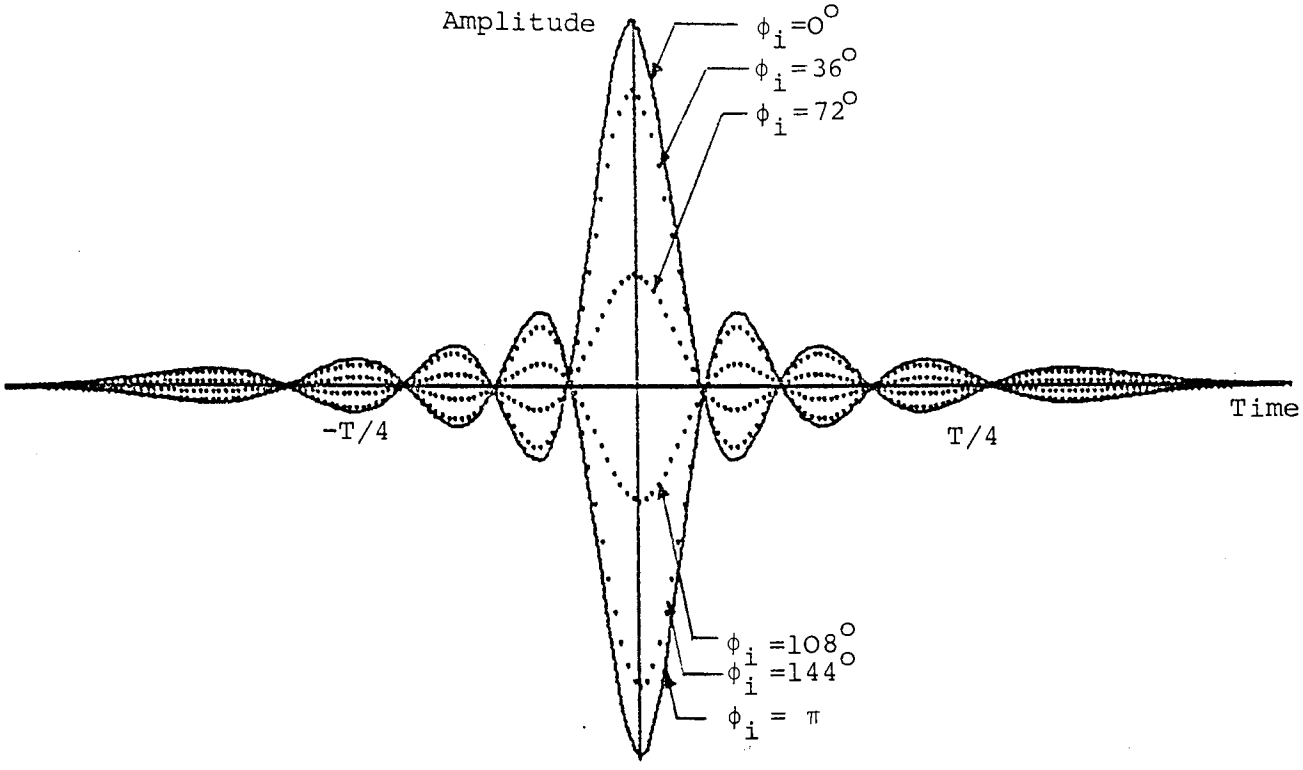

FIG. 6

ENVELOPES OF MARK AND SPACE SIGNALS AT THE OUTPUT OF P.C.M.F.

FOR DIFFERENT VALUES OF PHASE ANGLE (ϕ_i)

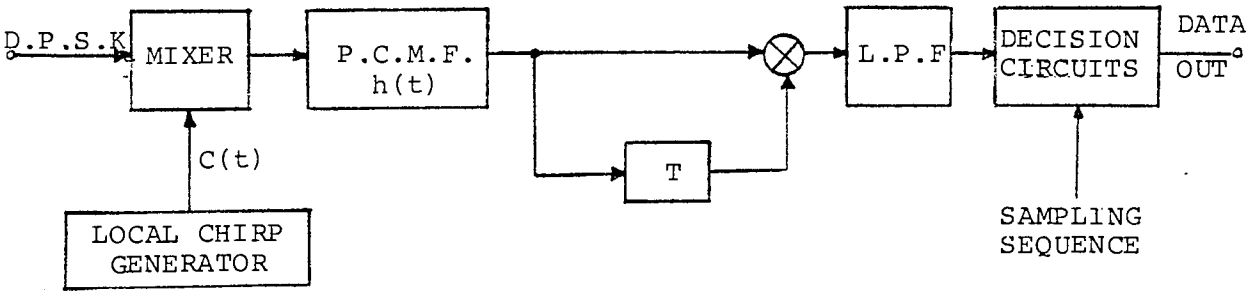

FIG. 7

OVERALL SCHEMATIC OF D.P.S.K. RECEIVER

different values of (ϕ_i). In the presence of doppler shift, the output envelope position is shifted on the time-axis away from the position of perfect match similar to that of the F.S.K. case considered earlier.

The choice between P.S.K. and D.P.S.K. detection schemes for a given channel depends mainly on whether a local phase reference is available at the receiver to perform the coherent detection process. In the D.P.S.K. case the phase reference is simply recovered from the received signal by employing a differential detector; while a P.S.K. signal must be detected coherently, in which case part of the P.S.K. spectrum may be used to send information about the reference carrier to the receiver. Thus D.P.S.K. detection is generally more elegant, simple and practical to use, despite its 3 dB disadvantage in performance to coherent P.S.K.. Fig. 7 illustrates the D.P.S.K. receiver in which a mixer-P.C.M.F. compound is incorporated with a differential detector followed by a low pass filter, and decision circuits. The receiver is implemented utilizing combined hardware and software, which will be discussed in Chapter 4.

2.2 Noise and Distortion Considerations

So far only the response of the mixer-P.C.M.F. compound to a noise-free data signal is considered. In this section white Gaussian noise is added to the data signal before reaching the mixer-P.C.M.F. compound to

show that the compound exhibits the capability of maximizing its output SNR. In this case its relation to the basic optimum predetectors (namely, the matched filter-sampler compound and correlator-sample compound), in A.W.G.N. will be shown. Also the effects of single carrier interference on the output of the P.C.M.F. for both F.S.K. and D.P.S.K. receptions are discussed, as well as the effects of two-tone interference for F.S.K. reception.

In practice, the non-ideal behaviour of the mixer-P.C.M.F. compound distorts the output A.C.F., in which case the detection system in which the compound is incorporated suffers a degradation in performance. The prime sources of distortion which include non-linearity and slopemismatch of the P.C.M.F., and frequency drifts of the local chirp generator (i.e. practical imperfections) are examined. Moreover, the failure of the local chirp generator to start at the arriving time of the data signal received, will be examined, together with its effects on the output A.C.F. of the P.C.M.F. for both F.S.K., and D.P.S.K. reception.

2.2.1 The Output SNR of the P.C.M.F.

Consider the mixer-P.C.M.F. compound of Fig. 1 to process a data signal contaminated by A.W.G.N. The noise part output from the mixer is then

$$n_i(t) = [n(t)][C(t)]^* \qquad (2.15)$$

Hence, the output of the P.C.M.F., using (1), is given by

$$n_o(t) = \int_0^\infty n(t-\tau)\,[C(t-\tau)]^* h(\tau)\,d\tau \qquad (2.16)$$

and the mean square value for (2.16) is

$$E[n_o^2(t)] = \int_0^\infty\int R_n(\tau_1-\tau_2)\,[C(t-\tau_1)]^*\,[C(t-\tau_2)]^* \; h(\tau_1)h(\tau_2)\,d\tau_1 d\tau_2 \qquad (2.17)$$

where, $R_n(\tau) = E\,[n(t)n(t-\tau)]$ is the A.C.F. of the noise.

If the noise bandwidth is wide compared with the signal and of power spectral density $s_n(2\pi f)$, then

$$s_n(2\pi f) = \frac{N}{2} \qquad |2\pi f| < \alpha$$

Since $s_n(2\pi f)$, and $R_n(\tau)$ are a Fourier transform pair then,

$$R_n(\tau) = \frac{N}{2}\,\delta(\tau) \qquad (2.18)$$

Making use of (2.18), (2.17) becomes

$$E[n_o^2(t)] = \int_0^\infty \frac{N}{2}[C^2(t-\tau)]^* h^2(\tau)\,d\tau \qquad (2.19)$$

If the P.C.M.F. bandwidth is narrow compared with the signal centre frequency and $h_c(\tau)$ is the complex envelope of its impulse response $h(\tau)$, then from (2.8)

$$\text{Re.}[h(\tau)] = \text{Re.}[h_c(\tau)\ \text{exp.}\,j(\omega_c t + \tfrac{1}{2}\mu t^2)], |t| \leq \frac{T}{2} \qquad (2.20)$$

where $h_c(\tau) = U(\tau) + jv(\tau)$

Making use of (2.1), and (2.20) respectively, the real values of $[C^2(t)]^*$, and $h^2(\tau)$ are given as follows, neglecting second harmonic terms

$$[C^2(t)]^* = \frac{1}{2} \text{ and } h^2(\tau) = \frac{1}{2} \text{Re.}[h_c(\tau)]^2, |t| \leq \frac{T}{2} \tag{2.21}$$

Therefore, the mean square value of the noise component at the output of the P.C.M.F. is found by using (2.19) and (2.21) as

$$E[n_o^2(t)] = \int_0^\infty \frac{N}{8} [h_c(\tau)]^2 \, d\tau \tag{2.22}$$

Consider the signal component assuming that both F.S.K. and D.P.S.K. signals are centred at the same frequency and may use the same mixer-P.C.M.F. compound without loss of generality. Making use of (2.2), the real value of the output of the mixer yields

$$\text{Re.}[M(t)] = \frac{E}{2}.\cos[\omega_c t + \theta(t)], \quad |t| \leq \frac{T}{2} \tag{2.23}$$

where E is the amplitude of the input signal to the P.C.M.F.

ω_c is the angular centre frequency

$$\theta(t) = \begin{cases} \pi RFt - \frac{1}{2}\mu t^2 & \text{for F.S.K. signal received} \\ \phi_i - \frac{1}{2}\mu t^2 & \text{for D.P.S.K. signal received} \end{cases}$$

Convolving (2.23) with (2.20) using (1), and

simplifying, the output of the P.C.M.F. becomes

$$\text{Re.}[g(t)] = \text{Re}\left\{ \int_0^{\infty} \frac{E}{4} h_c(\tau) \exp.j[\omega_c t + \theta(t-\tau)]\, dt \right\} \tag{2.24}$$

Hence, the peak signal power $= \left| \int_0^{\infty} \frac{E}{4} h_c(\tau)\, d\tau \right|^2$, and

$$\text{SNR} = \frac{\frac{E^2}{16}\left| \int_0^{\infty} h_c(\tau)\, d\tau \right|^2}{\frac{N}{8} \int_0^{\infty} |h_c(\tau)|^2 d\tau} \tag{2.25}$$

If the decision is made at $\tau = T$ (for a physically realizable linear filter)[2] then

$$\text{SNR} = \frac{E^2 T}{2N} \cdot \frac{\left| \int_0^{T} h_c(\tau)\, d\tau \right|^2}{\int_0^{T} |1|^2 d\tau \int_0^{T} |h_c(\tau)|^2 d\tau} \tag{2.26}$$

Applying Schwarz inequality, the output SNR reduces to the following well known result attainable by the matched filter detector[2],[3],[5].

$$\text{SNR} = \frac{E^2 T}{2N} = \gamma \tag{2.27}$$

which depends on the input signal energy rather than its time structure. Nevertheless, the same SNR can be obtained by the basic optimum predetectors namely, the matched filter-sampler compound, or its equivalence, the

correlator-sampler compound[2],[5],[34] which are illustrated in Fig. 8 together with the mixer-P.C.M.F. compound followed by a sampler. Thus the P.C.M.F. sampler, the correlator-sampler compound, and the matched filter-sampler compound are equivalent.

The waveform conversion process (i.e. the mixing process) is incorporated with the P.C.M.F.-sampler in practice to facilitate the ability of building a reasonable approximation to the matched filter in the form of the P.C.M.F. However, the SNR of (2.27) is attainable only when the P.C.M.F. is in perfect match with its input signal. This implies that in F.S.K. reception (section 2.1.1) the SNR is not attainable, since the mark and space compressed signals at the P.C.M.F. output are shifted in time away from the position of perfect match. However, in P.S.K. or D.P.S.K. reception, the perfect match state may be achieved, (by satisfying the requirements stated in section 2.1.2), in which case the SNR of (2.27) is attainable. Nevertheless, to utilize the SNR attainable in both F.S.K. and D.P.S.K. reception, accurate sampling at the peaking instant is required.

Consider both the F.S.K. and D.P.S.K. detection schemes operating in the presence of A.W.G.N. The noise component received by the P.C.M.F. comprises a different frequency pattern from the input chirp signal, which means that noise compression does not occur in the same way as the signal is compressed. Hence, the noise component

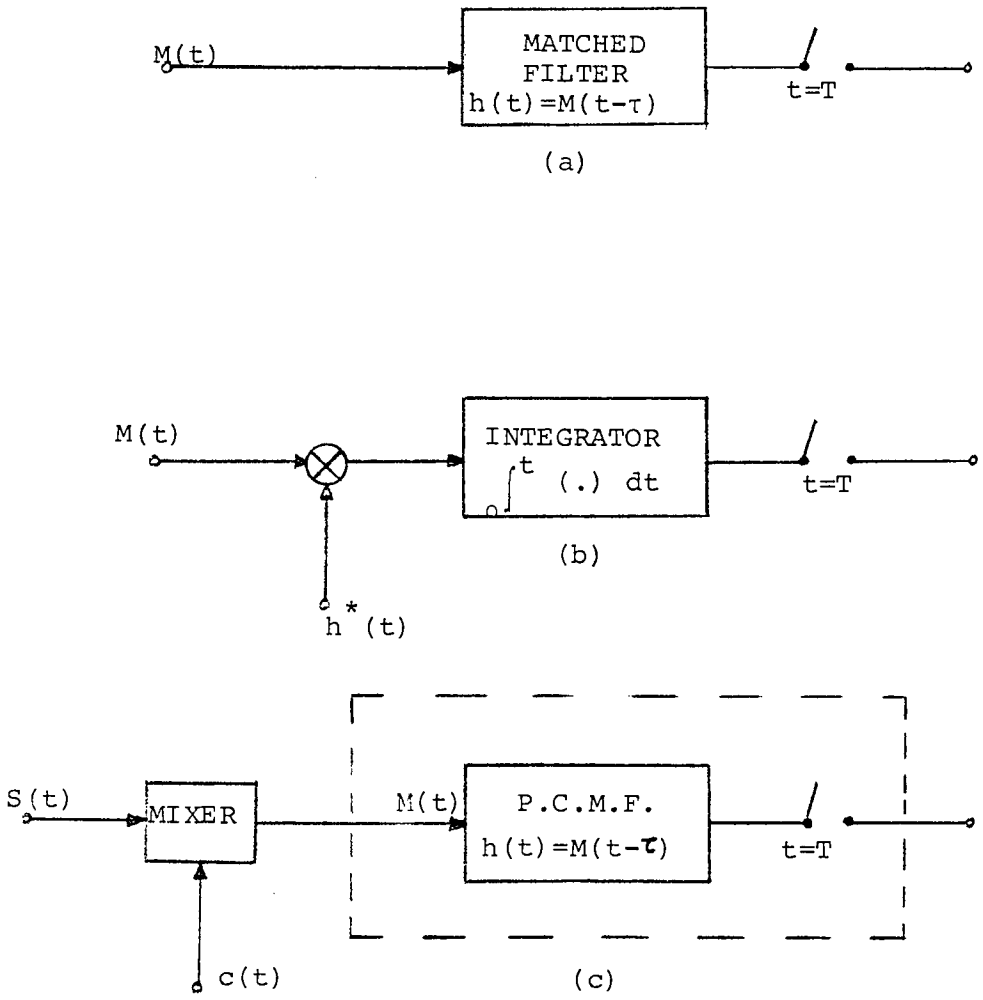

FIG. 8 BASIC OPTIMUM DETECTORS IN A.W.G.N.

(a) Matched Filter-Sampler Compund

(b) Correlator-Sampler Compound

(c) Mixer-P.C.M.F. Compund Followed by Sampler

passes throughout the mixer-P.C.M.F. compound essentially unchanged in amplitude. However, the signal may be replaced (or blocked) for occasional short periods of time by a noise component,which due to the random nature of noise causes an error in the received signal.

The error rate (i.e. the probability of error as a function of SNR) for the F.S.K. detection scheme was approximated by applying spectrum processing, which is the dual of signal processing, and assuming that the spectrum of a random noise components exceeds the spectrum of signal plus noise at the wanted frequency[11]. This gives

$$Pe = \frac{1}{2}\exp. - \frac{\gamma}{2} \qquad (2.28)$$

which is the same error rate obtained for a pair of orthogonal F.S.K. signals in the presence of A.W.G.N. utilizing non-coherent reception[4].

The error rate of the D.P.S.K. detection scheme by pulse compression is equivalent to the conventional D.P.S.K. system[35], which was given by

$$Pe = \frac{1}{2} \exp. - \gamma \qquad (2.29)$$

which may be achieved by a pair of orthogonal signals in the form of D.P.S.K. utilizing a differentially-coherent reception process in which the phase reference is established from the received signal[2],[4]. This latter fact made D.P.S.K. reception particularly attractive compared with coherent P.S.K.[36].

Both theoretical error rates presented above utilize the SNR at the output of the P.C.M.F. with the advantage of 3 dB in performance of the D.P.S.K. detection scheme over the F.S.K. non-coherent detection scheme. However, a critical evaluation of their performances in A.W.G.N. background can only be obtained by practical experiment.

2.2.2 Carrier Interference

In principle the general optimum receiver for a digital data transmission system operating in a combination of carrier interference and A.W.G.N. is essentially a matched filter type of receiver, to which both the F.S.K. and D.P.S.K. receivers described previously belong. Furthermore, for low frequency application of the pulse compression receivers, and in order to obtain a definable compressed pulse at the output of the P.C.M.F. (The number of cycles of the compressed pulse is given by $\frac{2f_o}{B}$), the input chirp signal to the P.C.M.F. must be long enough (i.e. the duration T sec. must be sufficient to give a useful time-bandwidth product). In this case the data rate is affected, for each local chirp generated at the receiver must accommodate one data signal received. Hence the duration of the data signal, which specifies the data rate is dictated by the time-bandwidth product necessary to obtain a definable compressed pulse at the output of the P.C.M.F. This implies that the data signal format (i.e. signal duration and rate), is suitable for utilization over H.F. channels, in which the presence of

interfering signals other than white noise is very likely[2],[3],[5]. However, the degree of freedom of a data signal to be distinguishable from another signal is specified by 2BT[38], accordingly wideband data signals such as chirp data signals[21],[31], are less likely to be corrupted by carrier interference. On the other hand, data signals such as F.S.K. and D.P.S.K. accept less interfering power, and are more likely to be used in a congested frequency spectrum, such as the H.F. channel, than wideband data signals[37].

Generally, if a single interfering carrier is added to the received data signal and the result is processed by the mixer-P.C.M.F. compound, the time domain output of the P.C.M.F. is similar to that of a single tone received signal (i.e. the interfering carrier emerges from the P.C.M.F. as a compressed pulse positioned in the time domain depending on its frequency). This stems from the fact that the mixer-P.C.M.F. compound furnishes the frequency spectrum of its input signal[11], with time as the analogue of frequency. This implies that signals with different frequencies received within the bandwidth of the P.C.M.F. may be resolved at the output with their positions in the time domain corresponding to discrete values of frequency.

In practice a random phase interfering carrier would be most destructive to the data signal when its amplitude, phase and frequency are respectively the same as, opposite

to, and the same as that of the signal. Thus the carrier-to-signal power ratio (CSR), as well as the similarity of the data signal and the interfering carrier, are important factors affecting the detection of the data signal in the presence of carrier interference. An interfering carrier of constant amplitude (C_1), angular frequency (ω_1), and random phase (θ_1) may be expressed as

$$I_1(t) = C_1 \exp.j(\omega_1 t + \theta_1) \qquad (2.30)$$

If $I_1(t)$ is added to the F.S.K. signal expressed by (2.5), and the result is processed by the same mixer-P.C.M.F. compound of (2.8), the output ACF (derived in Appendix B) is given by

$$g(t) = \sqrt{BT}\,(1-\frac{|t|}{T})\{A\,\mathrm{Sinc}\pi(Bt+\frac{Rh}{2})(1-\frac{|t|}{T})\cos(\omega_c+\frac{\pi Rh}{2T})t$$

$$+ C_1\,\mathrm{Sinc}\pi[Bt + (f_1-f_a)T](1-\frac{|t|}{T})\,\mathrm{Cos}(\omega_c t+\frac{\omega_1-\omega_a}{2}t+\theta_1)\} \qquad (2.31)$$

which indicates that the mixer-P.C.M.F. compound resolves the mark and space compressed signals from the interferring compressed signal. However, for $\theta_1 = \pi$, CSR $= \frac{C_1^2}{A^2} = 0$ dB, and $\omega_1 = \omega_a + \frac{Rh}{T}$, the output $|g(t)| = 0$ for either a mark or a space signal, indicating the worst case in the presence of single carrier interference.

Two tone interferers of constant amplitudes (C_1) and (C_2) angular frequencies (ω_1) and (ω_2), and random independent phases (θ_1) and (θ_2) may be expressed as

$$I(t) = C_1 \exp.j(\omega_1 t + \theta_1) + C_2 \exp.j(\omega_2 t + \theta_2) \tag{2.32}$$

In the presence of two tone interferers, the output A.C.F. of the mixer-P.C.M.F. compound is similarly found, and it resembles the addition of a third term to (2.31) comprising (C_2) for (C_1), (ω_2) for (ω_1), and (θ_2) for (θ_1) compared with the second term. The two interferers would be most destructive when the interfering angular frequencies $\omega_1 = \omega_a + \frac{h}{T}$, and $\omega_2 = \omega_a - \frac{h}{T}$, the CSR = $\frac{C_1^2 + C_2^2}{A^2}$ = 0 dB, and the phase angles $\theta_1 = \theta_2 = \pi$.

Consider the D.P.S.K. signal expressed by (2.11) is added to the interfering carrier of (2.30) and the result is processed by the mixer-P.C.M.F. compound. The output A.C.F. of the P.C.M.F. (derived in Appendix B) is given by

$$\bar{g}(t) = \sqrt{BT}\left(1 - \frac{|t|}{T}\right)\left\{GSinc\pi Bt\left(1 - \frac{|t|}{T}\right)Cos(\omega_p t + \phi_i) + C_1 Sinc\pi\left[Bt + (f_1 - f_b)T\right]\left(1 - \frac{|t|}{T}\right)\cos\left(\omega_p t + \frac{\omega_1 - \omega_b}{2}t + \theta_1\right)\right\} \tag{2.33}$$

which indicates that the worst case occurs when $\omega_1 = \omega_b$ CSR = 0 dB, and the phase angles (ϕ_i) and (θ_1) are antipodal. Nevertheless, the position on the time-axis

given by $t = (\frac{f_b - f_1}{B})T$, and the polarity of the compressed interfering signal is given by the value of (θ_1). However, the differential detection process performed on the output of the P.C.M.F. creates a phase dependency from one interfering signal to the next[39], unlike the F.S.K. case, where interference acts independently on each signal.

The mixer-P.C.M.F. compound is therefore able to resolve additive carrier interference and the data signal as long as they differ in frequency. However, the combination of A.W.G.N., and random phase carrier interference certainly degrades the performance of both receivers employing the mixer-P.C.M.F. compound. This degradation which depends on the (CSR), needs to be established by practical experiment.

2.2.3 Practical Imperfections

A complete feasibility study of incorporating the mixer-P.C.M.F. compound in both detection schemes under investigation necessitates the inclusion of distortion effects on the output A.C.F. due to the compound's non-ideal behaviour in practice. The fact that the chirp signal is a composite signal having several parameters, makes it less controllable in practice and, hence more liable to depart from the desired parameters during generation and/or processing. Of particular importance is the departure of the chirp parameters from those required to achieve the perfect match state with its P.C.M.F.

The mixer-P.C.M.F. compound utilizes two chirp signals, one for modulating the received data signal (i.e. the local chirp), and the other for pulse compression acting as the impulse response of the P.C.M.F. In practice local chirp generators are likely to drift in frequency, shifting the chirp signal spectrum from the desired centre frequency. Consider the local chirp signal of (2.1) to drift by ($\delta\omega$) from its angular frequency (ω_o), then it can be expressed as

$$\dot{C}(t) = \exp.j\left[(\omega_o - \delta\omega)t + \frac{1}{2}\mu t^2\right], \quad |t| \leq \frac{T}{2} \qquad (2.34)$$

In this case the output A.C.F. of the mixer-P.C.M.F. compound for an F.S.K. signal received may be found (using (2.5), (2.34), and (1), following the same method in Appendix A) to be

$$g(t) = A\sqrt{BT}\left(1-\frac{|t|}{T}\right)\mathrm{Sinc}\pi\left[\left(Bt+\frac{Rh}{2}+\delta fT\right)\left(1-\frac{|t|}{T}\right)\right]$$

$$\cos\left(\omega_c + \frac{\pi Rh}{2T} + \frac{\delta\omega}{2}\right)t, \qquad |t| \leq T \qquad (2.35)$$

which indicates that the mark and space signals are shifted in time from the mark and space sampling times of (2.10) by $\frac{\delta fT}{B}$. Similarly for a D.P.S.K signal received, the output A.C.F. may be found (using (2.11), (2.34), and (1)) to be

$$g(t) = G\sqrt{BT}\left(1-\frac{|t|}{T}\right)\mathrm{Sinc}\pi\left[(Bt+\delta fT)\left(1-\frac{|t|}{T}\right)\right]$$

$$\cos\left(\omega_p t + \frac{\delta\omega}{2}t + \phi_i\right), \quad |t| \leq T \qquad (2.36)$$

which shows a time shift of $\frac{\delta f T}{B}$ from the state of perfect match. Moreover, a doppler shift in the received data signal would produce the same time shift produced by the frequency drift ($\delta\omega$).

A common type of mismatch which occurs between the P.C.M.F. impulse response and its input chirp signal is the slope mismatch[16]. In this case the impulse response chirp does not have the correct slope to match the input chirp and may be expressed as

$$h'(t) = \exp.j(\omega_o t + \frac{1}{2}\mu' t^2), \quad |t| \leq \frac{T}{2} \tag{2.37}$$

while the linear-FM law is preserved, a slope mismatch factor (D) may be defined as

$$D = \frac{\mu - \mu'}{\mu} \tag{2.38}$$

where (μ') is the departed slope from the correct slope (μ).

To approach more exactly the practical case, the departure of the impulse response, from the linear-FM law is considered, and may be expressed as

$$h''(t) = \exp.j(\omega_o t + \frac{1}{2}\mu t^2 + \frac{\delta\mu t^3}{3}), \quad |t| \leq \frac{T}{2} \tag{2.39}$$

where a quadratic term weighted by (δ) is added to the chirp signal argument, indicating the degree of non-linearity present in the impulse response of the P.C.M.F.

The effects produced by slope mismatch, and non-linearity of the P.C.M.F. on the A.C.F. for an M-ary F.S.K. signal received were theoretically approximated yielding some limits on both type of imperfections[40]. Generally the effects produced by practical imperfections considered (i.e. frequency drift of the local chirp, and slopemismatch and non-linearity of the P.C.M.F.) on the output A.C.F. (for F.S.K., and D.P.S.K. receptions) are, time shift of the compressed output which leads to inaccurate sampling, reduction in amplitude and widening of the compressed pulse width. This implies that a degradation in performance of both detection schemes in the presence of practical imperfection is inevitable. However,the amount of degradation in performance needs to be established in practice by estimating the error rate in the presence of each type of imperfection.

2.2.4 Time Delay

For optimum processing to take place by the mixer-P.C.M.F. compound, each local chirp signal generated must accommodate one data signal received. This implies that the chirp generator must know the arrival time of the data signal (i.e. the local chirp signal must be generated periodically, and in synchronism with the data signal).

In practice active or passive techniques may be used to generate the local chirp signal. A conventional active generation technique is to synthesize the chirp signal

from a clock signal from which a ramp signal, of the same period of the chirp signal to be generated, is processed, to drive a voltage controlled oscillator (V.C.O.)[16]. Another digital technique made feasible by the advent of (L.S.I.) is to store one element of the chirp signal in a programmable-read-only-memory (PROM), then read it out periodically using a binary counter. The digital output of the (PROM) is fed to a digital-to-analogue converter (D/A) to provide the local chirp signal. Passive generation of the chirp signal may be obtained by exciting a conjugate of the P.C.M.F. employed for pulse compression[16],[22]. In any generation technique used, the time start of the local chirp generator may be achieved by sending a synch pulse together with the data signal. However, a clock signal may be extracted from the received data signal, to perform two functions, first to synthesize the local chirp signal, and secondly to make a decision on the binary bit received, as is usually the case in any digital communication receiver. The chirp generation process and/or a delay of the data signal in the channel leads to a time delay between the local chirp signal and the data signal received. Accordingly, a degradation in the performance of the mixer-P.C.M.F. compound may be expected.

On a pulse-by-pulse basis, the compressed envelope at the output of the P.C.M.F. in the presence of time delay for both F.S.K. and D.P.S.K. reception, may be found after introducing a time delay (Δ) in the local chirp signal

of (2.1) as follows

$$C(t-\Delta) = \exp.j\left[\omega_o(t-\Delta) + \frac{1}{2}\mu(t-\Delta)^2\right], \quad -\frac{T}{2} - \Delta \leq t \leq \frac{T}{2} - \Delta \tag{2.40}$$

The output of the envelope detector present at the output of the P.C.M.F. is found in Appendix C for an F.S.K. signal received, and is given by

$$\eta = A\sqrt{BT}\ (1-\frac{\Delta}{T})\ \text{Sinc}\pi\left[B(\Delta-t) + \frac{Rh}{2}\right](1-\frac{\Delta}{T}) \tag{2.41}$$

If compared with the envelope of (2.9) this indicates that it suffers a time shift of (Δ), a loss in amplitude, and widening in the pulse width.

Similarly, for a D.P.S.K. signal received, the envelope of the A.C.F. is found in Appendix C as

$$\eta_1 = G\sqrt{BT}(1-\frac{\Delta}{T})\text{Sinc}\pi B(\Delta - t)(1 - \frac{\Delta}{T}) \tag{2.42}$$

which shows again that the envelope suffers a time shift, a loss in amplitude, and widening of the pulse width driving the A.C.F. away from the state of perfect match.

Hence as a result of time delay, inconsistency in the values of the peaking instant of the compressed envelope at the output of the mixer-P.C.M.F. compound is produced. Consequently, a degradation in the performance of both detection schemes may be expected.

CHAPTER THREE

IMPLEMENTATION OF THE EXPERIMENTAL SYSTEM

3. IMPLEMENTATION OF THE EXPERIMENTAL SYSTEM

3.1 INTRODUCTION

The advent of microprocessors has made it possible to implement experimental systems without recourse to actual, and often expensive, hardware. Software is not only less expensive, but it also offers several other very important advantages over hardware: it is more flexible, it is easier to implement, more efficient, and more reliable. Together, the hardware and software may be utilized to create a more versatile experimental system. Furthermore, by using a versatile microprocessor system (e.g. TMS-9900 system)[41] many tasks can be tackled, and the development cost can be shared by using the microprocessor for several applications[42].

Fig. 9 illustrates the general layout of the experimental system which is supervised by the TMS-9900 microprocessor system. Signals used are generated and digitized using the TEKTRONIX 1405 minicomputer, while noise is obtained from the HP 3722A Gaussian noise generator, and digitzed using an analogue-to-digital (A/D) converter. The digital output of the signal processing is converted back to analogue for further processing. Software was written using the TMS-9900 instruction set[41],[43]. In order to allow for more universal usage, flow diagrams are provided for the purpose of illustration.

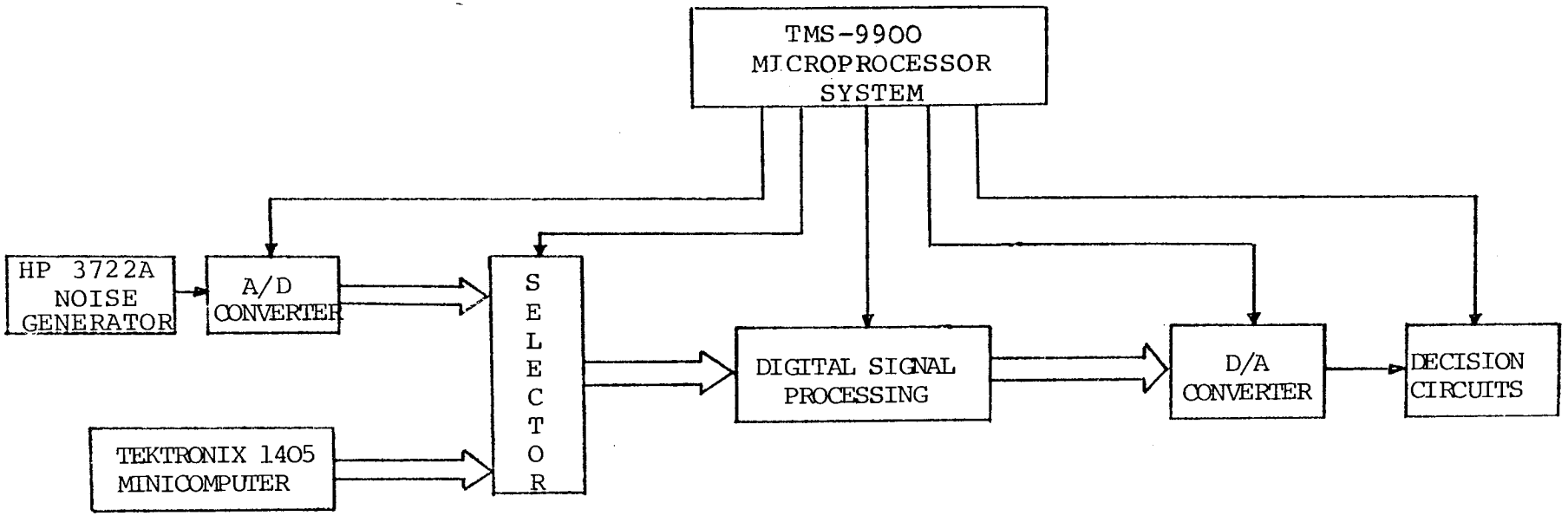

FIG. 9 GENERAL LAYOUT OF EXPERIMENTAL SYSTEM

Experimental error-rate models for both F.S.K. and D.P.S.K. detection schemes are implemented utilizing the experimental system. Also a random phase carrier interference model is implemented which may be operated in conjunction with any of the error-rate models.

3.2 SIGNALS DIGITIZATION AND PROCESSING

Any operation performed on a signal by an analogue signal processor may also be performed by a digital signal processor, providing that the signal is sampled and quantized (i.e. digitized) before any digital operation takes place. Sampling must be performed at least at the Nyquist rate (i.e. a signal must be sampled at twice the highest frequency in the signal). However, in practice sampling is performed at higher sampling rates to avoid any loss of information due to sampling[44]. With the availability of digital computers, signals can be generated in digital form using software, otherwise the digitization process must be performed by an A/D converter circuit.

Known signals (e.g. F.S.K., P.S.K., and chirps) are generated in digital form using a minicomputer, while noise needed to represent the A.W.G.N. channel in the experimental system is obtained from a Gaussian noise generator, and digitized using an A/D converter circuit. Fig. 10 illustrates the software of the signal-generator, which samples a (T) seconds-long signal into (L) samples, quantizes it into (2ε) levels, converts each sample into

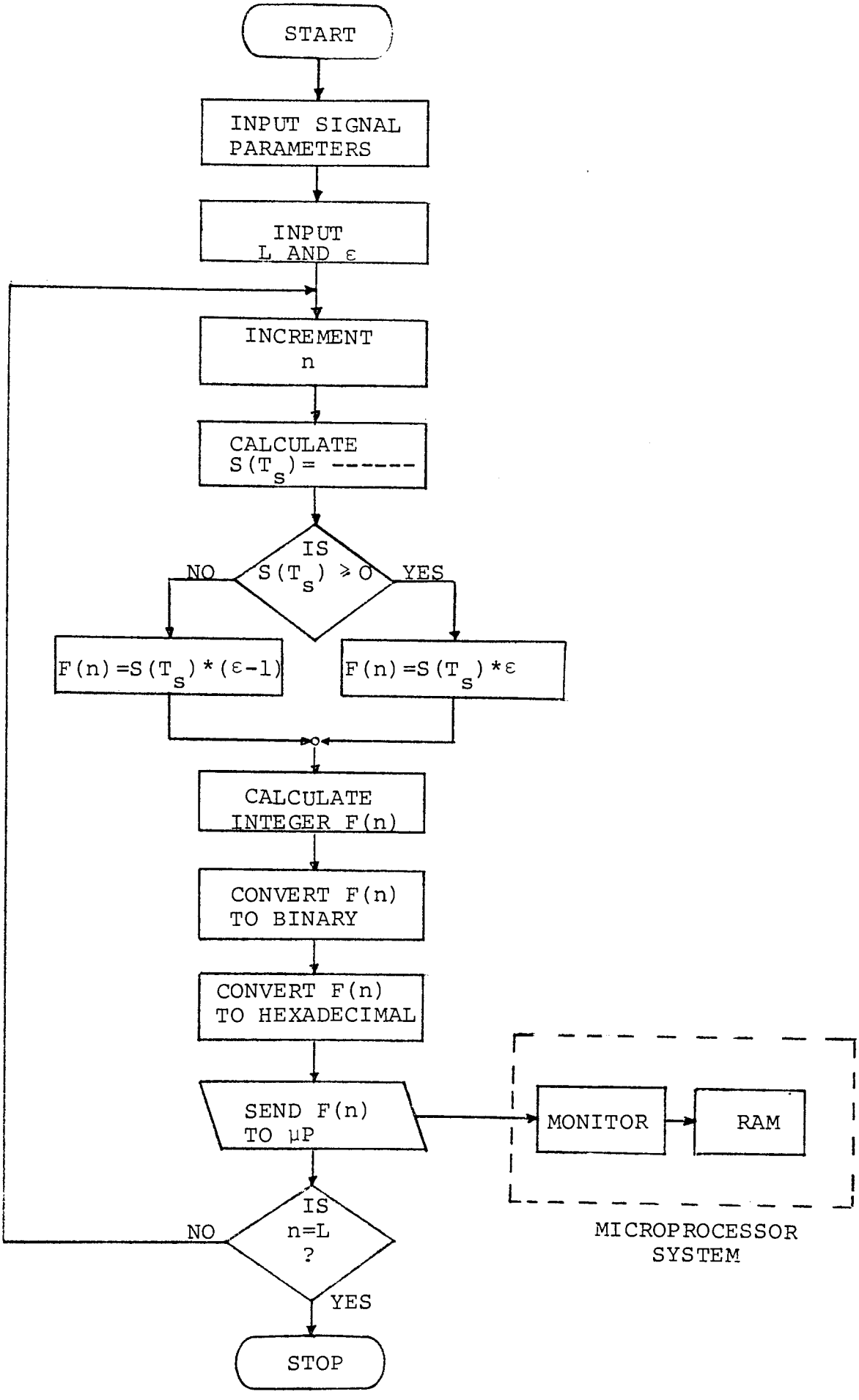

FIG. 10 SIGNAL GENERATOR SOFTWARE

binary and then into Hexadecimal format. The latter format of each sample is sent to the random-access-memory (RAM) of the microprocessor system through its monitor. The F.S.K., P.S.K., and chirp signals used are expressed respectively in (3.1), (3.2), and (3.3) as a function of the sampling interval (T_s)

$$S(T_s) = \text{Sin}(\omega_a + \pi RF)T_s \qquad (3.1)$$

$$S_i(T_s) = \text{Sin}(\omega_p T_s + \phi_i) \qquad (3.2)$$

$$C(T_s) = \text{Sin}\left[\omega_o T_s + \frac{1}{2}\mu (T_s)^2\right] \qquad (3.3)$$

where $T_s = \frac{nT}{L}$

L is the total number of samples

n = 1, 2, ----, L

Thus, the minicomputer is performing two functions which may be performed by a signal generator, followed by A/D converter. However, the former method provides more flexibility regarding the change of signal parameters needed for experimental purposes.

3.2.1 Modulation and Convolution

The main object of the digital-signal-processing part in the experimental system of Fig.9 , is the implementation of the mixer-P.C.M.F. compound, which is used by both detection schemes under investigation, in software. Other signal processing techniques involving the detection schemes are also implemented in software, for example, signal and noise addition, envelope calculation,

data generation and encoding, and random phase shift generation.

Modulation, and convolution are the two processes which form the mixer-P.C.M.F. compound process. Modulation is implemented using the following known relation.

$$M(n) = X_c(n)\left[u+mX_s(n)\right], \quad n = 1,2, \text{---},L \qquad (3.4)$$

where $X_c(n)$ are samples of the carrier

$X_s(n)$ are samples of the signal

u is the D.C. level (constant)

m is the modulation index (constant)

$X_c(n)$, and $X_s(n)$ may represent respectively, the digital numbers stored in RAM for the local chirp signal and the data signal (i.e. F.S.K. or D.P.S.K.) which were originally generated using the software generator of Fig. 10 . A flow diagram of the modulator software is illustrated in Fig.11 . Each two samples to be multiplied or divided must be checked for polarity in advance.

The P.C.M.F. is completely defined by its impulse response, which is a chirp signal (suitably delayed) opposite in slope to that of the input chirp signal. The output of the P.C.M.F. is calculated by convolving the impulse response with the input chirp signal. For a signal M(n), and an impulse response h(L-r) delayed by L-samples, the convolution sum may be expressed as

$$g(s) = \sum_{\substack{n=1 \\ r=n-1}}^{s} M(n)h(L-r), \quad 1 \leq s \leq L \qquad (3.5)$$

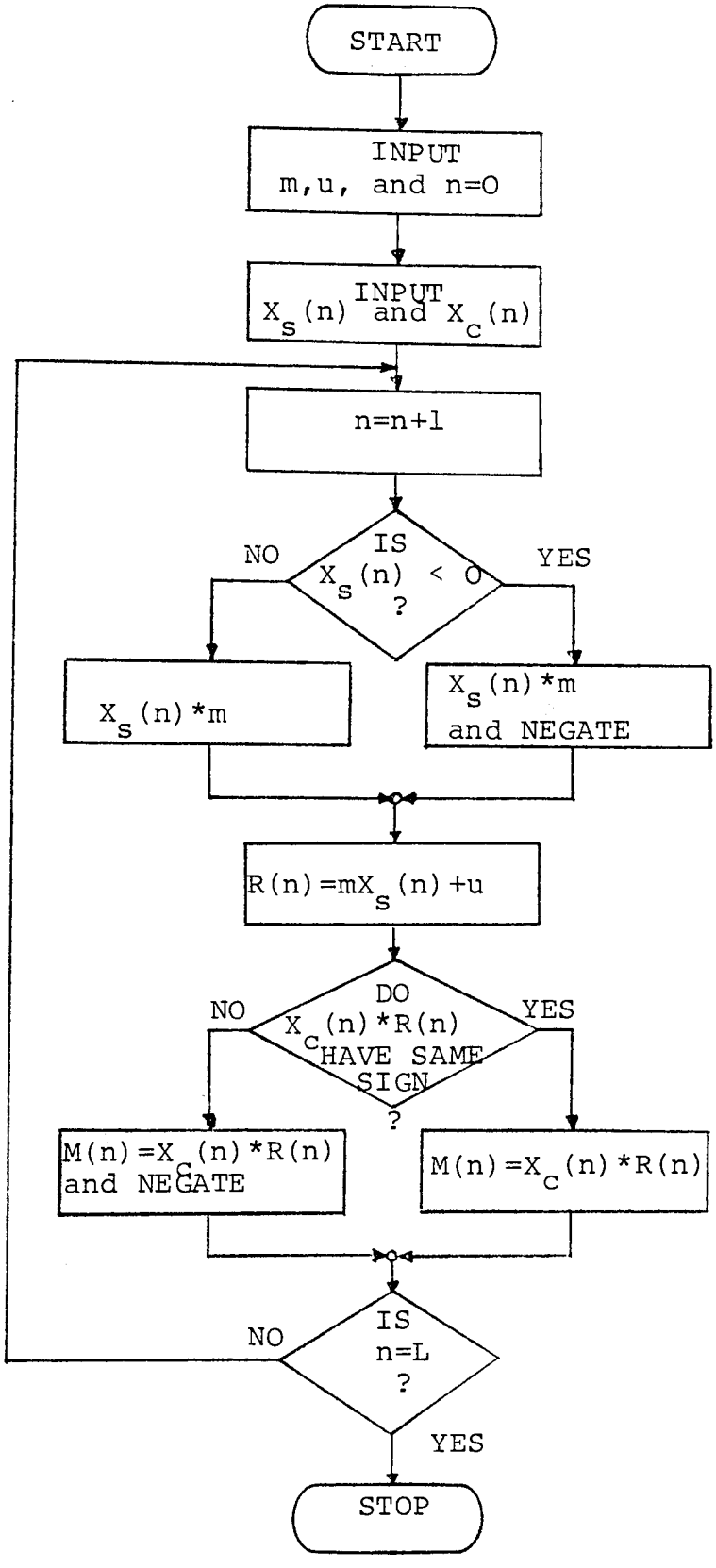

FIG.11 MODULATOR SOFTWARE

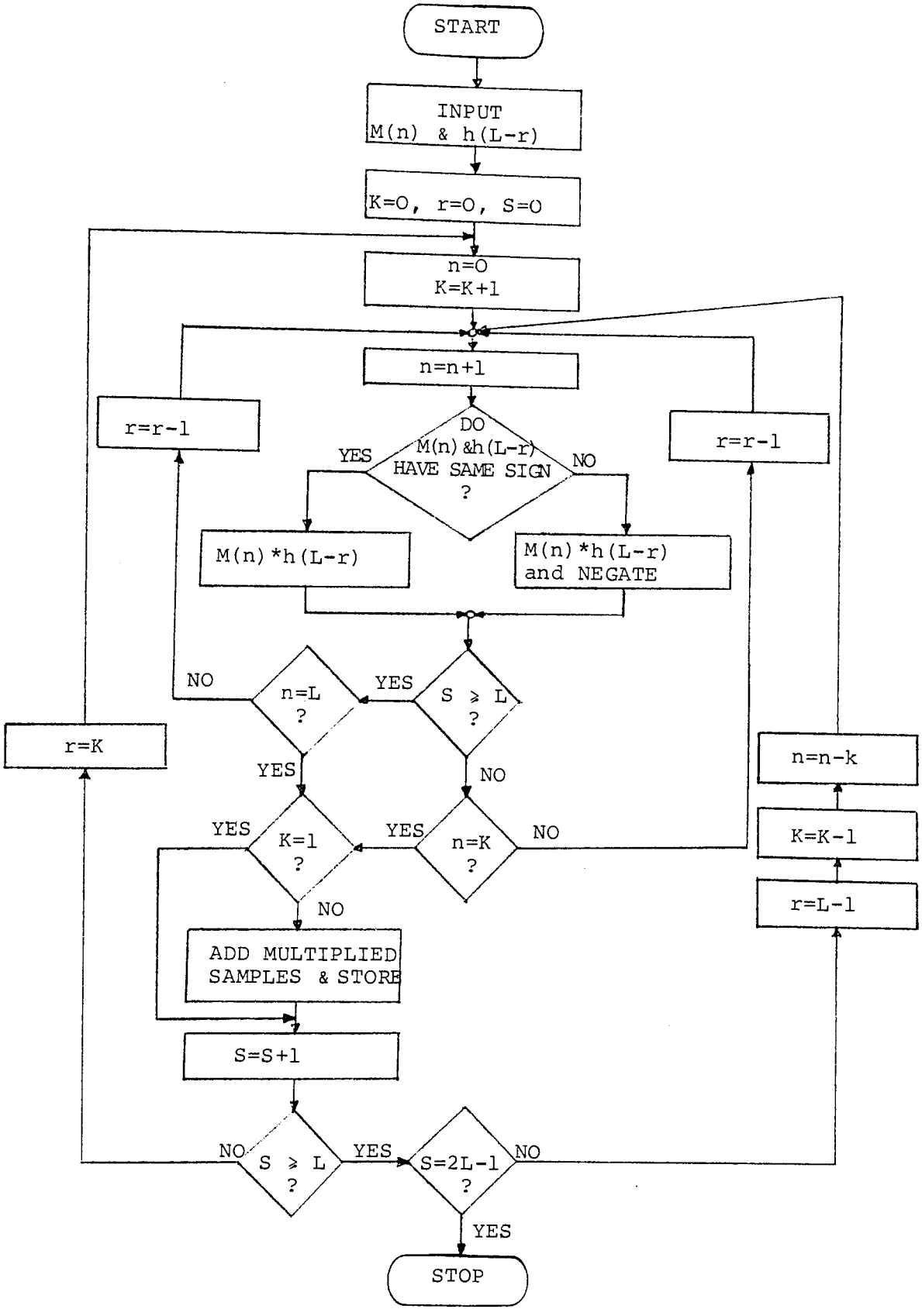

FIG.12 P.C.M.F. SOFTWARE

M(n), and h(L-r) are each L-samples long, and M(n) is the output sequence of the modulator of (3.4), whereas h(L-r) is generated in digital form using the software generator of Fig.10 . A flow diagram of the P.C.M.F. software is illustrated in Fig.12 . This calculates the complete convolution of M(n), and h(L-r) sequences by shifting the two sequences by one sample with respect to each other, after each calculation of the convolution sum. Accordingly the output of the P.C.M.F. is (2L-1) samples long.

The parameters of both the local chirp and the impulse response chirp which represents the mixer-P.C.M.F. compound may therefore be easily changed using the software generator of Fig.10 . This facilitates, for experimental purposes, the insertion of non-linearity, slope mismatch, envelope weighting, and frequency drift.

3.2.2 A/D and D/A Conversion

The A/D converter circuit is mainly used for digitizing Gaussian noise when it is required for digital signal processing. After signal processing is accomplished, the D/A circuit is used for constructing the analogue equivalent of a set of digital numbers stored anywhere in RAM or PROM. Both the A/D and D/A circuits are microprocessor controlled, and are identified to the processor as unique memory locations by their own addresses. Fig. 13 illustrates a flow diagram of the A/D-software routine used in conjunction with the A/D circuit. To eliminate the D.C. level intro-

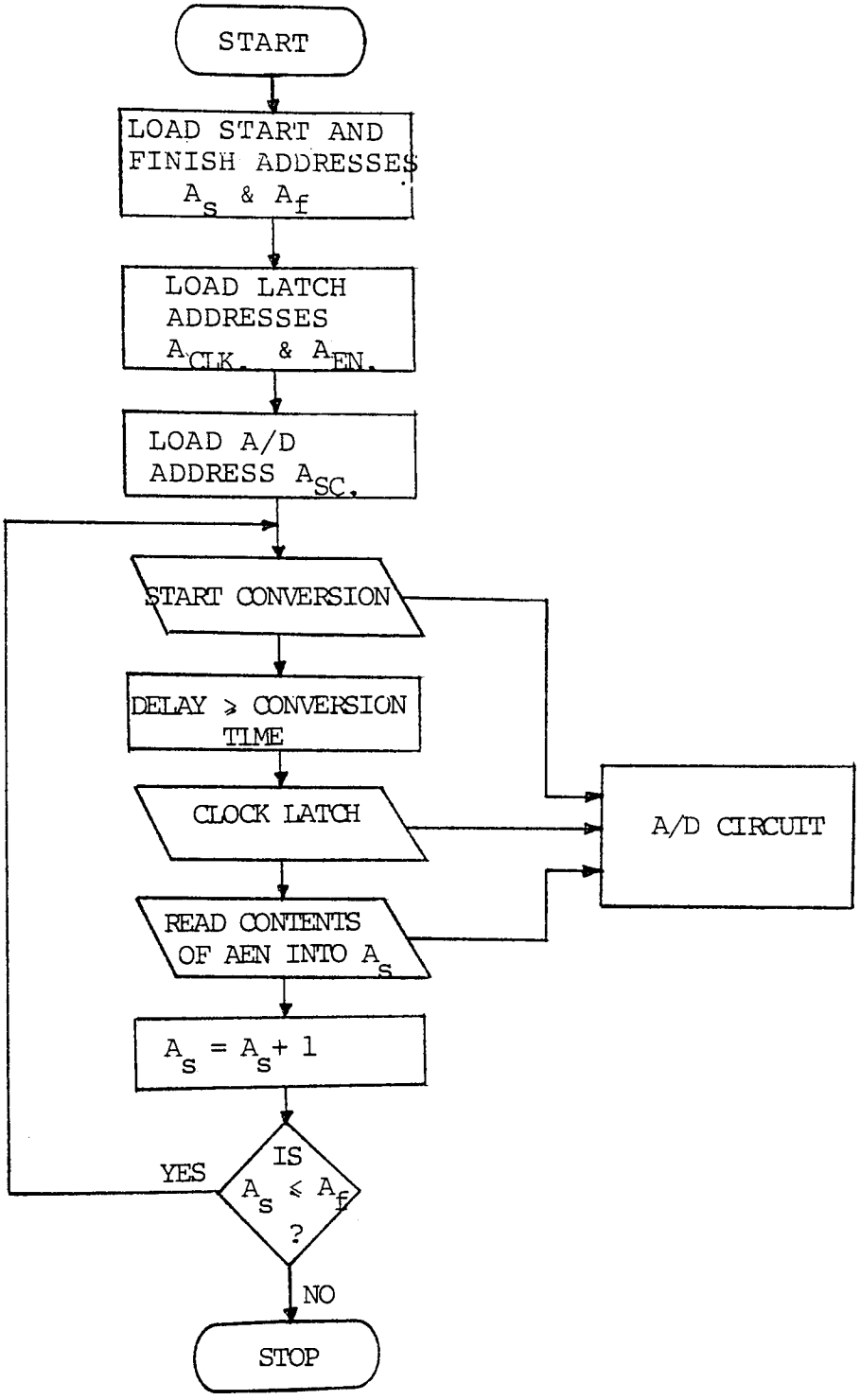

FIG.13 A/D SOFTWARE

duced by the A/D circuit on a bipolar input signal, the mean value (H_x) of the digital output is calculated, and then subtracted from each sample value X(n). This gives the zero mean digital output $\overline{X}(n)$ as follows

$$\overline{X}(n) = X(n) - H_x \qquad (3.6)$$

$$\text{where } H_x = \frac{1}{L} \sum_{n=1}^{L} X(n)$$

The D/A converter routine begins with loading the start and finish addresses within which the digital sequence to be converted to analogue is stored. Each time the contents of the start address is read out into the D/A converter circuit, an increment is added. This continues until the start and finish addresses are equal.

Latches are used to interface both the A/D and D/A circuits with the Data-Bus of the microprocessor system, as will be described in the next section.

3.3 THE HARDWARE INTERFACE

The hardware interface circuits supported by software, causes the experimental system to perform special tasks under microprocessor control. Moreover, the hardware facilitates communication of the experimental system with the outside world[45],[46]. Fig. 14 illustrates a block diagram of the hardware interface.

Unique addresses are decoded from the Address-Bus of the microprocessor system for the A/D converter circuit,

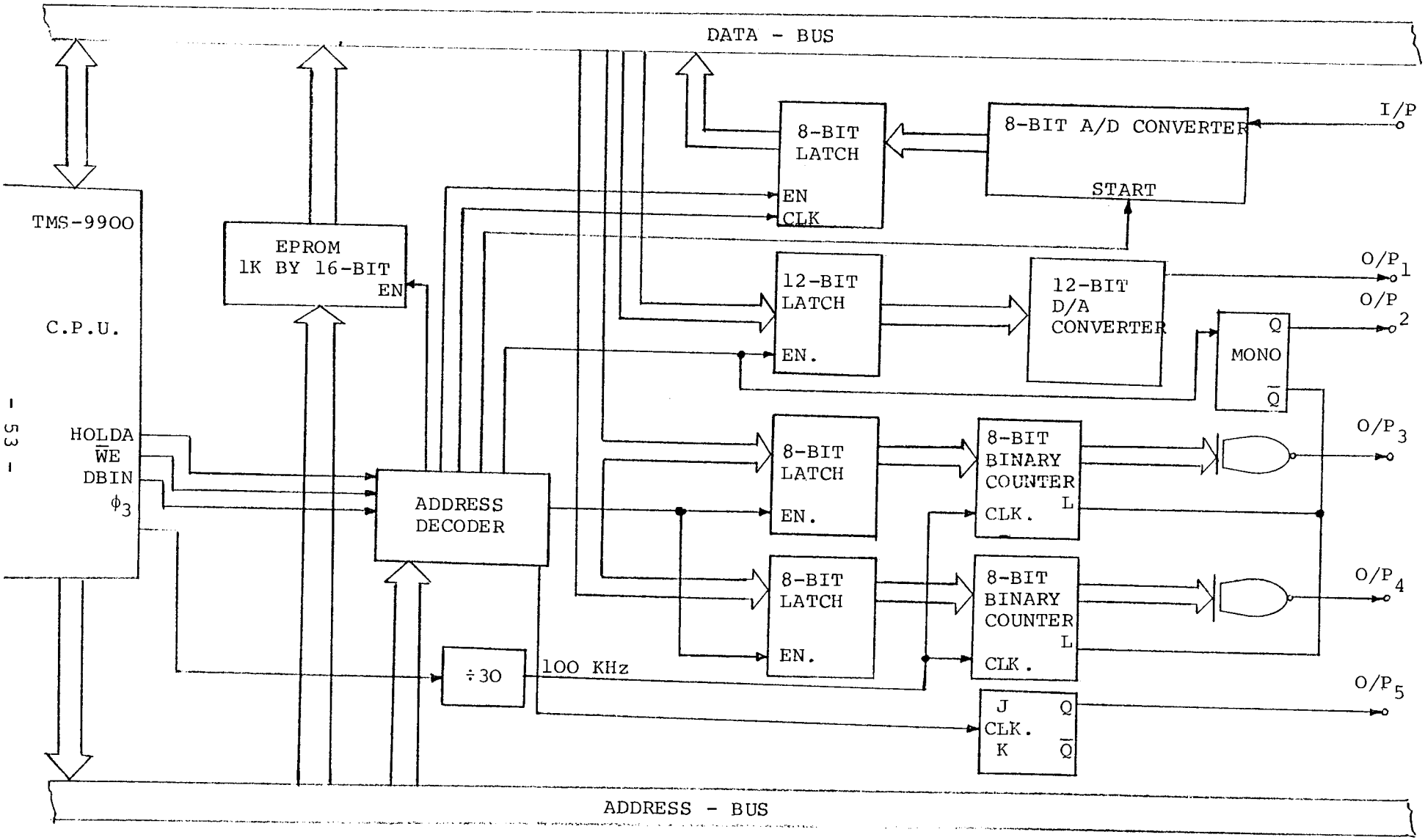

FIG.14 "HARDWARE INTERFACE"

D/A converter circuit, two programmable frequency dividers, a data pattern generator, and a PROM. The address decoder is controlled by HOLDA (Hold Acknowledge), $\overline{WE}$ (Write enable), and DBIN (Data Bus In) of the TMS-9900 microprocessor[41]. DBIN-active means that data may be written into memory (i.e. RAM) using the A/D converter circuit; $\overline{WE}$-active means that data may be read out of memory into a given address (e.g. D/A converter circuit, frequency dividers, or data pattern generator); and HOLDA is used for reading out the PROM in which programs necessary for digital signal processing are stored.

The result of digital signal processing is converted to analogue by latching the digital sequence into a 12-bit latch, then this is enabled, and finally the sequence is clocked into a 12-bit D/A converter. The time taken by the processor to load the addresses required for operating the D/A circuit is detected using a retriggerable monostable. This detected time provides timing markers representing the start and finish times of reading out a digital sequence into the D/A circuit. Moreover, it is used for resetting the two 8-bit binary counters employed in the programmable frequency dividers.

The programmable dividers are used to provide timing signals for driving the decision circuits employed in both F.S.K. and D.P.S.K. detection schemes. An 8-bit binary number is latched into an 8-bit latch, and once this is enabled then the counter divides down its 100 KHz clock

signal which is processed from one of the clock signals originally used by the C.P.U. Divisions can be made by any number in the range (1-255). Consequently, a sampling pulse from each divider can be provided within the start and finish times of reading out a digital sequence from memory to the D/A converter circuit.

The transmitted data pattern is provided for comparison with the recovered data pattern using a J-K flip-flop, which changes its state under processor control when the transmitted data changes state.

After digital signal processing is accomplished, a digital sequence in memory will be ready to be read out into the D/A converter circuit. Fig. 15 illustrates a flow diagram of reading out the digital sequence, followed by the required timing information, and next the transmitted data pattern.

3.4 THE ERROR RATE MODELS

The error rate models are structured to simulate F.S.K., and D.P.S.K. communication systems utilizing the experimental system described earlier. Moreover, these models are designed to compute the probability of error for a given input SNR,when F.S.K. or D.P.S.K. signals are received in a background of A.W.G.N. and/or the following conditions:

(a) Non-linearity, slope mismatch, and envelope weighting of the impulse response chirp of the

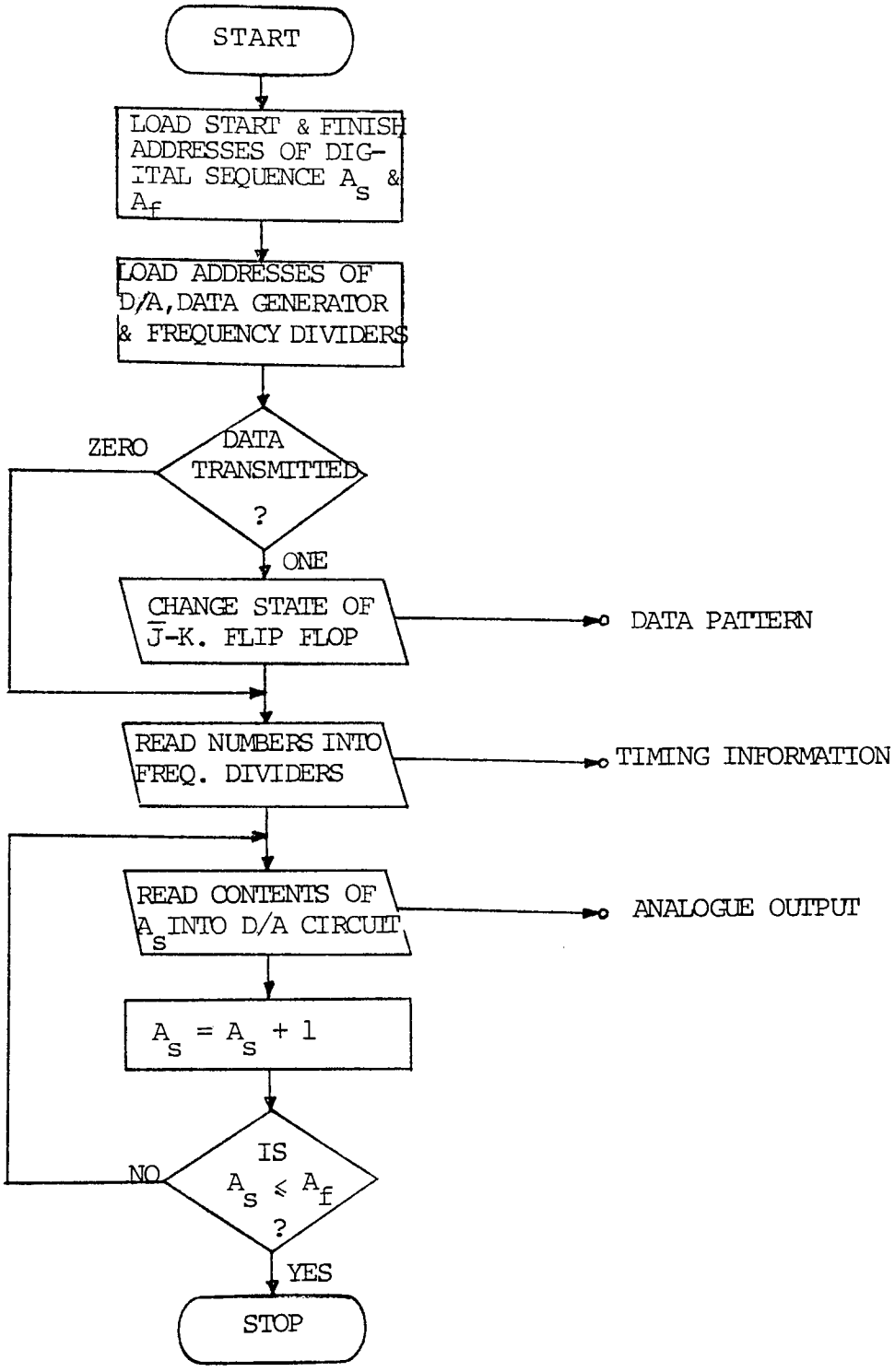

FIG.15 OUTPUT SOFTWARE

P.C.M.F. as well as frequency drift of the local chirp signal. These are implemented utilizing the software signal-generator of Fig. 10 .

(b) The failure of the local chirp generator to start at the arrival time of the received data signal. This is implemented by shifting the local chirp samples stored in memory each time a time delay is required.

(c) The presence of random phase additive interference, in both F.S.K. and D.P.S.K. reception. A carrier interference model is implemented which may be operated in conjunction with both error rate models, as will be described later.

Different input SNR's are specified by first storing the same r.m.s. values of signal and noise, and secondly dividing each, using software to set a specific SNR. Having set the SNR, the user can operate the error rate model and compute the probability of error P_e as follows

$$P_e = \frac{\text{Number of Errors (e)}}{\text{Number of Transmitted signals (x)}} \qquad (3.7)$$

3.4.1 The F.S.K. Error Rate Model

Fig. 16 shows a flow diagram of the F.S.K. error-rate model in which two F.S.K. signals are sequentially selected, added to noise, modulated, convolved, full wave

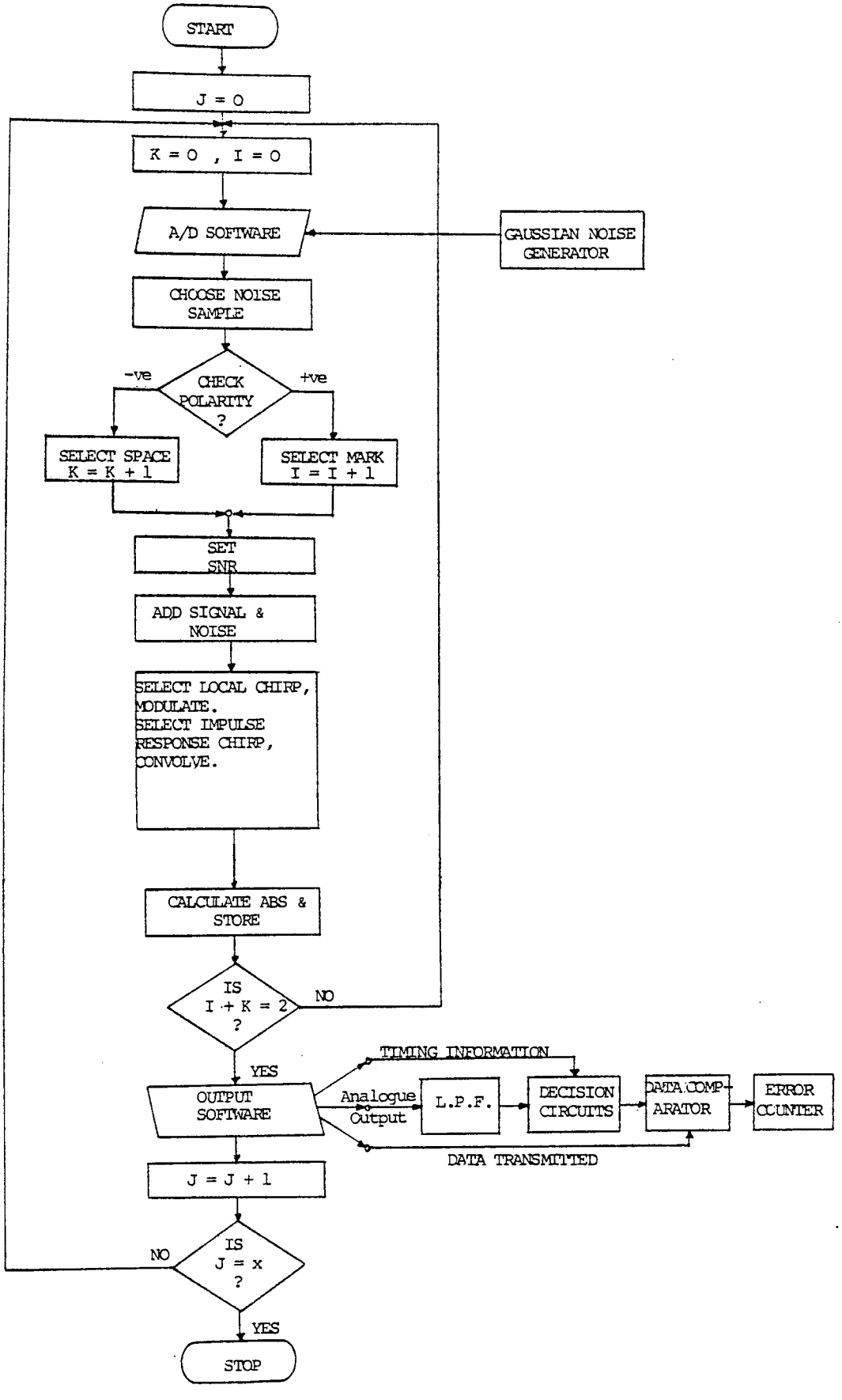

FIG.16 F.S.K. ERROR RATE MODEL

rectified, and the result is converted to analogue for further processing.

Each F.S.K. signal is selected according to the transmitted data pattern, which depends on the polarity of a given noise sample. New samples of white Gaussian noise are added to each F.S.K. signal after the SNR is specified. Modulation and convolution are performed using the appropriate local chirp and impulse response chirp, respectively. Each output compressed signal of the convolver (i.e. P.C.M.F.) is full-wave rectified to define its envelope. Once two signals have been processed, the outputs of the full-wave rectifier are sequentially read out into the D/A converter circuit, while timing information and the data transmitted are sent to the decision circuits.

The analogue output is low pass filtered, then sent to the decision circuit to decide on the received binary bit. The recovered data is compared with the transmitted data, and the output is fed to an error counter. After the required number of signals (x) for a given input SNR has been processed the probability of error is readily calculated using (3.7).

3.4.1.1 Decision Circuits

The envelope of the compressed signal peaks at either the mark or space time, depending upon the received data pattern. Hence, the decision criterion employed is to

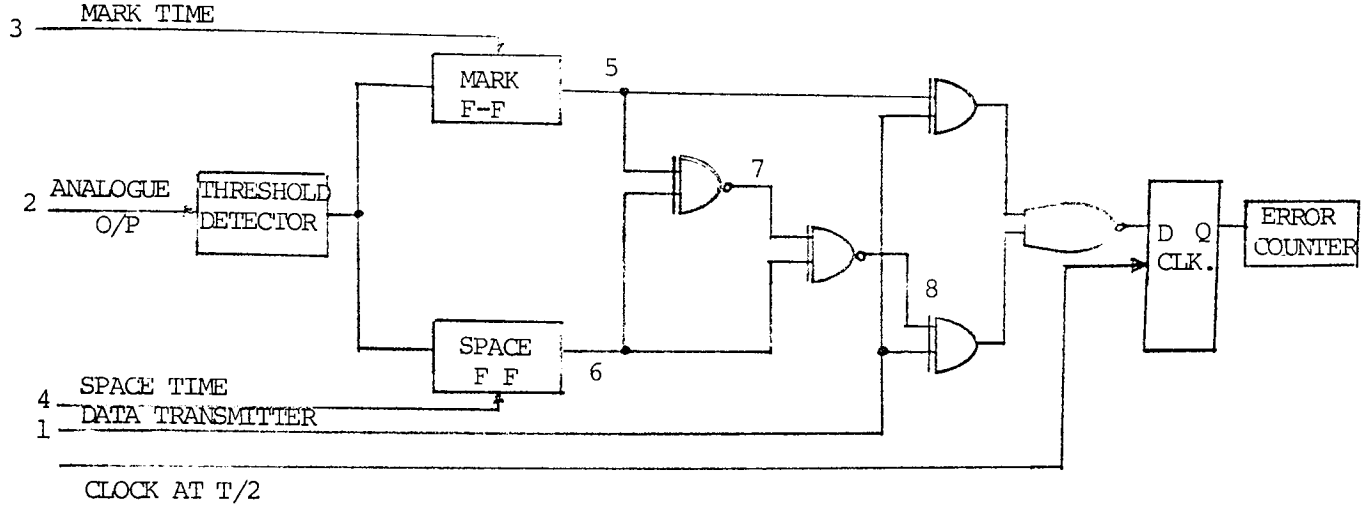

FIG. 17a DECISION CIRCUITS

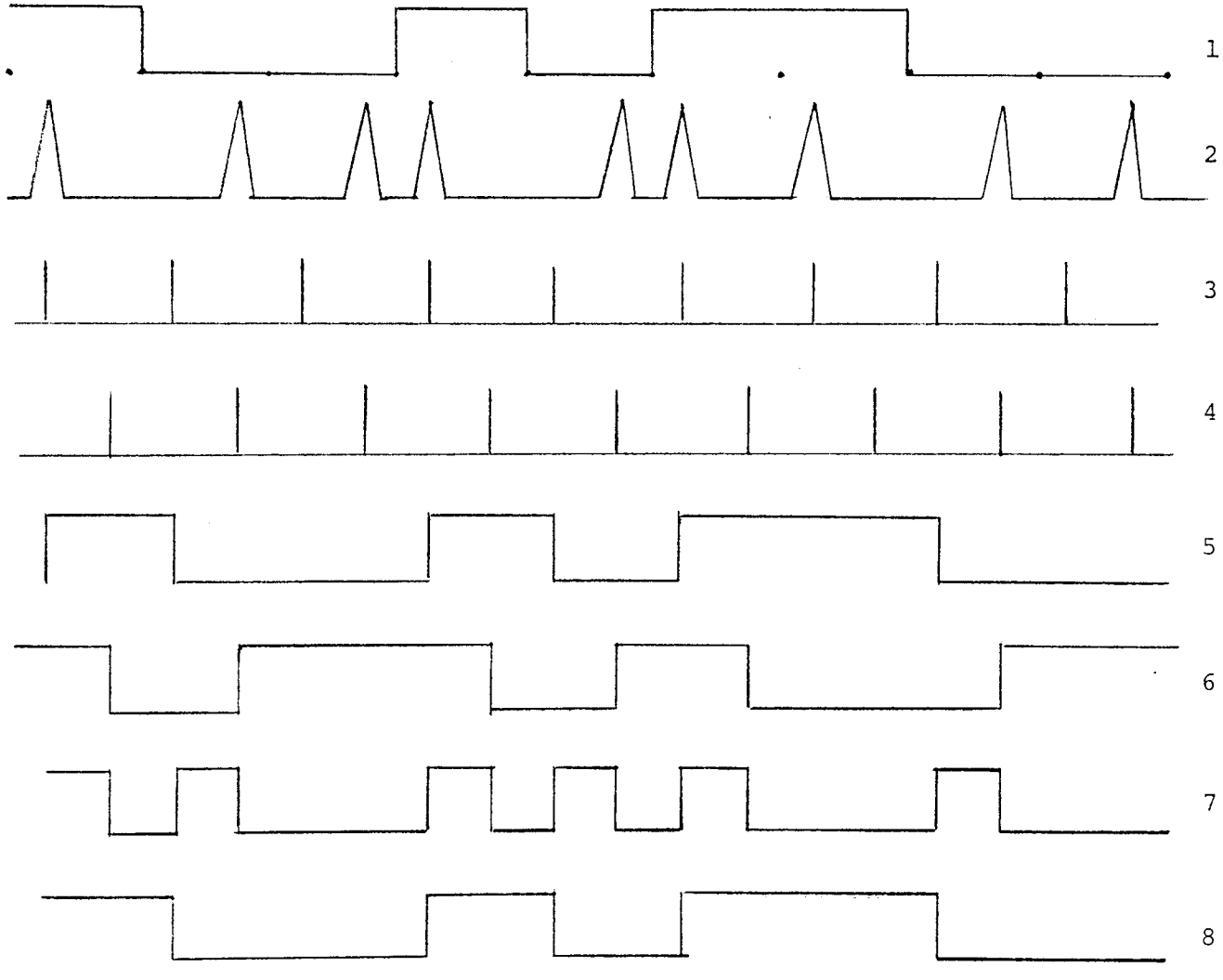

FIG. 17b MECHANISM OF DECISION CIRCUITS

detect two signals of the same polarity at two different times, one corresponding to a received mark, and the other to a received space, bearing in mind that only one signal is present at a time.

Fig. 17a shows schematicly the decision circuits which sample the output of the threshold detector at times (t_s), and (t_m), deciding logic "1" if signal is present, and logic "0", if noise is present. The mark and space flip-flops give the same output sequences, but delayed from each other by the time difference between a mark and a space signal. Each sequence represents the transmitted data, if no error occurs. The delay time between both sequences is recovered using two "Exclusive OR" gates. Both sequences are then compared to the transmitted data, and the outputs are fed to a "NOR" gate, which decides logic "0" if error is present, and logic "1" if no error is present. Finally, the output of the "NOR" gate is clocked through a flip-flop to increment a counter when error is present. The mechanism of the decision circuits for the transmission of random data is illustrated in Fig. 17b .

3.4.2 The D.P.S.K. Error Rate Model

Fig. 18 illustrates a flow diagram of the D.P.S.K. error rate model in which data is selected according to the polarity of a noise sample. The data is then differentially encoded to select one of two antipodal signals stored in memory. Similarly, another two D.P.S.K.

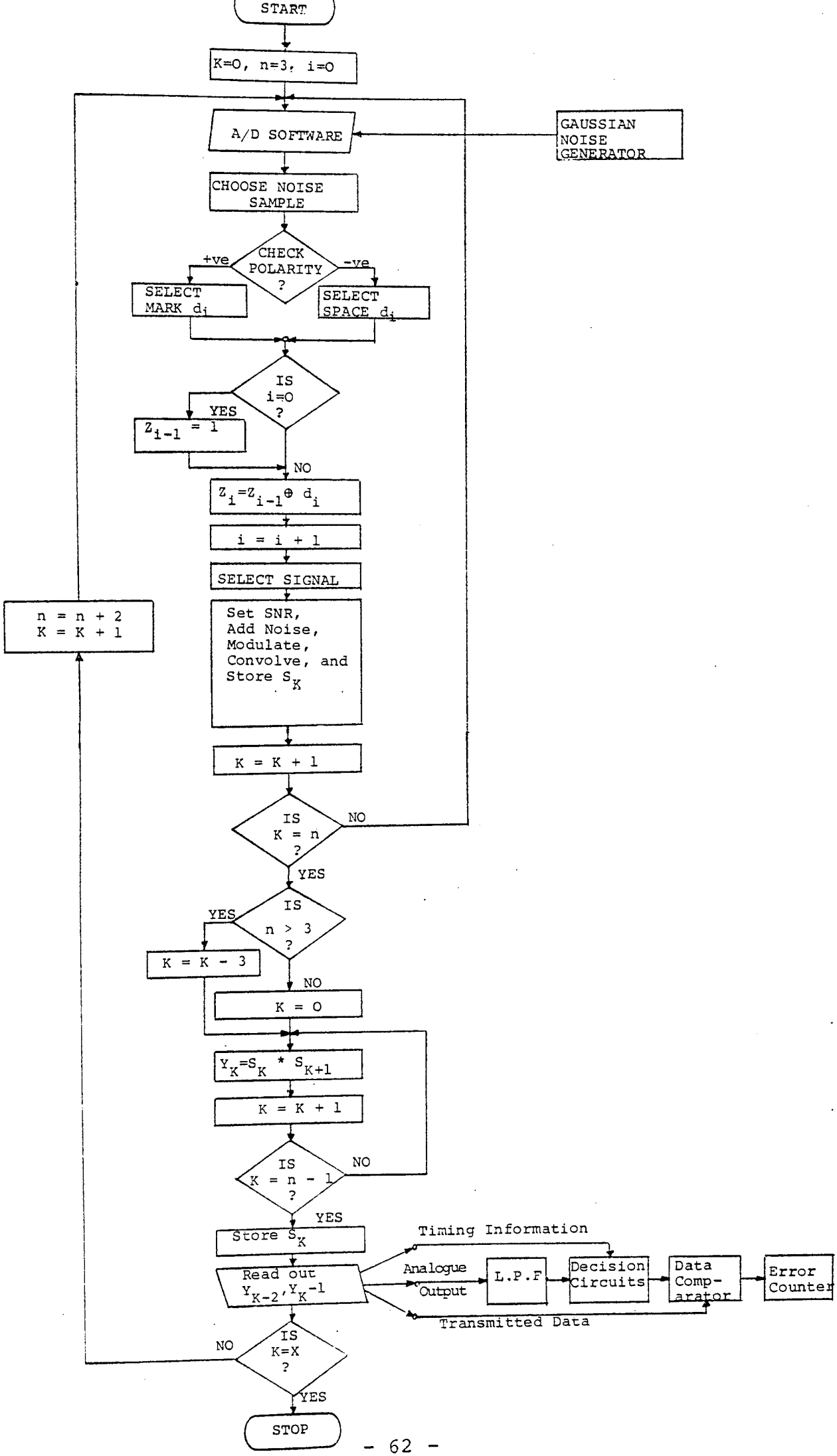

FIG. 18 D.P.S.K. ERROR RATE MODEL

signals are formed. After the SNR has been selected, each D.P.S.K. signal is added to noise and the resultant is modulated by, and then convolved with, the appropriate local and impulse response chirps respectively. The first signal output from the P.C.M.F. is compared with the second signal, and the second with the third, simulating the differential detector process. The third signal is stored to be used for comparison in the second round. Thus in each round, two signals are processed, the last signal of which is used for comparison in the next round. The two signals output from the comparator are read out sequentially into the D/A converter.

The analogue output of the D/A converter is low-pass filtered and then sent to the decision circuits to decide on the received binary bit. Timing information and the transmitted data are provided to drive the decision circuits, and the data comparator respectively.

3.4.2.1 Decision Circuits

The envelopes of the mark and space signals output from the low pass filter peak at the same instant of time, but have antipodean polarities depending whether a mark or a space is received. Hence, they are readily detected by sampling at the peaking instant, then decide logic "0", or logic "1" for negative, or positive polarity, respectively.

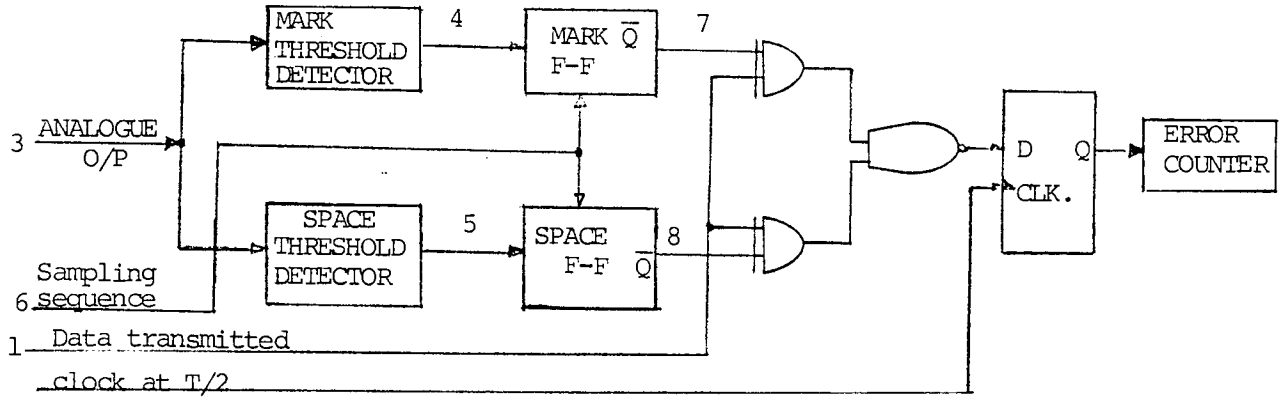

FIG. 19a DECISION CIRCUITS

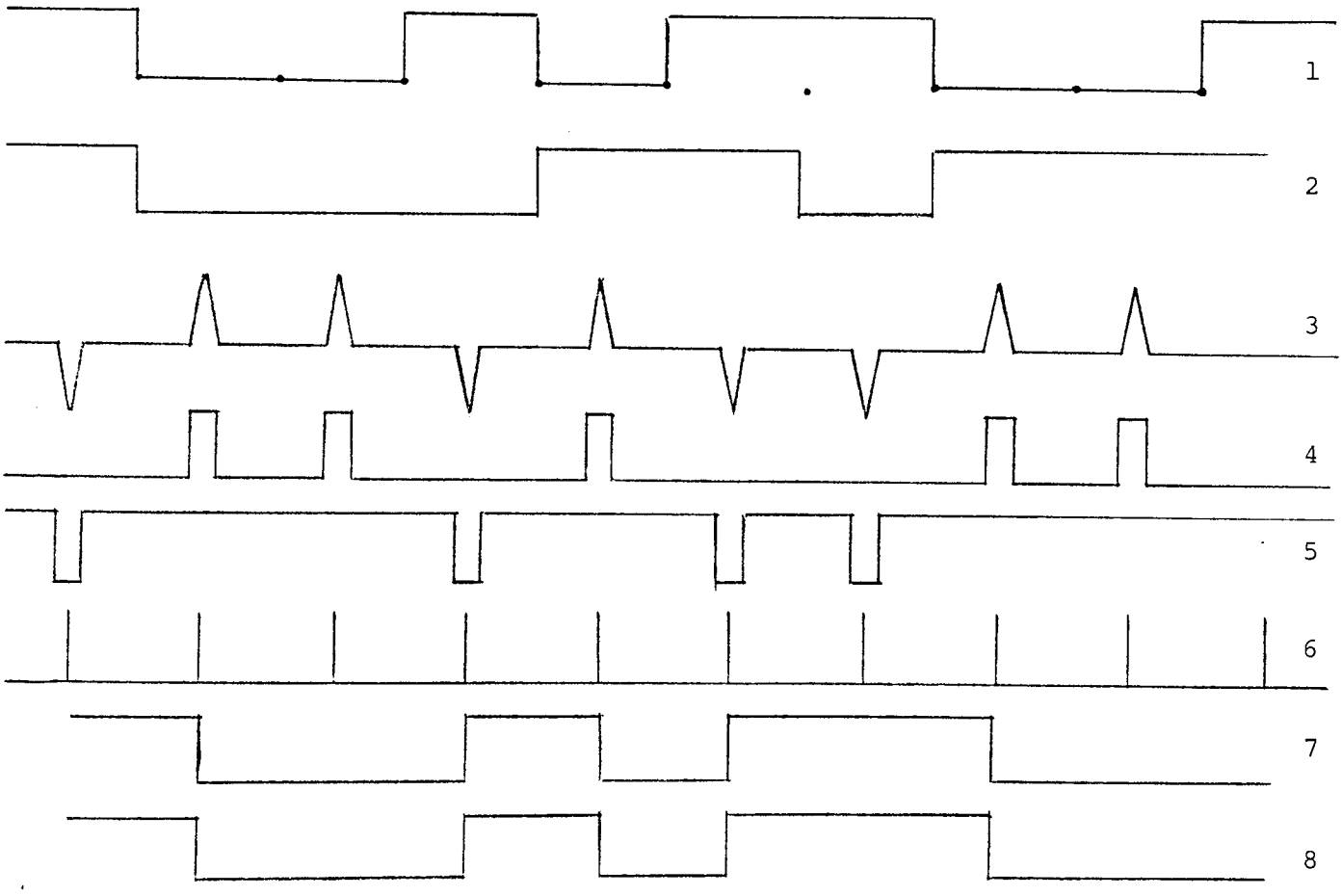

FIG. 19b MECHANISM OF DECISION CIRCUITS
TO DIFFERENTIALLY ENCODED DATA

Fig. 19a illustrates the decision circuits in which the output of the low pass filter is sent to a pair of threshold detectors, one detects the positive polarity signal, and the other detects the negative polarity signal. Both threshold levels are kept at 0 volt. The outputs of the detectors are sent to two flip-flops, together with the sampling sequence, to decide on the polarity of each. The inverted outputs of both flip-flops would give the same sequence if no error occurs in the transmitted data during transmission and/or processing.

The outputs of the flip-flops are compared with the transmitted data using two comparators. The compared sequences are then sent to a "NOR" gate which decides logic "0" for an error, and logic "1" for no error present. Finally, the output of the "NOR" gate is clocked through a flip-flop to increment a counter when error is present. The mechanism of the decision circuits for the transmission of random data is illustrated in Fig. 19b .

3.4.3 The Carrier Interference Model

Fig. 20 illustrates the carrier interference model which may be used in conjunction with the F.S.K. or D.P.S.K. error-rate models. Interfering signals are generated in digital form and stored in memory using the software signal-generator decribed earlier. Thus the amplitude, and frequency of interfering signals are specified in advance by the user of the error-rate models when these are operated in conjunction with the carrier

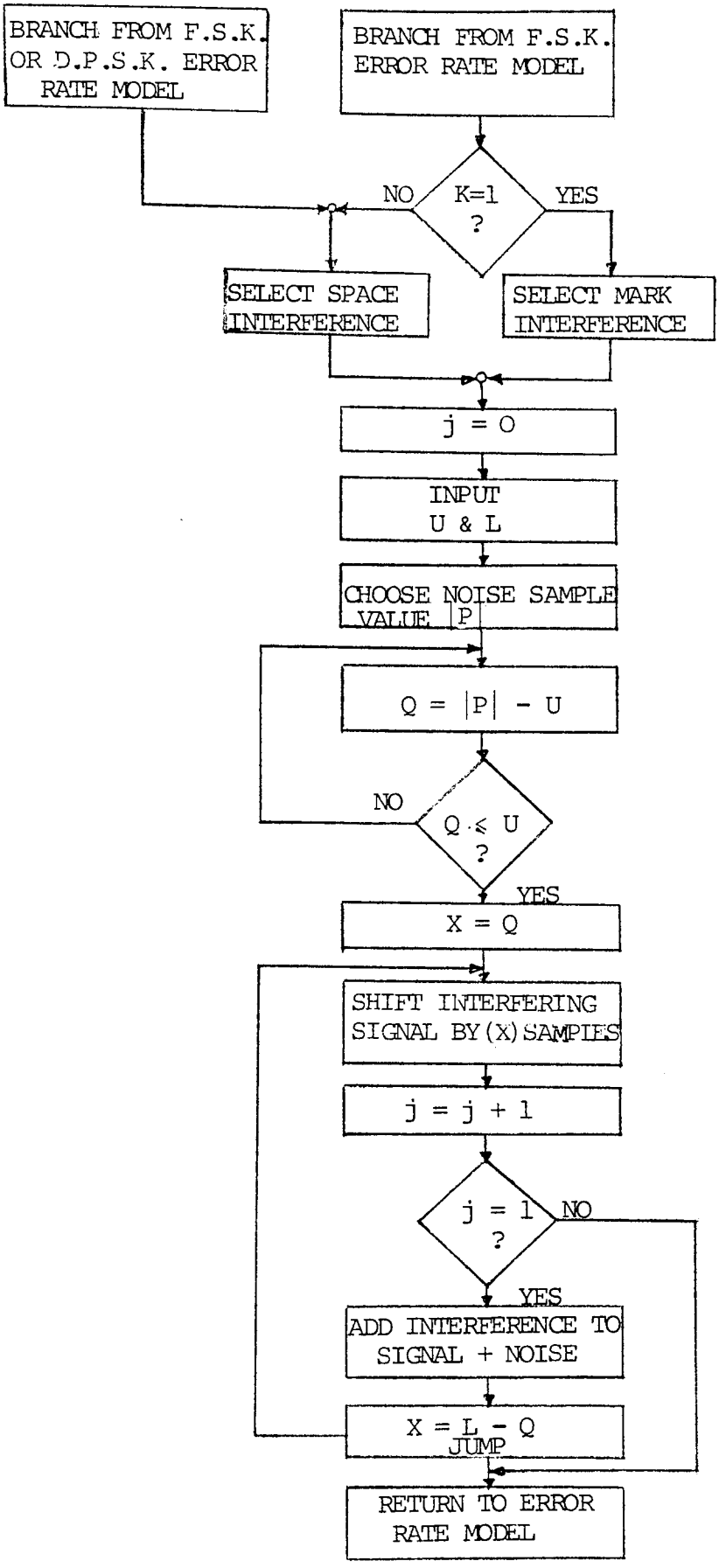

FIG. 20 CARRIER INTERFERENCE MODEL

interference model.

In operation, either a single interfering signal or two interfering signals are added to the noisy F.S.K. signal, whereas a single interfering signal is added to the noisy D.P.S.K. signal. The carrier interference model is thereby executed after the signal-plus-noise step in each error-rate model has been performed.

In each error-rate model, new noise samples are fetched into memory each time a new signal is selected. The value of a given noise sample (P) is used to implement a phase shift in the interfering signal. This phase shift may be expressed as

$$\theta_i = 2\pi \frac{Q}{U} \quad , \quad 0 \leq Q \leq U \qquad (3.8)$$

where Q is the number of samples shifted

U is the number of samples/cycle

The phase (θ_i) is implemented by shifting the interfering signal by (Q) samples with respect to the F.S.K. or D.P.S.K. signal transmitted. After the interfering signal has been added to signal plus noise, the phase shift (θ_i) is reset to zero in order to implement the next possible (θ_i) in the next round. However, the values of possible phase shifts are governed by the total number of samples (L) employed to represent the interfering signal. Thus, the number of possible values of (θ_i) increases by increasing the total number of samples (L).

CHAPTER FOUR

MEASUREMENTS AND EXPERIMENTAL RESULTS

4. MEASUREMENTS AND EXPERIMENTAL RESULTS

Both F.S.K. and D.P.S.K. detection schemes incorporate the mixer-P.C.M.F. compound as their predetector processor for optimizing their detection capabilities in a background of A.W.G.N. It is appropriate first to define the local chirp and the impulse response chirp parameters (i.e. define the mixer-P.C.M.F. compound) and, secondly, examine experimentally, then analyse, the tolerance of the output of the compound to practical imperfections and time delay. After the mixer-P.C.M.F. compound has been defined and analysed, then it can be incorporated in both F.S.K. and D.P.S.K. detection schemes to perform error-rate measurements, using the error-rate models developed in Chapter 3.

Employing the same mixer-P.C.M.F. compound in both detection schemes facilitates the comparison of their performancesin A.W.G.N., practical imperfections, time delay and carrier interference. However, the error-rate results established for each detection scheme will be discussed, and then compared with published error-rate results for conventional detection schemes.

4.1 THE MIXER-P.C.M.F. COMPOUND

To examine and analyse the compressed envelope at the output of the mixer-P.C.M.F. compound, the system of (Fig. 21) was assembled. This uses the signal-

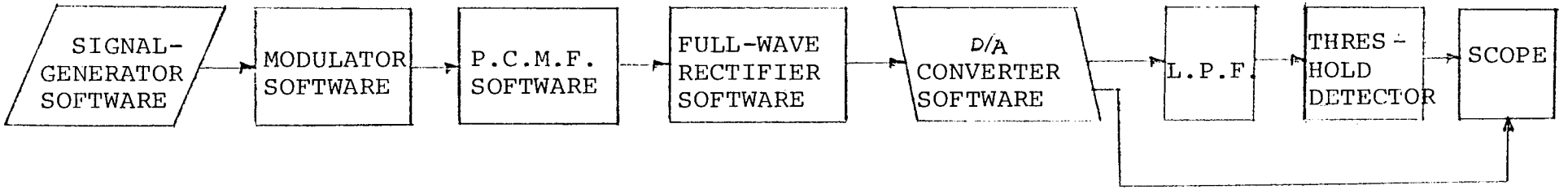

FIG. 21

EXPERIMENTAL SYSTEM FOR THE MIXER-P.C.M.F. COMPOUND

Parameters	Local Chirp	Impulse Response Chirp
B KHz	10	10
T msec.	2	2
f_1 KHz	15	3
f_2 KHz	25	13
f_o KHz	20	8

TABLE 1

PARAMETERS OF LOCAL CHIRP AND IMPULSE RESPONSE CHIRP

generator software, modulator software, P.C.M.F. software, full-wave rectifier software and the D/A converter software, which were described earlier in Chapter 3. The output of the D/A converter is low-pass filtered to remove the steps from the envelope of the compressed signal and then observed using an oscilloscope. The threshold detector is used when required, in order to measure the pulse-width of the compressed envelope.

The local chirp and the impulse response chirp signals were generated and stored in RAM using the signal-generator software. Parameters of both chirp signals are given in Table 1. These parameters are suitable for implementing the P.C.M.F. in hardware, using CCD technology (see Section 1.1.1).

To define the envelope of the compressed output of the P.C.M.F. with reasonable accuracy, L = 256 samples with 8-bit accuracy are used to represent each chirp signal. Consequently, the output compressed envelope of the P.C.M.F. has zero values outside $0 \leq t \leq (2L-1)\lambda$, where ($\lambda$) is the time taken by the processor to read out one sample from RAM into the D/A converter. The time taken by the TMS-9900 microprocessor (ψ) to execute each of its instructions is given by[41].

$$\psi = tc(C+W.M) \qquad (4.1)$$

where tc is the clock period

C number of clock cycles

W number of wait states

M memory access time

Four instructions are required in ordering the TMS-9900 microprocessor to read out samples from RAM into the D/A converter circuit after the start address (As) and the finish address (Af) have been loaded. These four instructions are as follows

```
┌→ MOV  move contents of As into D/A converter
│  INCT increment As
│  C    compare As and Af
│  JLE  jump if As ≤ Af
```

Each time the above loop is executed, one sample is read out from RAM into the D/A converter. Hence, making use of (4.1), λ = 17.316μsec.

Measurements were carried out by scanning the frequency spectrum of the P.C.M.F., using 256-samples sinewave generated by the signal-generator software used in the system of Fig. 21. The time-shift and the amplitude of the compressed envelope were measured for each frequency of the input sinewave. Fig. 22a shows the measured amplitude and the time-shift of the compressed envelope. This represents the envelope of the A.C.F. (see Section 2.1), where the maximum attainable amplitude is considered to occur at zero time shift, which corresponds to 12 KHz of the input sinewave. The ripple in the envelope of the A.C.F. is due to the relatively low

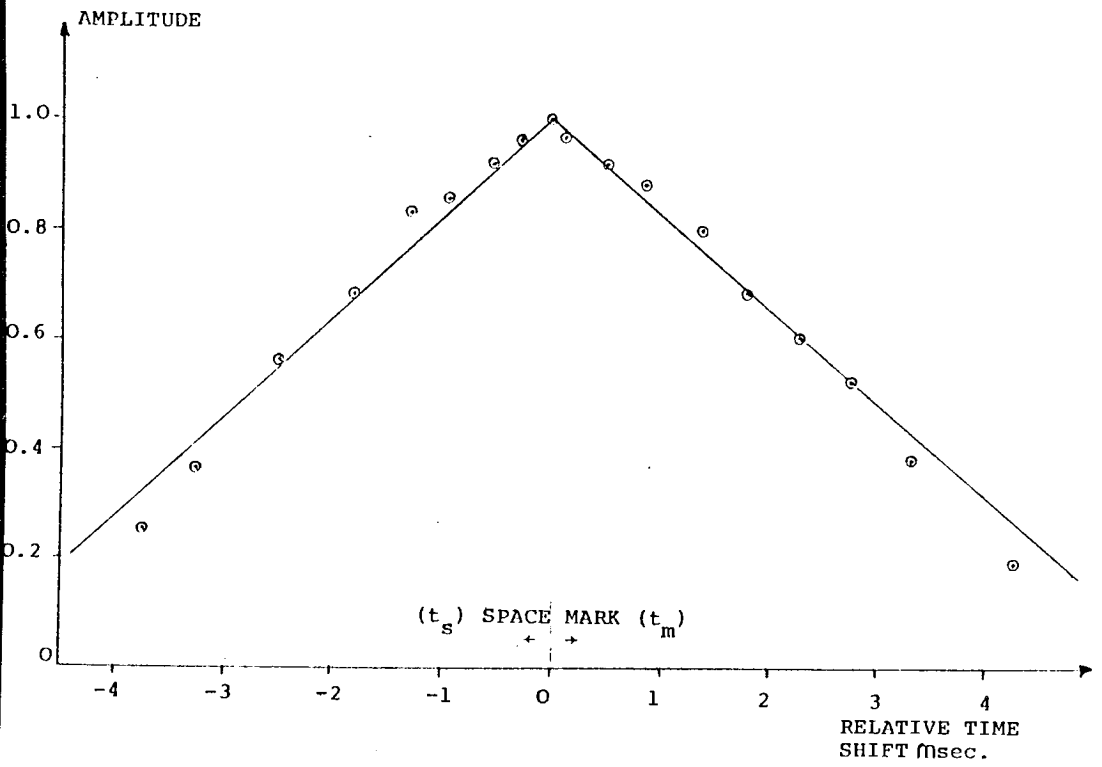

FIG. 22a

AMPLITUDE-TIME RELATIONSHIP

OF MIXER-P.C.M.F. COMPOUND

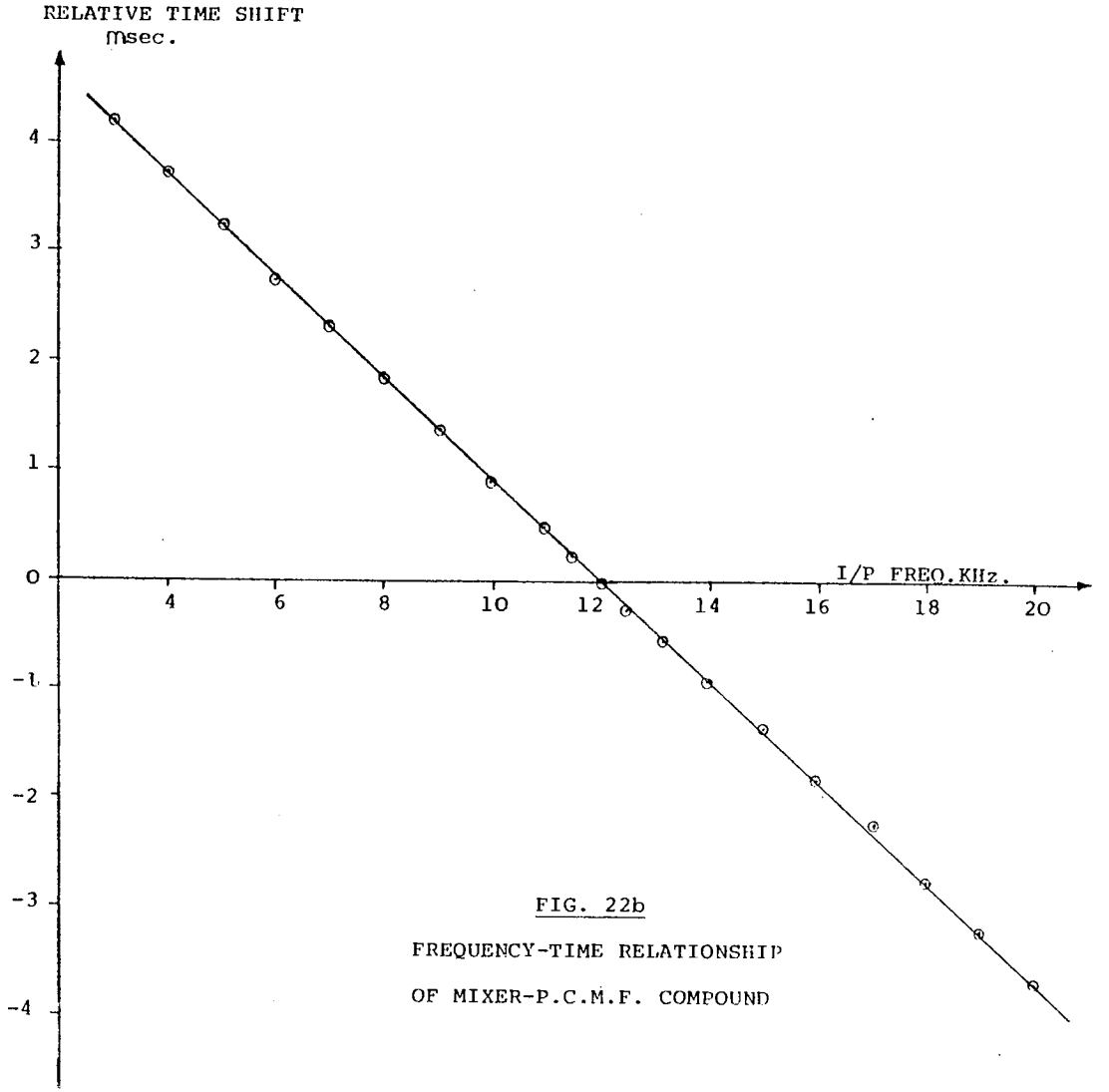

FIG. 22b

FREQUENCY-TIME RELATIONSHIP

OF MIXER-P.C.M.F. COMPOUND

time-bandwidth product used; the higher the time-bandwidth product of a chirp signal, the smaller are the oscillations in the envelope of its frequency spectrum[29],[34]. The frequency/time relationship of the mixer-P.C.M.F. compound is shown in Fig. 22b. This relationship shows the linearity that the compound enjoys, as well as the dependency of the position in time of the output envelope peak on the frequency of the input signal.

The frequency response of the P.C.M.F. is shown in the photograph, Fig. P1. This was produced by processing a chirp signal centred at 12 KHz by the mixer-P.C.M.F. compound of Fig. 21, which furnishes the frequency spectrum of its input signal. Fig. P2 shows the A.C.F. of the matched filter before and after filtering. This was produced by processing a single tone sinewave, at the centre frequency of the P.C.M.F., by the mixer-P.C.M.F. compound. In this case the P.C.M.F. is perfectly matched to its input chirp signal. The timing markers specify the output window of the P.C.M.F.. Fig. P3 shows the envelope of the A.C.F. This was produced by matching the P.C.M.F. to a single tone sinewave.

Thus, the mixer-P.C.M.F. compound is defined experimentally. However, an experimental evaluation of its tolerances to practical imperfections, and time delay now may be performed. These include the examination of the compressed envelope characteristics at the output of

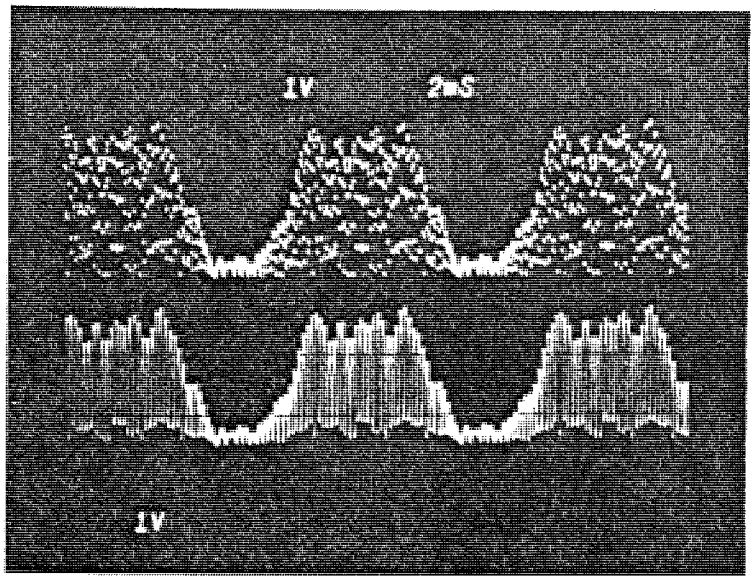

FIG. P1

THE FREQUENCY SPECTRUM OF THE P.C.M.F. BEFORE AND AFTER FILTERING

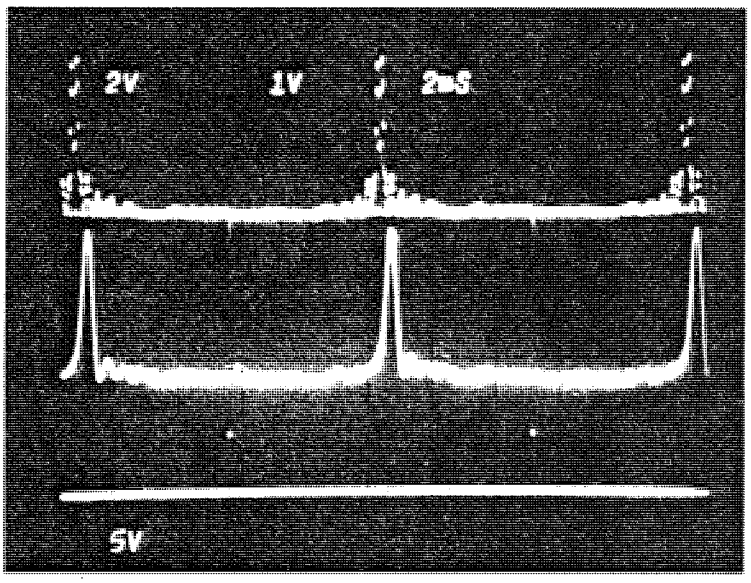

FIG. P2

THE ENVELOPE OF THE A.C.F. OF THE MATCHED FILTER FOR THE PERFECT MATCH STATE BEFORE AND AFTER FILTERING

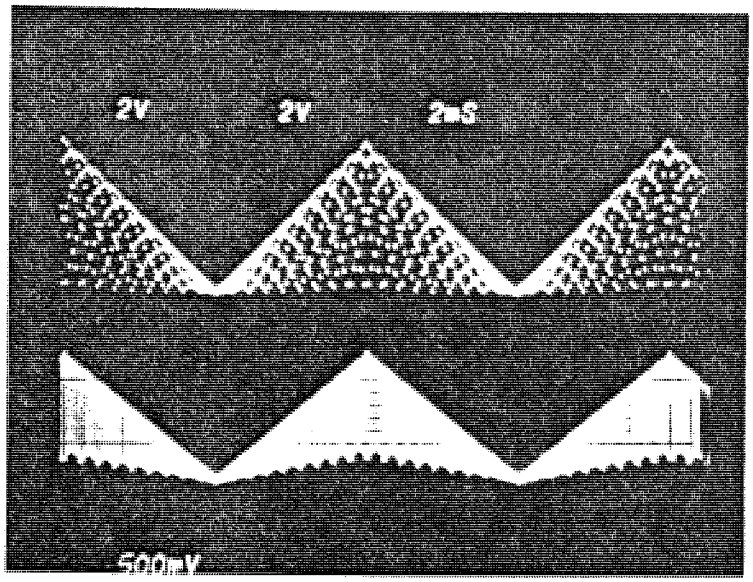

FIG. P3

THE ENVELOPE OF THE A.C.F. BEFORE AND AFTER FILTERING

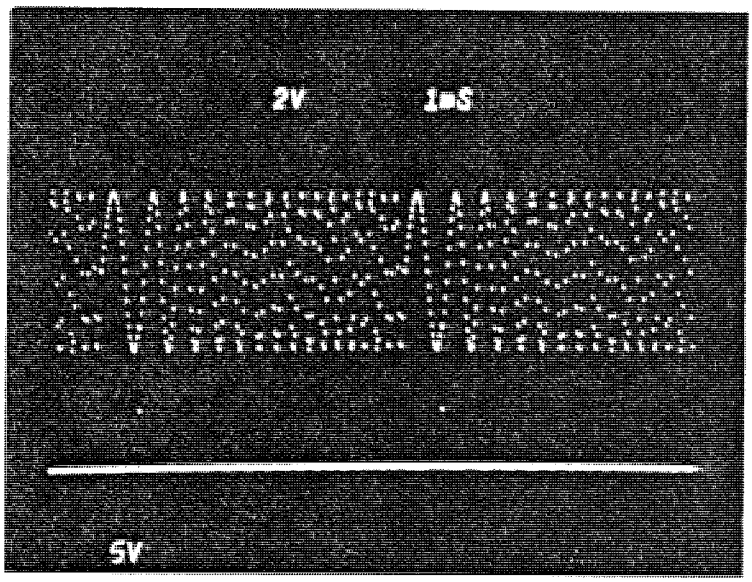

FIG. P4

LOCAL CHIRP SIGNAL DELAYED BY SEVERAL SAMPLES FROM SIGNAL ARRIVAL TIME

the P.C.M.F., in the presence of practical imperfections and time delay.

4.1.1 Practical Imperfections

The compressed envelope at the output of the mixer-P.C.M.F. compound carries the vital information about the incoming signal by its amplitude, peaking instant, and pulse width. Hence, measurements were carried out, using the system of Fig. 21, to find the effects produced by non-linearity and slope mismatch of the P.C.M.F., and frequency drift of the local chirp signal on the compressed envelope characteristics.

Non-linearity, slope mismatch, and frequency drift were implemented (see Section 2.2.3) by adding a third term to the argument of the impulse response chirp, varying the duration of the impulse response chirp, and varying the centre frequency of the local chirp respectively. The normalized amplitude, time shift, and pulse width are plotted respectively, against percentage non-linearity $\delta\%$, percentage frequency drift $\frac{\delta f}{B}\%$, and slope mismatch factor D%. Fig. 23a, Fig. 23b, and Fig. 23c show respectively, the effects produced by practical imperfections on the amplitude, the peaking instant, and the pulse width of the compressed envelope. The amplitude, the peaking instant, and the pulse width (measured at 3 dB below the peak value) are all measured with reference to the characteristics of the compressed envelope at the state

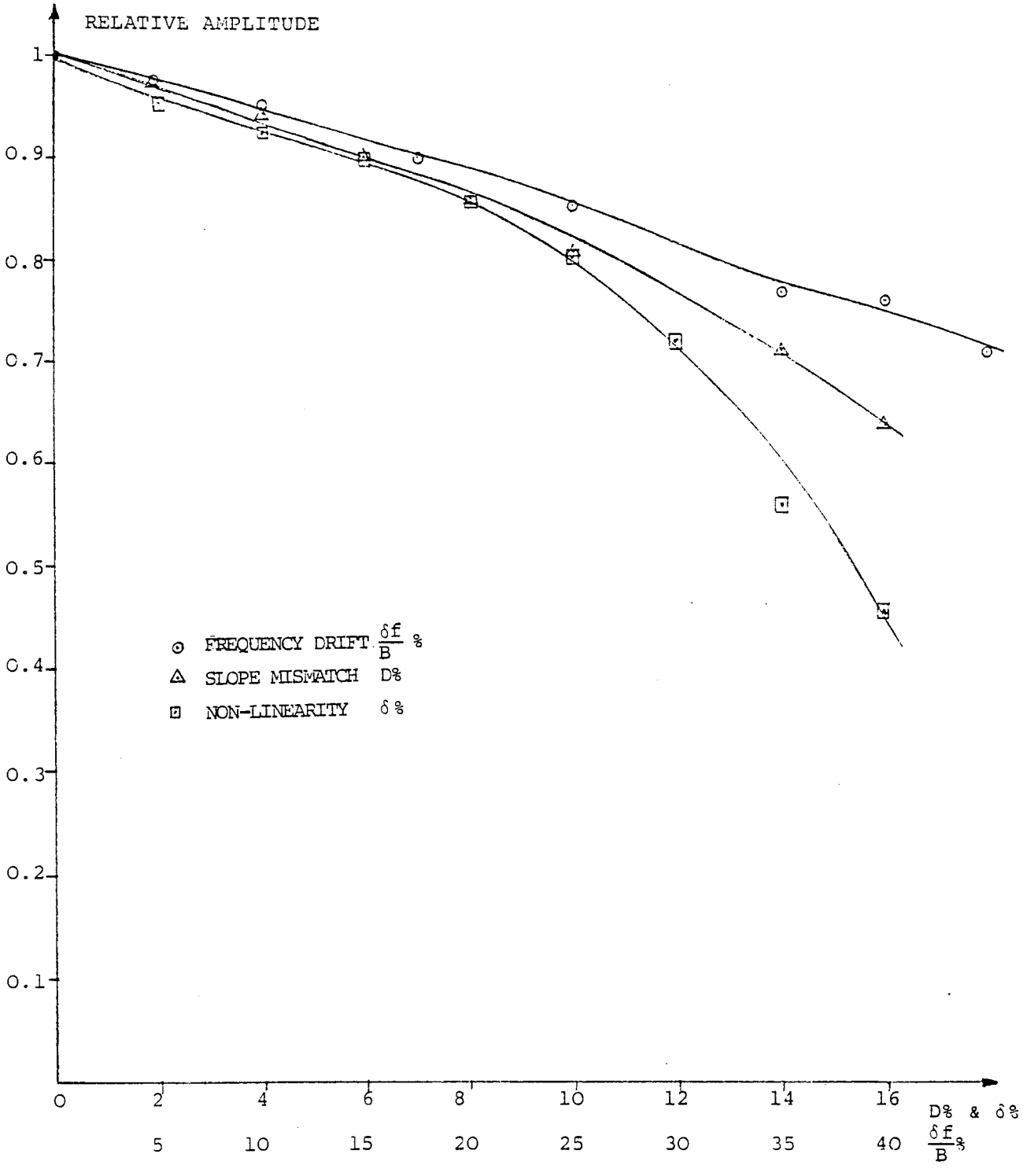

FIG. 23a

EFFECTS OF PRACTICAL IMPERFECTIONS ON AMPLITUDE OF THE COMPRESSED ENVELOPE

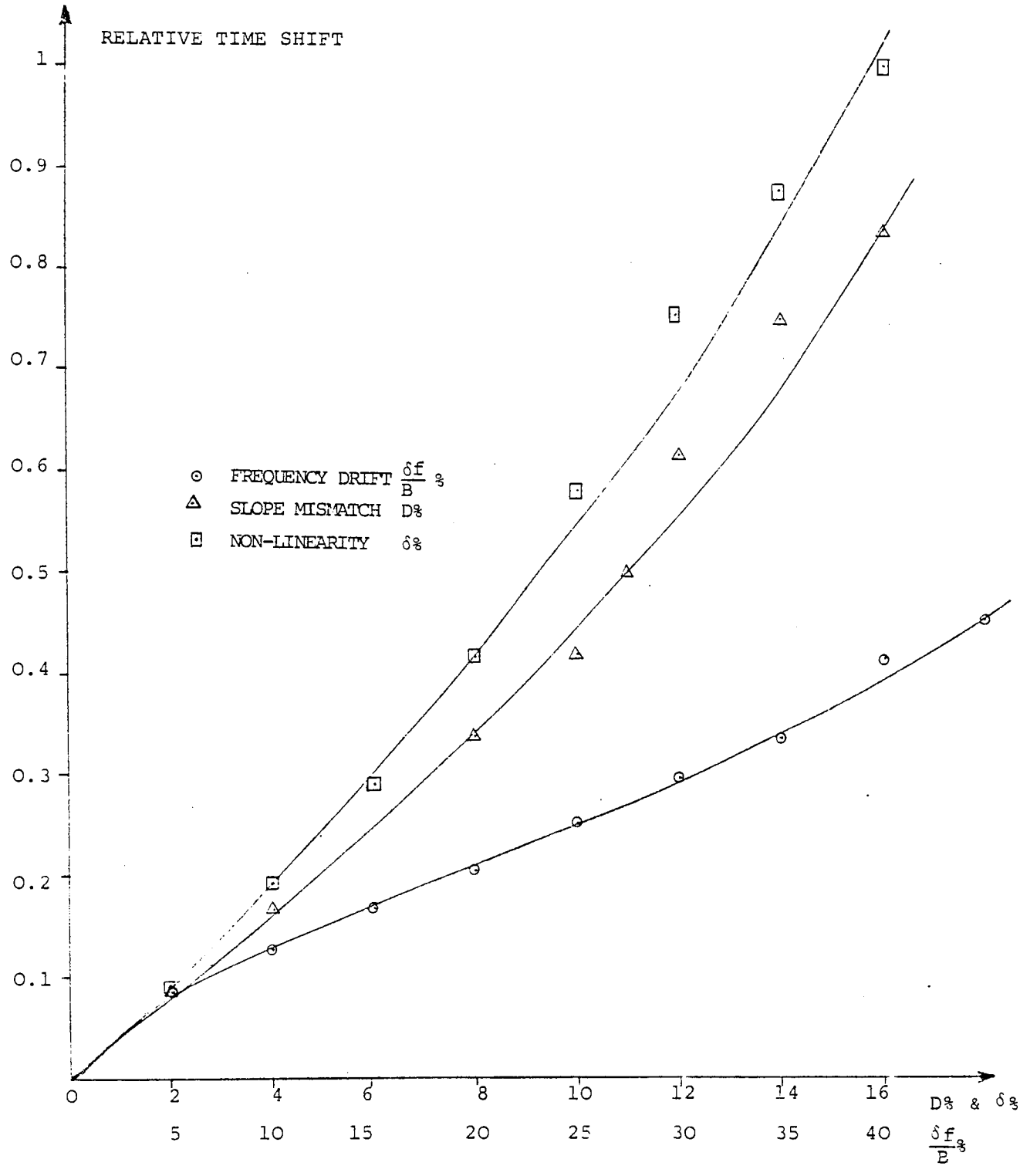

FIG. 23b

EFFECTS OF PRACTICAL IMPERFECTIONS ON TIME SHIFT OF THE COMPRESSED ENVELOPE

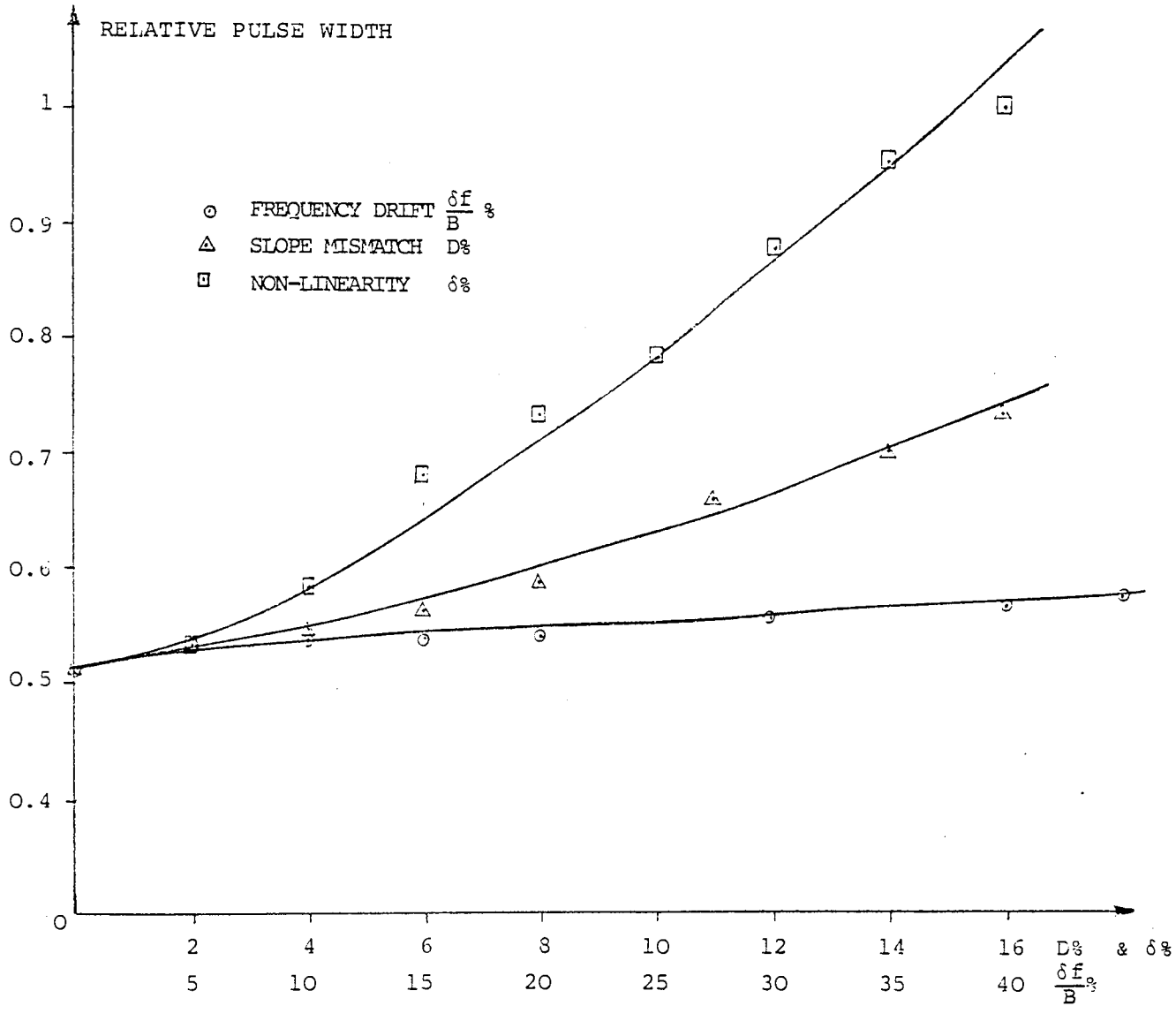

FIG. 23c

EFFECTS OF PRACTICAL IMPERFECTIONS ON PULSE WIDTH OF THE COMPRESSED ENVELOPE

of perfect match.

Results indicate that non-linearity of the P.C.M.F. produces the most damaging effects on the characteristics of the compressed envelope. This is because the mixer-P.C.M.F. compound is a linear system. However, it may be expected at this stage that the presence of non-linearity would produce higher error-rates when the compound is incorporated in the F.S.K. and D.P.S.K. detection schemes later.

Furthermore, these results offer maximum values of non-linearity, slope mismatch, and frequency drift that the mixer-P.C.M.F. compound can tolerate. Thus, an upper limit is specified for each type of imperfection, above which error-rate measurements in the presence of practical imperfections are not practicable.

4.1.2 Time Delay

Time delay between the local chirp signal and the received signal by the mixer-P.C.M.F. compound prevents the local chirp signal from accommodating one complete received signal. As was anticipated in Chapter 2, this causes deterioration of the performance of the compound by deviating the compressed envelope from its ideal characteristics.

Measurements were conducted to find the effects produced by time delay on the output of the compound, using the system

of Fig. 21. The amplitude, peaking instant, and pulse width were measured, while varying the time delay between the local chirp signal and the received signal. Time delay was implmented by shifting the samples of the local chirp stored in RAM. Fig. P4 shows the local chirp signal delayed by several samples from the signal arrival time, which is specified by timing markers.

Fig. 24 illustrates the deviation of the compressed envelope characteristics from the ideal characteristics as a function of the number of samples delayed. The actual time delay may be calculated by multiplying the number of samples delayed by the time the processor takes to read out one sample from RAM into the D/A converter (i.e. λ = 17.316μsec.).

The above results are meant to serve as guidelines to perform error-rate measurements for both F.S.K. and D.P.S.K. detection schemes in the presence of time delay.

4.2 THE F.S.K. SYSTEM

After the mixer-P.C.M.F. compound has been defined and its tolerances to practical imperfections and time delay have been found, it may be incorporated with an envelope detector, a low pass filter, and the decision circuits, described in Section 3.4.1.1, to form the F.S.K. detection scheme.

A pair of F.S.K. signals were generated, and stored

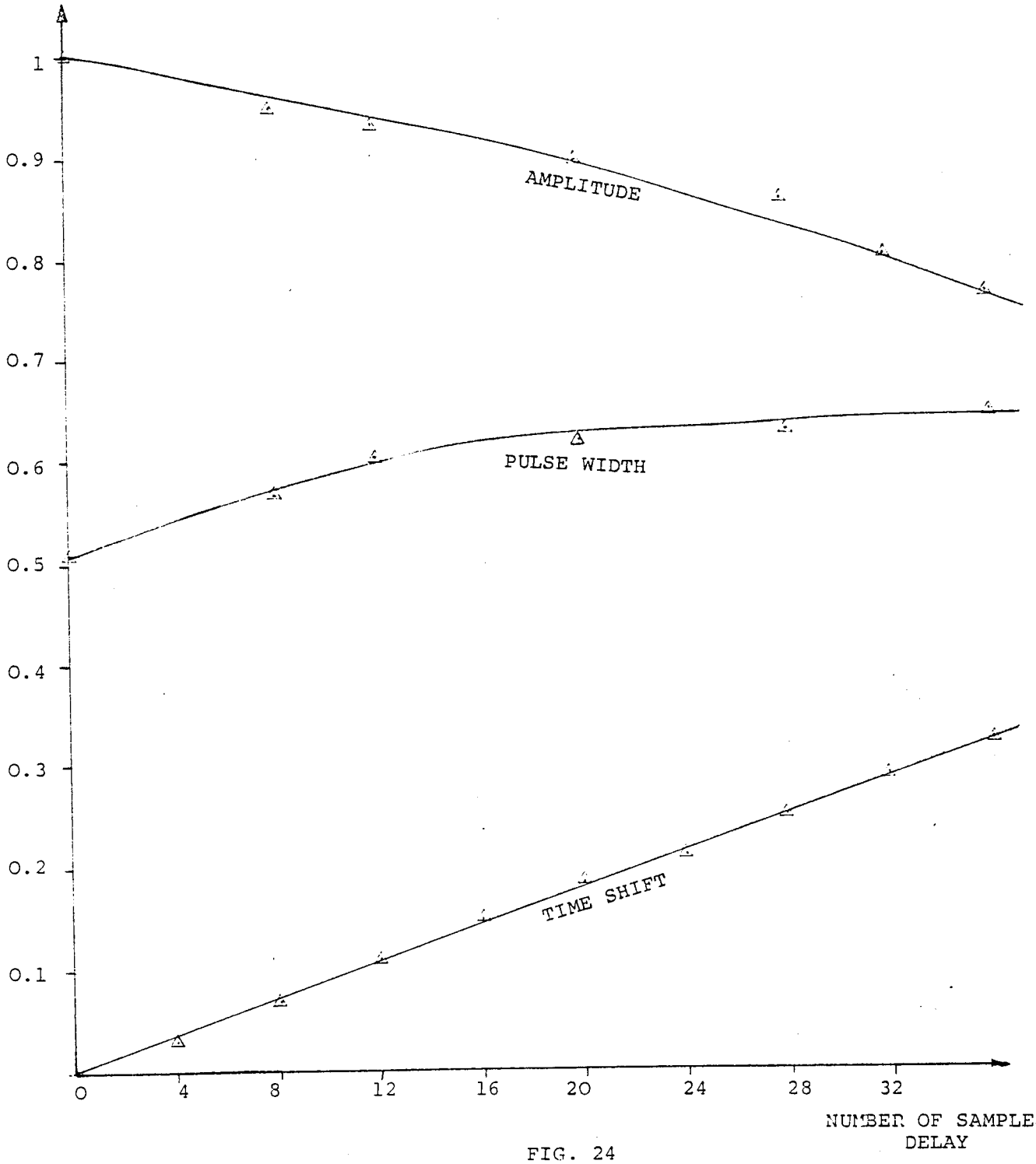

FIG. 24

EFFECTS OF TIME DELAY ON THE COMPRESSED ENVELOPE CHARACTERISTICS

in RAM. Each F.S.K. signal is 2 msec. long, and digitized into 256 samples with an 8-bit accuracy. The mark frequency is 11 KHz, whereas the space frequency is 13 KHz, giving a modulation index of (h=4). Thus the F.S.K. signal is centred at 12 KHz, which if mixed with the centre frequency of the local chirp signal (i.e. 20 KHz), would result to a difference frequency of 8 KHz, which is the centre frequency of the P.C.M.F.

4.2.1 Error-rate Measurements

Error-rate measurements for the F.S.K. detection scheme were conducted in the presence of A.W.G.N., by running the F.S.K. error-rate model described in Section 3.4.1 for different input SNR's. The same r.m.s. values of noise and signal are stored in RAM. Different SNR's are set by dividing the signal for input SNR's < 0 dB and dividing the noise for input SNR's > 0 dB. 256 samples of noise are fetched into RAM each time an F.S.K. signal is selected, as was described previously. The probability of error was estimated for different SNR's by comparing the recovered data with the transmitted data pattern and counting the errors due to noise. Fig. P5 shows the output compressed envelope of the P.C.M.F. for a received F.S.K. signal before and after filtering. The time shift due to an alternate mark-space F.S.K. signal can be observed by looking at the timing markers, which represent the output window of the P.C.M.F.. Fig. P6 shows the output of the threshold

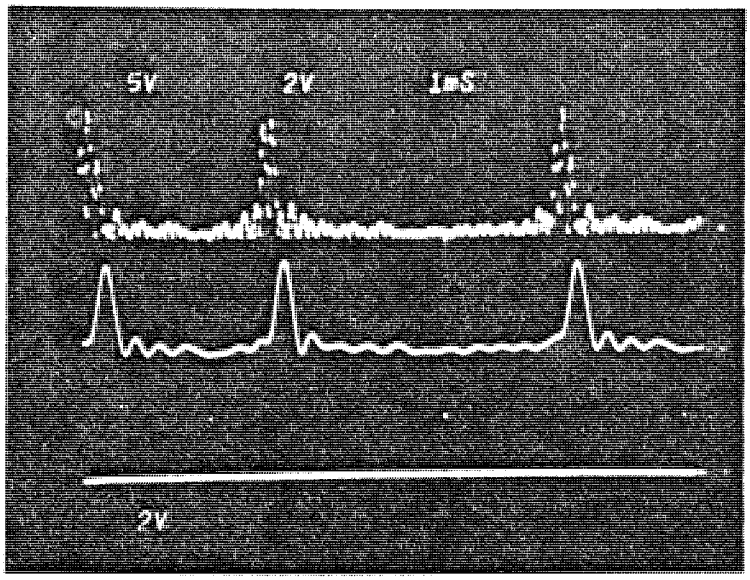

FIG. P5

THE COMPRESSED OUTPUT ENVELOPE FOR A RECEIVED F.S.K. SIGNAL BEFORE AND AFTER FILTERING

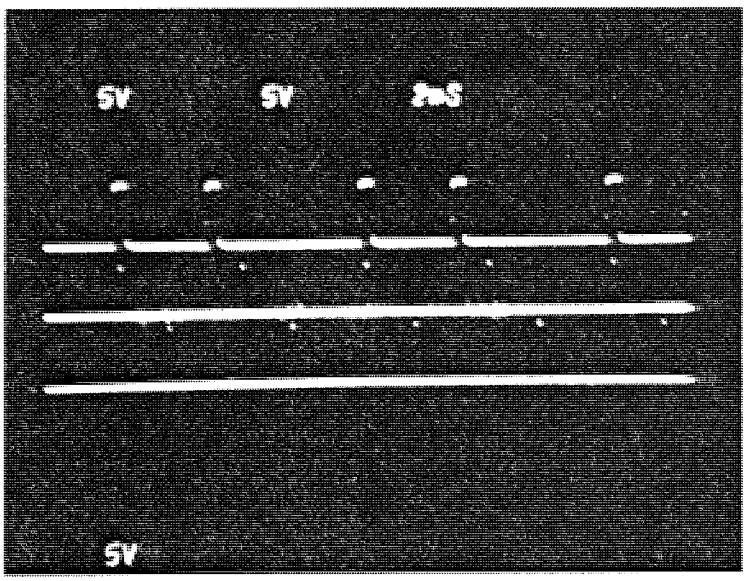

FIG. P6

THE OUTPUT OF THRESHOLD DETECTOR FOR RECEIVED F.S.K. SIGNAL AND SAMPLING SEQUENCES

detector, together with one of the sampling sequences and the output window of the P.C.M.F.

The noise added to the signal adds random processes to the frequency spectrum of the signal furnished by the mixer-P.C.M.F. coumpound. Hence, noise is expected to introduce two different types of errors on the output compressed envelope. These are as follows:

(a) Signal Blocking

The presence of a noise component of the same frequency, opposite phase, and opposite amplitude to that of the signal would block the signal from appearing at the output of the P.C.M.F. Consequently, an error occurs due to the absence of signal.

(b) False Signal

Sampling of the output of the threshold detector is performed at two different times (i.e. mark time, tm, and the space time, ts, of 2.10). Consequently, the presence of a noise component, say, at the space frequency when a mark is received, and vice versa, would introduce a false signal in either the mark or space decision circuit. However, this type of error can only occur when the false signal due to noise appears above the threshold level, which is set at 3 dB below the peak signal output from the P.C.M.F.

Extensive runs of the F.S.K. error-rate model were performed to compute the final estimate of the probability

of error for each input SNR. The performance of the F.S.K. detection scheme by pulse compression was found by counting 1000-errors for low SNR's (i.e. - 6 dB to 2dB), and counting 500-errors for higher SNR's (i.e. 3 dB- 14 dB). Moreover, error counts, when repeated gave different (Pe) for the same input SNR. These were averaged to arrive at the final estimate of (Pe) for each SNR. Fig. 25 shows the experimental error-rate results plotted together with the theoretical error-rate calculated using (3.7) for an F.S.K.matched filter receiver (i.e. optimum for a pair of orthogonal F.S.K. signals in the presence of A.W.G.N). Experimental results indicate that the performance of the F.S.K. detection scheme is approximately (1.5 dB) below optimum for practical probabilities of error (i.e. $Pe \leqslant 10^{-2}$). For the range of errors investigated, the F.S.K. detection scheme performance may be considered acceptable. This will be confirmed when the obtained performance is compared with conventional F.S.K. detection schemes performances later.

In an attempt to improve the performance of the F.S.K. detection scheme in A.W.G.N., time weighting of the impulse response of the P.C.M.F. was employed. Weighting reduces the sidelobes of the compressed envelope at the output of the P.C.M.F.[14]-[16]. Consequently, the interfering effects between adjacent signals are reduced. Weighting also reduces the

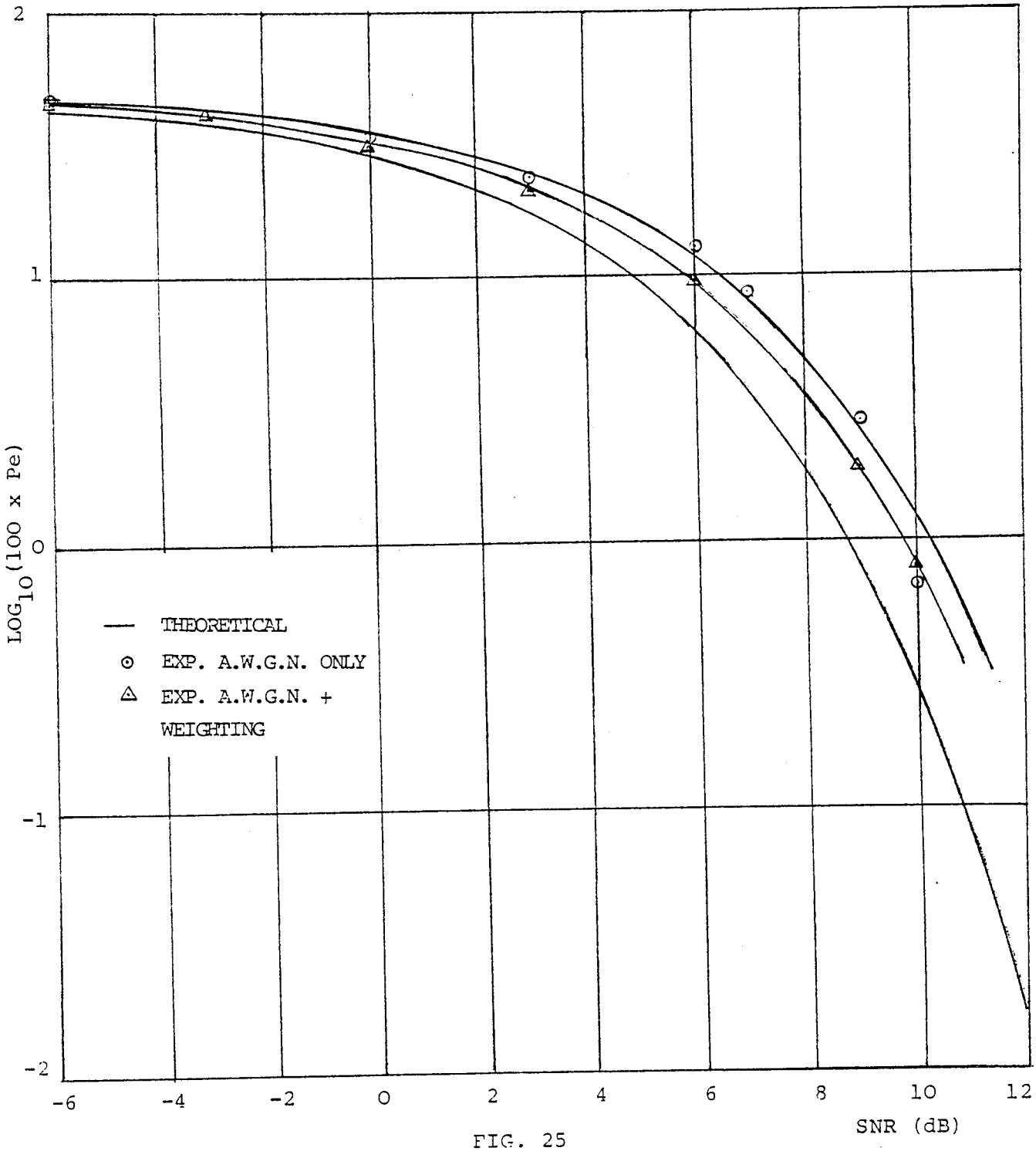

FIG. 25

ERROR-RATES OF F.S.K. DETECTION SCHEME IN THE PRESENCE OF A.W.G.N.

possibility of false signal occurring, since noise and sidelobes may enhance each other to cause an error due to false signal. However, weighting has its own effects on the compressed envelope main lobe, for example, pulse width widening, amplitdue reduction, and mismatch[16]. Nevertheless, error-rate measurements were conducted after weighting the impulse response chirp, using the following weighting function[16].

$$W(t) = z + (1-z)\cos^2\frac{\pi t}{T}, \quad |t| \leq \frac{T}{2} \qquad (4.2)$$

where $z = 0.08$, for Hamming

The above function was multiplied by the impulse response chirp to form the weighted impulse response, then fed to RAM, using the software signal-generator of Fig. 10. The weighted impulse response, together with the frequency spectrum of the P.C.M.F., are shown in Fig. P7. The frequency spectrum of the P.C.M.F. was produced using the system of Fig. 21. Comparing the spectra of the P.C.M.F. before weighting (Fig. P1), and after weighting (Fig. P7), it is clear that the ripple in the envelope of the frequency spectrum is reduced by weighting. Nevertheless, error-rate results show that weighting has improved the performance of the F.S.K. detection scheme in A.W.G.N. A 0.5 dB in SNR, at $Pe \leq 10^{-2}$, is the improvement obtained by weighting, as is shown in Fig. 25. At higher Pe (i.e. lower SNR's)

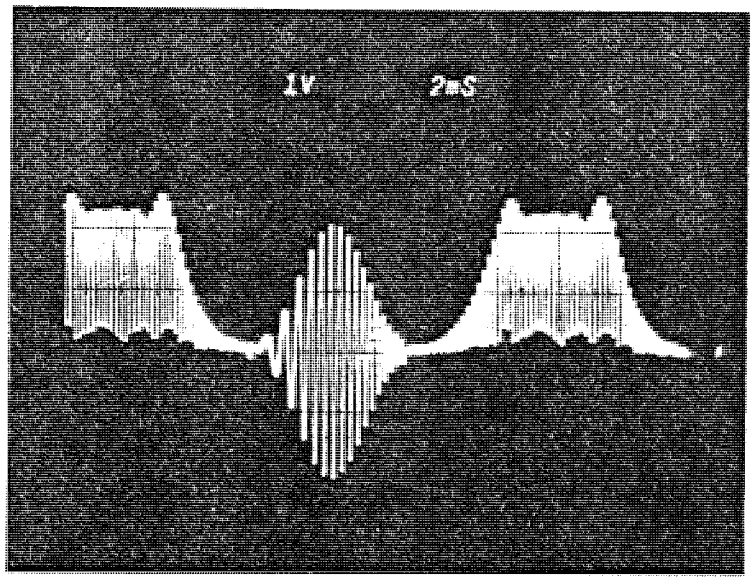

FIG. P7

WEIGHTED IMPULSE RESPONSE CHIRP AND FREQUENCY SPECTRUM OF P.C.M.F.

the improvement is slightly more than 0.5 dB. This confirms the effectiveness of weighting in reducing the number of errors due to A.W.G.N.

4.2.1.1 Practical Imperfections

Using the same definitions used before for non-linearity, slope mismatch and frequency drift, error-rate measurements were conducted in the presence of each type of imperfection, and A.W.G.N. for different SNR's.

Fig. 26a, Fig. 26b, and Fig. 26c show the obtained error-rate results in the presence of non-linearity, slope mismatch, and frequency drift respectively. Results indicate that the F.S.K. detection scheme tolerates frequency drift of the local chirp, and slope mismatch of the P.C.M.F. more than non-linearity. This is expected, since the compressed envelope characteristics at the output of the P.C.M.F. are degraded most in the presence of non-linearity, as was shown previously. Degradations in the performance of the F.S.K. detection scheme due to each type of imperfection may be found from the graphs provided by comparing them with the performance in A.W.G.N. only. However, for practical probabilities of error, the worst degradations in performance are 3 dB for 12% non-linearity, 1.8 dB for 45% frequency drift, and 1.5 dB for 12% slope mismatch.

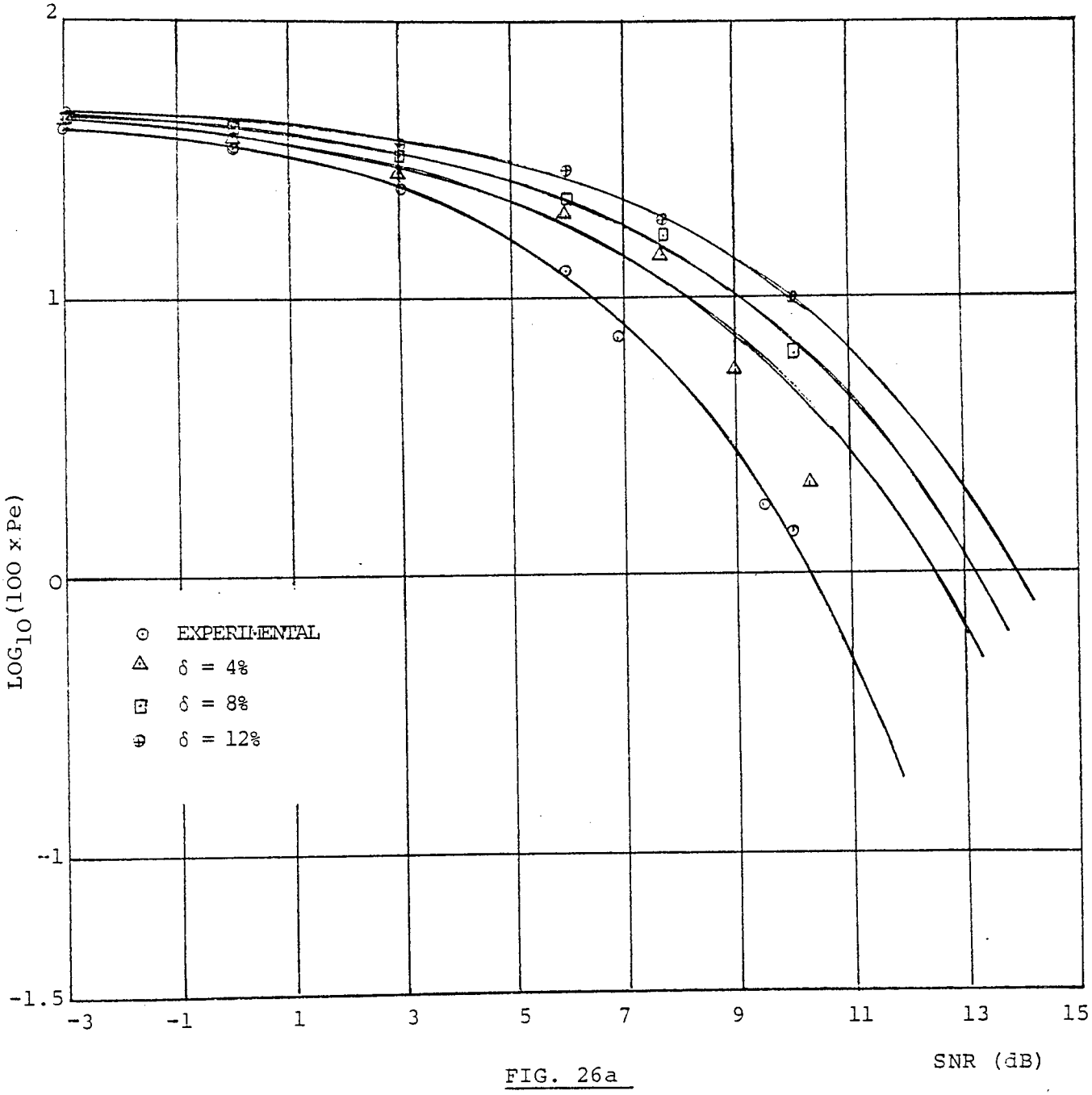

FIG. 26a

ERROR-RATES OF F.S.K. DETECTION SCHEME IN THE PRESENCE OF NON-LINEARITY

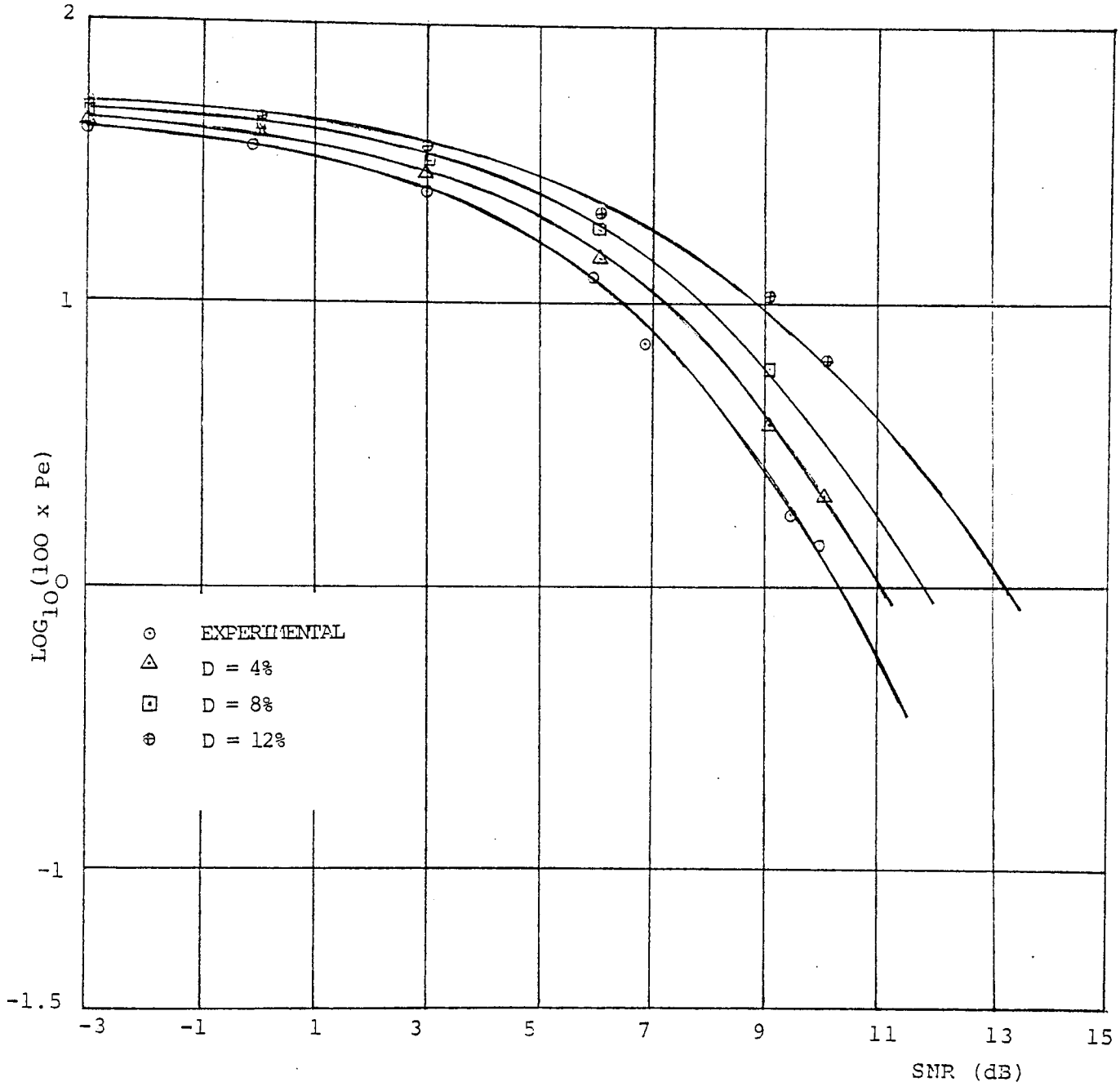

FIG. 26b

ERROR-RATES OF F.S.K. DETECTION SCHEME IN THE PRESENCE OF SLOPE MISMATCH

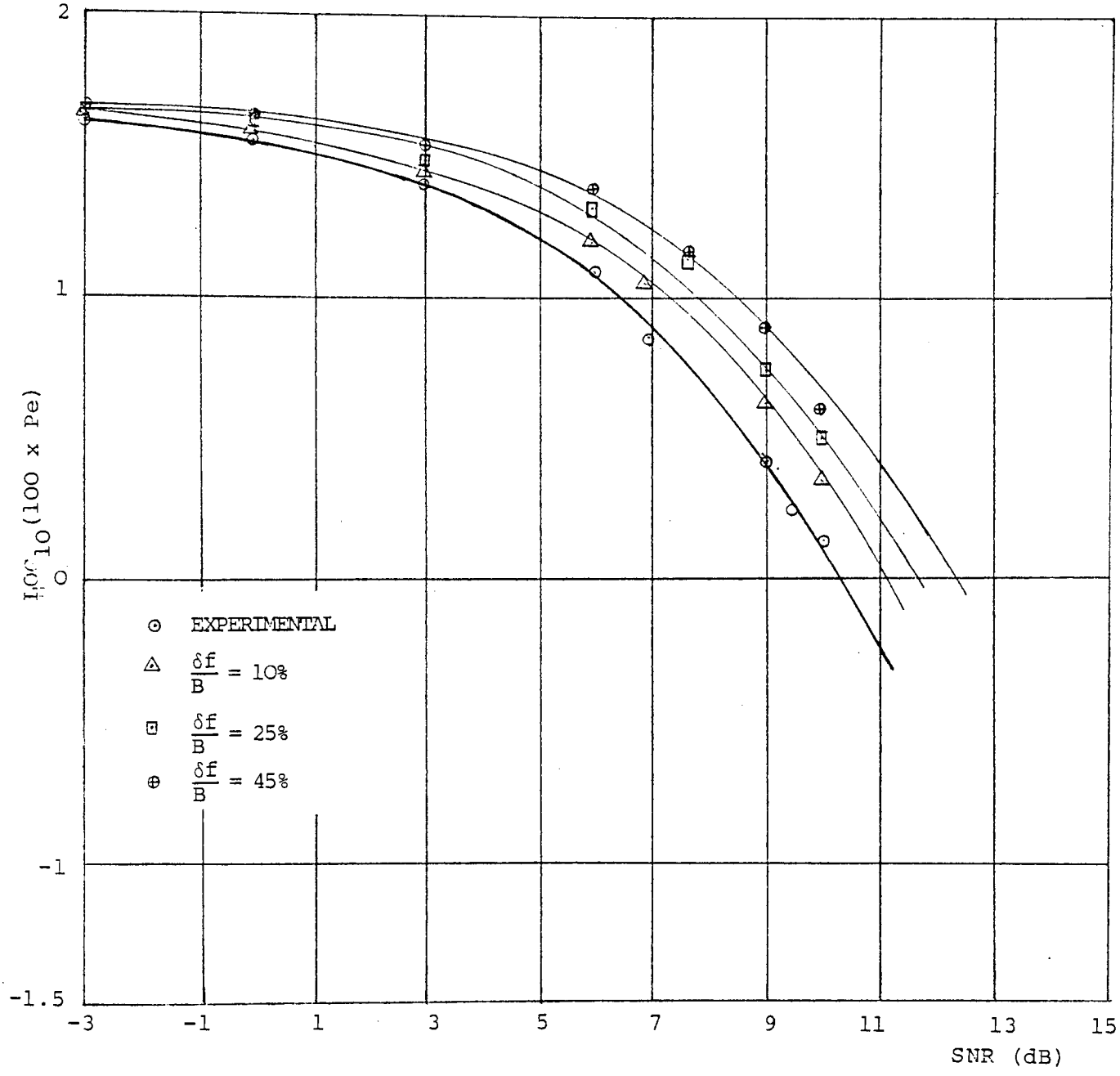

FIG. 26c

ERROR-RATES OF F.S.K. DETECTION SCHEME IN THE PRESENCE OF FREQUENCY DRIFT

4.2.1.2 Time Delay

Error-rate measurements in the presence of A.W.G.N. and different time delays of the local chirp signal were conducted. The values of time delays used, are selected in the light of the results obtained earlier concerning the degradations of the compressed envelope characteristics in the presence of time delay.

Fig. 27 shows the error-rate results obtained for different time delays, plotted together with the experimental performance of the F.S.K. detection scheme in A.W.G.N. It was observed during error-rate measurements that errors due to time delay tended to occur as a result of time-shift of the compressed envelope, which led to inaccurate sampling. However, results indicate that 12-samples delay (i.e. $\Delta = 0.46875T$) of the local chirp signal degrades the performance by 2 dB for $Pe \leq 10^{-2}$. This result highlights the considerably high tolerance of the F.S.K. detection scheme to time delay.

4.2.1.3 Carrier Interference

The carrier interference model of Fig. 20 was used in conjunction with the F.S.K. error-rate model, to perform error-rate measurements in the presence of both A.W.G.N. and additive carrier interference. Single interfering signal and two-tone interferers, at the transmitted mark and space frequencies of the F.S.K.

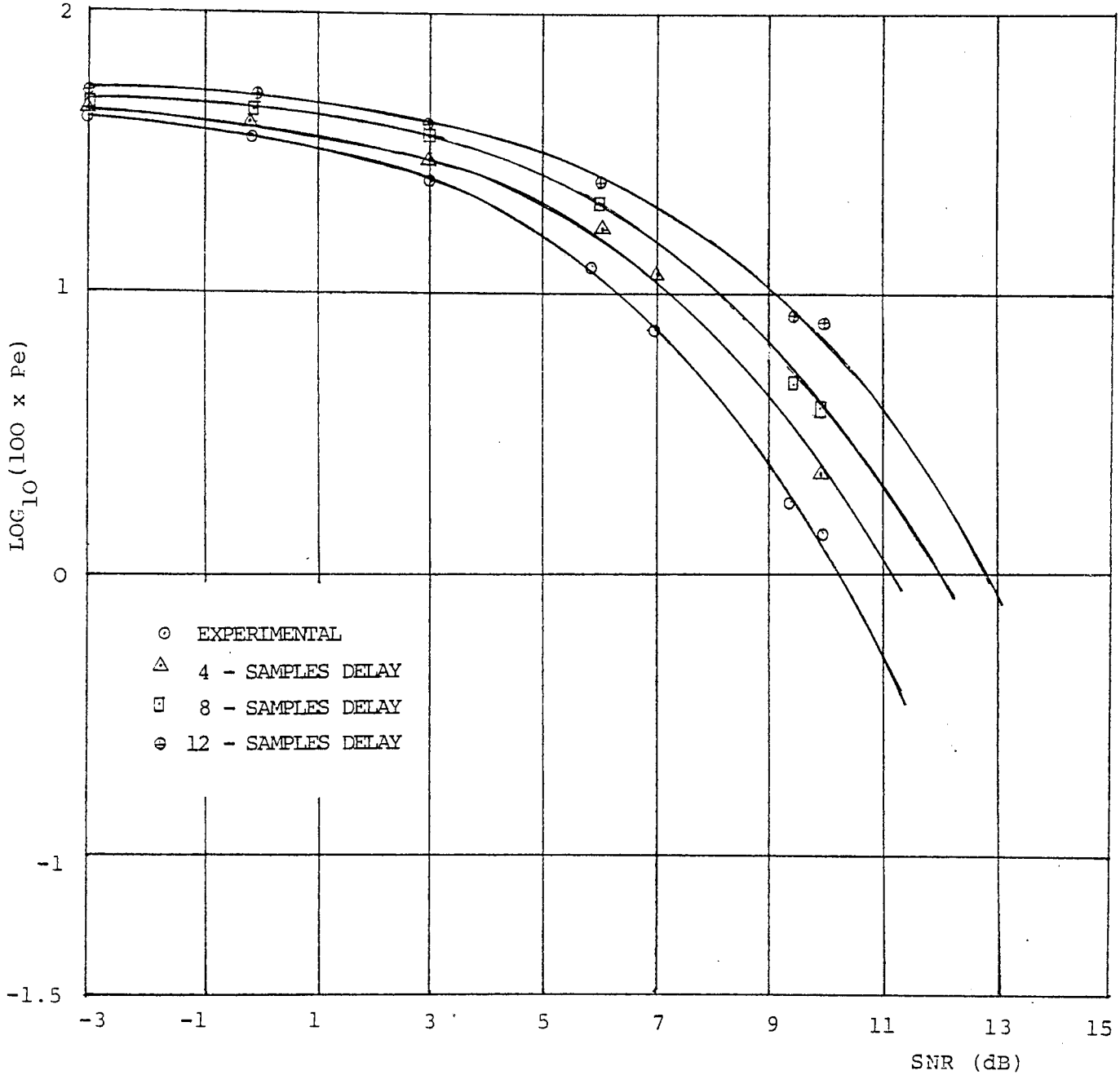

FIG. 27

ERROR-RATES OF F.S.K. DETECTION SCHEME IN THE PRESENCE OF TIME DELAY

signal,were investigated. Prior to conducting error-rate measurements, interfering signals were generated and fed to RAM each time a new CSR is required, using the signal-generator software.

Since the phase of the interfering signal depends on the polarity of a given noise sample (see Section 3.4.3), then the worst case that may happen, is when a noise component enhances a destructive interfering signal (i.e. when the interfering signal, and the wanted signal are opposite in phase). However, the other extreme is when the signal and the interfering signal are in phase. Both extremes are applicable to the two-tone interference case. Thus the probability of error computed for a given CSR, is due to both A.W.G.N. and carrier interference.

The theoretical error probability of a non-coherent F.S.K. system, which uses two bandpass filters followed by two envelope detectors, has been evaluated in the presence of both A.W.G.N. and two-tone interferers by Wang, L[47]. A special case of the evaluated error probability includes the case of single carrier interference. Thus, the error-rate results produced for both single-carrier interference and two-tone interference may be used for comparison with the experimental error-rate results of the present F.S.K. detection scheme by pulse compression.

The experimental error-rate results obtained are

shown in Fig. 28a, Fig. 28b, and Fig. 28c for single carrier interference, two-tone interferers with equal power, and two-tone interferers with 3 dB power difference respectively. Error-rate results are plotted together with the theoretical results obtained by Wang, L.[47], for CSR's of - 10 dB and - 15 dB.

Results indicate that, at Pe $\leq 10^{-2}$, the F.S.K. detection scheme performance is degraded due to single-carrier interference by 0.5 dB for CSR = - 15 dB, and 1 dB for CSR = - 10 dB. In the presence of two-tone interferers with equal power, degradations are 1.5 dB for CSR = -15 dB and 1 dB for CSR = - 10 dB., whereas in the presence of two-tone interferers with 3 dB power difference, degradations are approximately 1.5 dB for CSR = - 15 dB, and 0.5 dB for CSR = - 10 dB.

Altough the range of errors investigated is limited, the error-rate results obtained do establish the tolerance of the F.S.K.detection scheme by pulse compression to both single-carrier interference and two-tone interfers for the CSR's considered. Moreover, the performance of the present F.S.K. detection scheme in the presence of two-tone interfers with 3 dB power difference out-perform that in the presence of two-tone interferers with equal power. This result was theoretically substantiated for the conventional non-coherent F.S.K. detector[47].

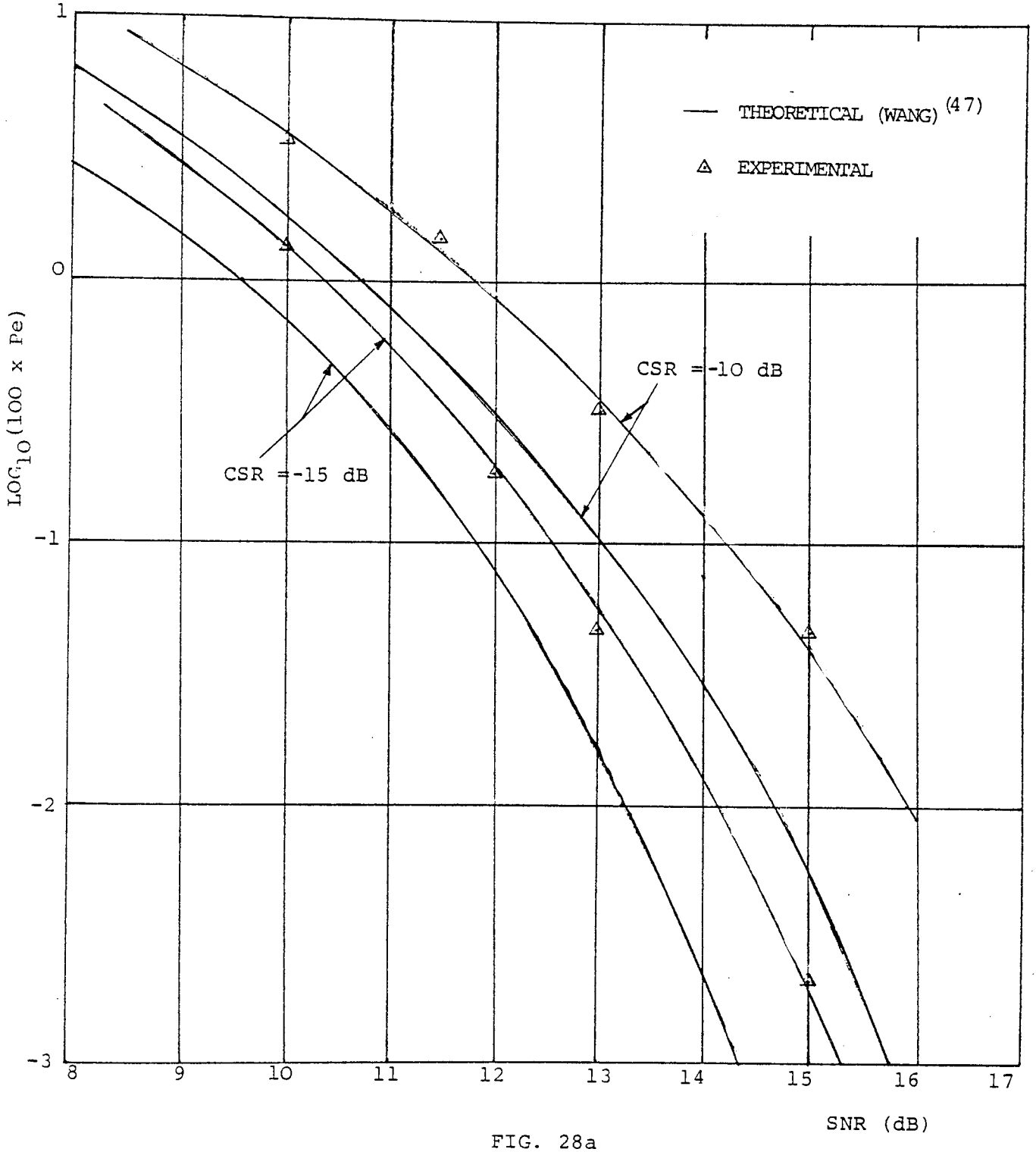

FIG. 28a

ERROR-RATES of F.S.K. DETECTION SCHEME IN THE PRESENCE OF SINGLE CARRIER INTERFERENCE

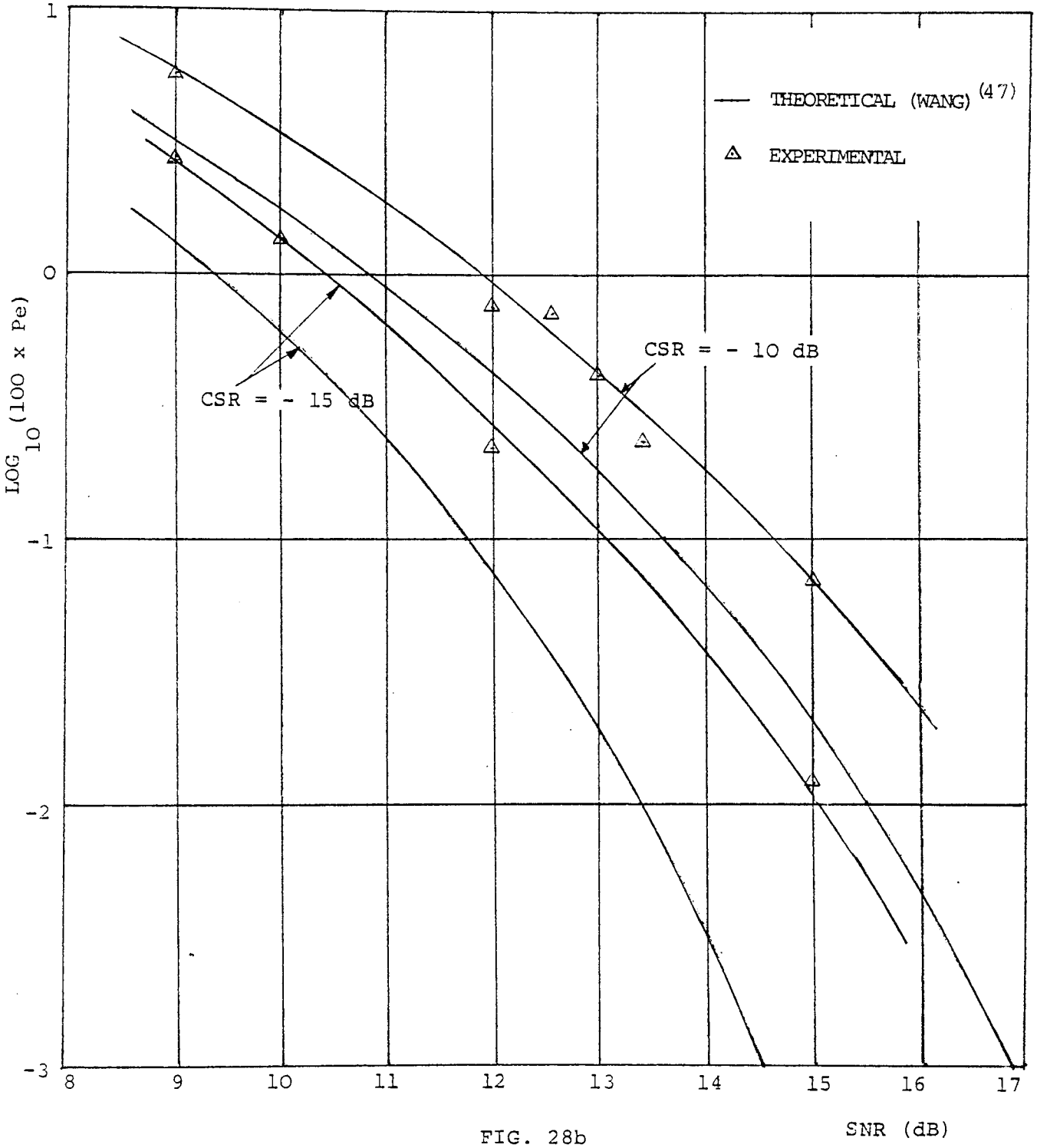

FIG. 28b

ERROR-RATES OF F.S.K. DETECTION SCHEME IN THE PRESENCE OF TWO-TONE INTERFERERS WITH EQUAL POWER

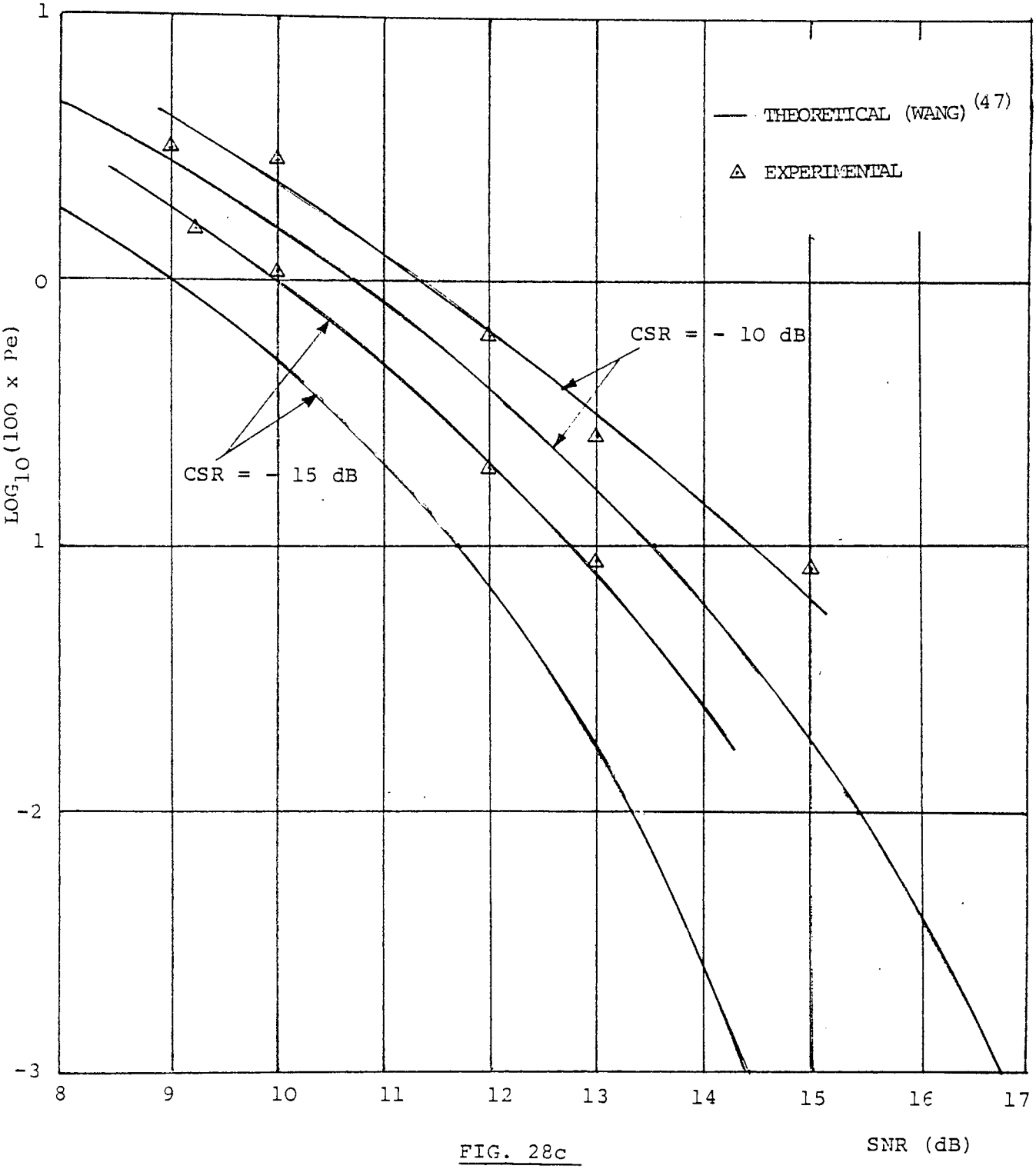

FIG. 28c

ERROR-RATES OF F.S.K. DETECTION SCHEME IN THE PRESENCE OF TWO-TONE INTERFERERS WITH 3 dB POWER DIFFERENCE

4.2.2 Discussion

The good performance of the F.S.K. detection scheme by pulse compression in A.W.G.N. does verify that this detection scheme is of practical interest. However, error-rate measurements were carried out using a combined software and hardware experimental system, which requires less instrumentation compared with an all hardware experimental system. Hence the obtained performance, which is 1.5 dB below the theoretical performance, may be considered as an optimistic result, since the experimental system used to perform error-rate measurements is nearly an ideal system. On the other hand, the range of errors investigated to establish the performance is limited.

Weighting of the impulse response of the PC.M.F. has improved the established performance in A.W.G.N. by 0.5 dB for practical probabilities of error. This was at first sight unexpected, due to the mismatch and loss of amplitude introduced by weighting. However, due to the nature of the decision scheme, a false signal (see Section 4.2.1) may cause an error in the recovered binary bit. Hence, it may be expected that the improvement in performance gained by weighting is due to minimizing the occurrence of false signal.

Measurements were carried out on one pulse basis to examine the compressed envelope characteristics in

the presence of practical imperfections and time delay, using the system of Fig. 21. Results of these measurements have established a range of values, beyond which error-rates are not practical in the presence of each type of imperfection and time delay. Thus, the performances of the F.S.K. detection scheme were established in the presence of each type of imperfection, as well as in the presence of different time delays. These performances may serve as guidelines for the hardware designer of the F.S.K. detection scheme by pulse compression.

A comparison technique was established by Hansen, R.C.[48], and used by Robin, H.K.[49], to compare the performances of various data transmission systems under random noise conditions. This technique may be employed to compare the established experimental results of the F.S.K. detection scheme by pulse compression with several other data transmission systems. The technique employs a parameter (ρ), which was defined as[49]

$$\rho = (SNR)(B_o.T)\ dB \qquad (4.3)$$

$$= \frac{\text{Signal energy per bit}}{\text{Noise power per unit bandwidth}}$$

where B_o is the bandwidth where noise is measured

T is the duration of one bit

For the F.S.K. detection scheme by pulse compression, the noise was measured in a bandwidth equal to that occupied

by the F.S.K. signal.

Hence, $\rho = (SNR)(F.T)$

Comparison is carried out for the following systems

(a) 32-tone piccolo

(b) F.S.K. $\pm$ 50% shift

(c) F.S.K. $\pm$ 425% shift

(d) F.S.K. chirp, $B_o.T = 50$

(e) F.S.K. by pulse compression, FT = 4

The performances of the binary systems (d and e) above are given in the form of bit error-rate, whereas the performances of the systems (a - c) are given in character error-rate. In this case it was assumed that the binary systems are used to send 5-bit characters and therefore the probability of error for 5-bit character is equivalent to five times the bit error-rate[49]. The error-rate of the binary chirp system[21] and the present F.S.K. system under investigation are converted to be equivalent to the rest of the systems involved in the comparison, and compared on the basis of character error-rate (i.e. equivalent to an alphabet of 32-characters). Fig. 29 shows the systems a - e plotted on ρ vs B_oT so that at the same character error-rate, the better system is the one which has the lowest ρ.

Error-rate results concerning the performance of the F.S.K. detection scheme in the presence of carrier interference and A.W.G.N., compare reasonably satisfactorily

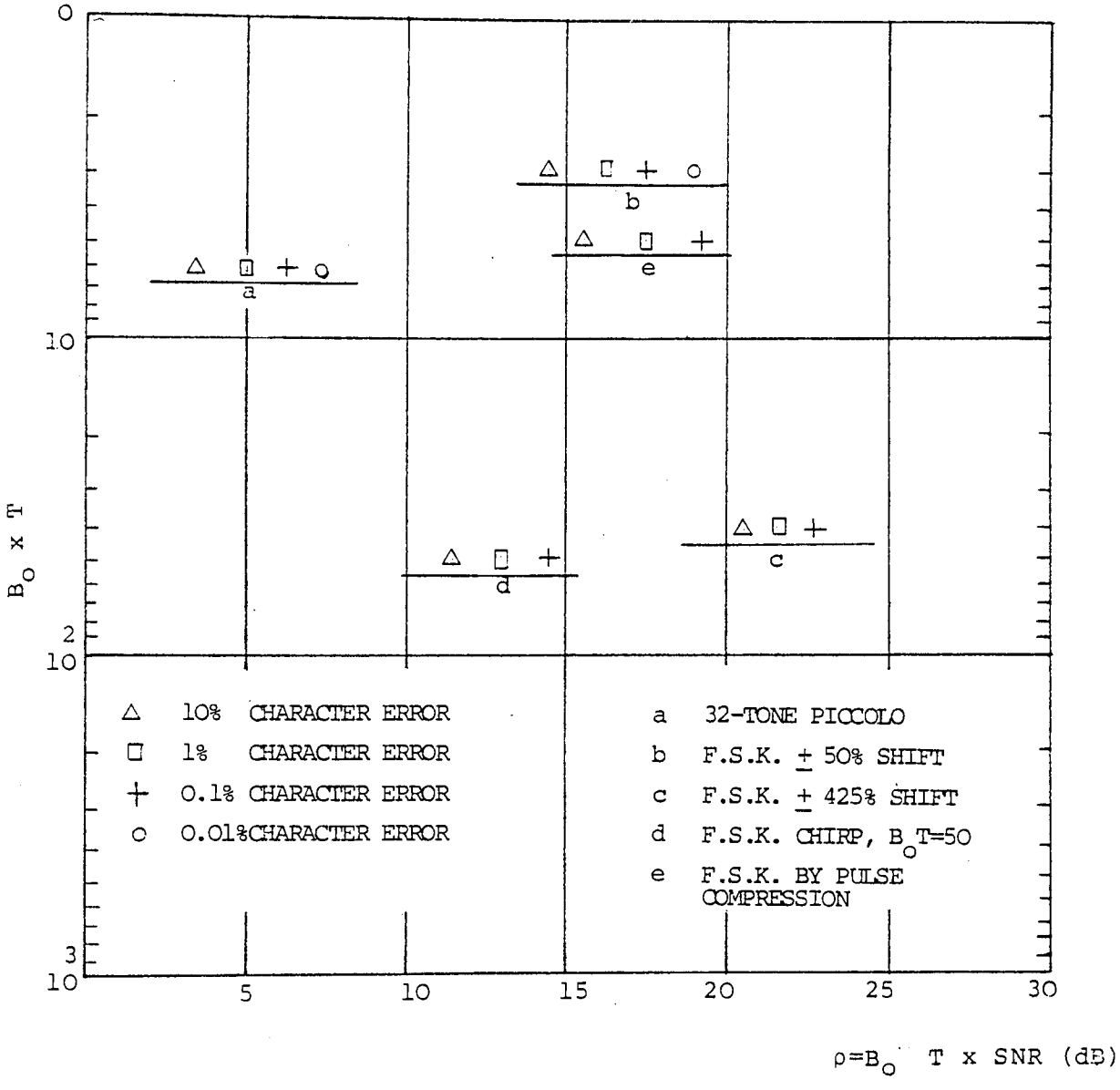

FIG. 29

COMPARISON OF PERFORMANCE OF VARIOUS F.S.K. SYSTEMS UNDER NOISE CONDITIONS

with the theoretical performance of the conventional non-coherent F.S.K. detector[47]. Unfortunatley, no experimental results were found for other F.S.K. detection schemes[50] to be used for comparison with the present detection scheme in the presence of carrier interference.

The case of one interfering signal or two interfering signals, but with different frequency from that of the signal, being within the bandwidth of the P.C.M.F., and random phase is less damaging to the performance of the F.S.K. detection scheme. This stems from the fact that the mixer-P.C.M.F. compound is capable of resolving the interfering signal from the wanted signal at its output (see Section 2.2.2). Furthermore, the interfering signal would be positioned away from the wanted signal depending on its frequency, in which case weighting may be used to minimize its effects on the output compressed envelope of the true signal.

In the light of the results obtained, it may be concluded that the F.S.K. detection scheme is of practical interest. Moreover, the performance obtained highlights the candidacy of this detection scheme for consideration for use in digital data transmission.

4.3 THE D.P.S.K. SYSTEM

The D.P.S.K. system is formed by incorporating the same mixer-P.C.M.F. compound used previously in the F.S.K. detection scheme, with a differential detector. The

differential detector comprises a delay and a multiplier, followed by a low pass filter. The multiplier is implemented in software, whereas low-pass filtering is performed at the output of the D/A converter as was shown in the D.P.S.K. error-rate model. A pair of antiphase sinusoidal signals are digitized into256-samples and fed into RAM, using the signal-generator software, to represent the transmitted data signals. Each signal is 2 msec. long with a carrier frequency of 12 kHz.

4.3.1 Error-rate Measurements

Error-rate measurements were conducted in the presence of A.W.G.N. by running the D.P.S.K. error-rate model described in Section 3.4.2 for different input SNR's. As in the F.S.K. case before, 1000-errors were counted for low SNR's, and 500-errors for higher SNR's to arrive at the final estimate of the probability of error for each SNR. Fig. 30 shows the experimental performance obtained plotted together with the ideal performance of a D.P.S.K. system in A.W.G.N. (i.e. equation 2.29)[35]. Error-rate results indicate that the D.P.S.K. detection scheme by pulse compression performs remarkably well in A.W.G.N. Its performance is less than 1 dB below the ideal performance for practical probabilities of error (i.e. $Pe \leq 10^{-2}$).

Unlike the F.S.K. detection scheme, a false signal due to noise or any other kind of interference would not cause an errorin the D.P.S.K. detection scheme. This is

because the decision on the binary bit in the D.P.S.K. decision circuits (see Section 3.4.2.1) is made by sampling once within every bit period. Thus, even if a false signal is detected by the threshold detector, it would be ignored by the decision circuits. This may be considered an advantage of the D.P.S.K. detection scheme over the F.S.K. detection scheme, in addition to the 3 dB superiority in performance of the former over the latter in the presense of A.W.G.N. Fig. P8 shows the output of the differential detector before and after filtering, together with two timing markers, which represent the output window of the P.C.M.F. Fig. P9 shows the output of the differential detector after filtering, the output of the threshold detector and the sampling sequence.

Weighting of the impulse response of the P.C.M.F. was used as was described in section 4.2.1, in an attempt to improve the performance of the D.P.S.K. detection scheme in A.W.G.N. . However, the results obtained show no significant improvement over the performance without weighting, as shown in Fig. 30. This may be due to the mismatch and loss of amplitude created by weighting[16]. Furthermore, the differential detection process makes the current and the reference noisy signals dependent[35]. This dependency causes errors to occur in pairs. This was observed occasionally during error-rate measurements.

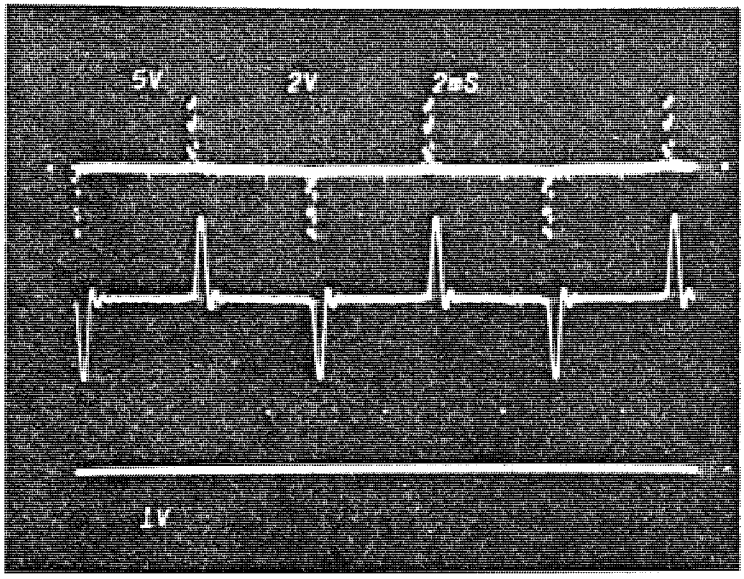

FIG. P8

OUTPUT OF DIFFERENTIAL DETECTOR BEFORE AND AFTER FILTERING

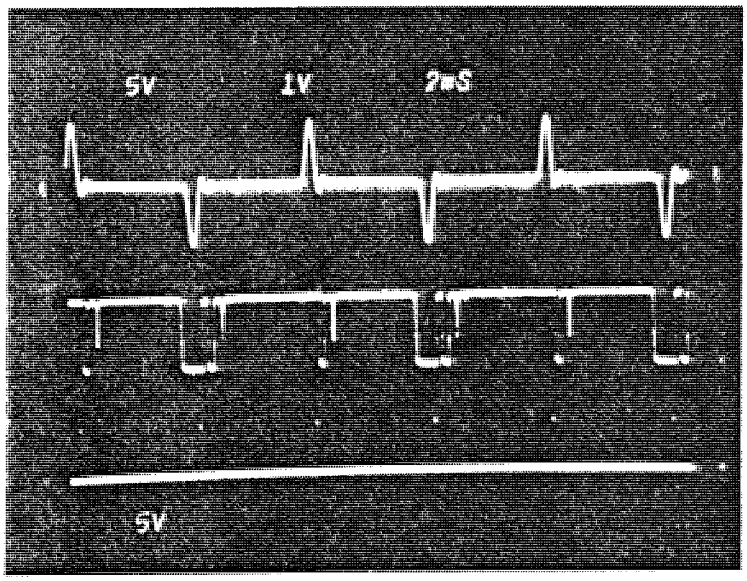

FIG. P9

OUTPUTS OF DIFFERENTIAL DETECTOR, THRESHOLD DETECTOR, AND SAMPLING SEQUENCE

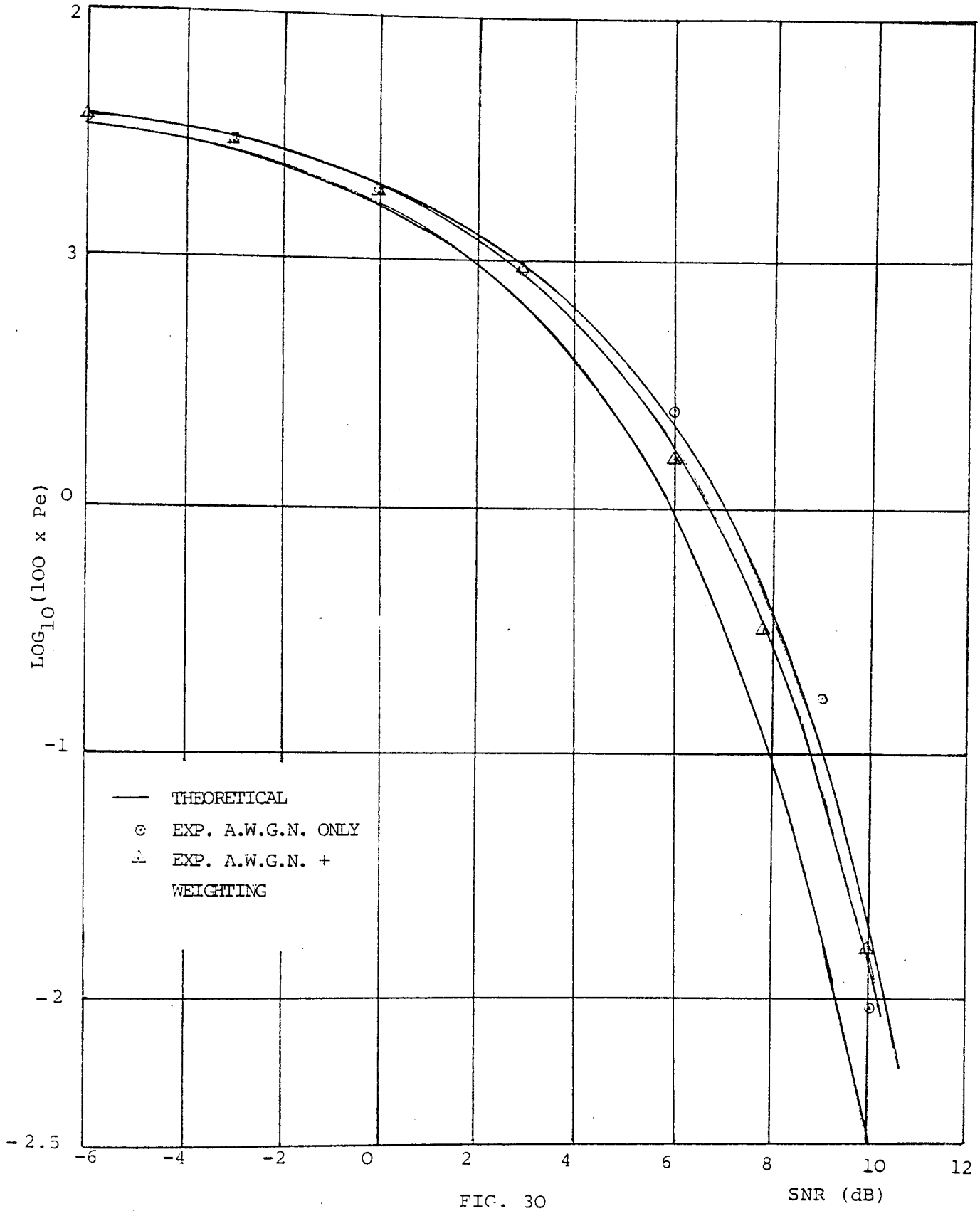

FIG. 30

ERROR-RATES OF D.P.S.K. DETECTION SCHEME IN THE PRESENCE OF A.W.G.N.

4.3.1.1 Practical Imperfections

Error-rate measurements were conducted in the presence of each type of imperfection, and A.W.G.N. The same values of practical imperfection used in the F.S.K. case are used in the D.P.S.K. case to facilitate comparison of error-rate results for both detection schemes in the presence of practical imperfections.

The error-rate results obtained in the presence of non-linearity, slope mismatch, and frequency drift are plotted respectively in Fig. 31a, Fig. 31b, and Fig. 31c, together with the performance of the D.P.S.K. detection scheme in A.W.G.N. The results show that non-linearity produces the most damaging effects among the considered practical imperfections on the performance of the D.P.S.K. detection scheme. For example, the performance in A.W.G.N. is degraded by 5.5 dB, at Pe $\leq 10^{-2}$ for 12% non-linearity in the impulse response of the P.C.M.F.. Thus, the D.P.S.K. detection scheme suffers more than the F.S.K. detection scheme in the presence of non-linearity. Moreover, if the performance of each detection scheme in A.W.G.N. is compared with its performance in the presence of slope mismatch, and frequency drift, the D.P.S.K. detection scheme seems to suffer more. A comparison of the performances of both detection schemes will be given later.

4.3.1.2 Time Delay

Error-rate measurements in the presence of time delay

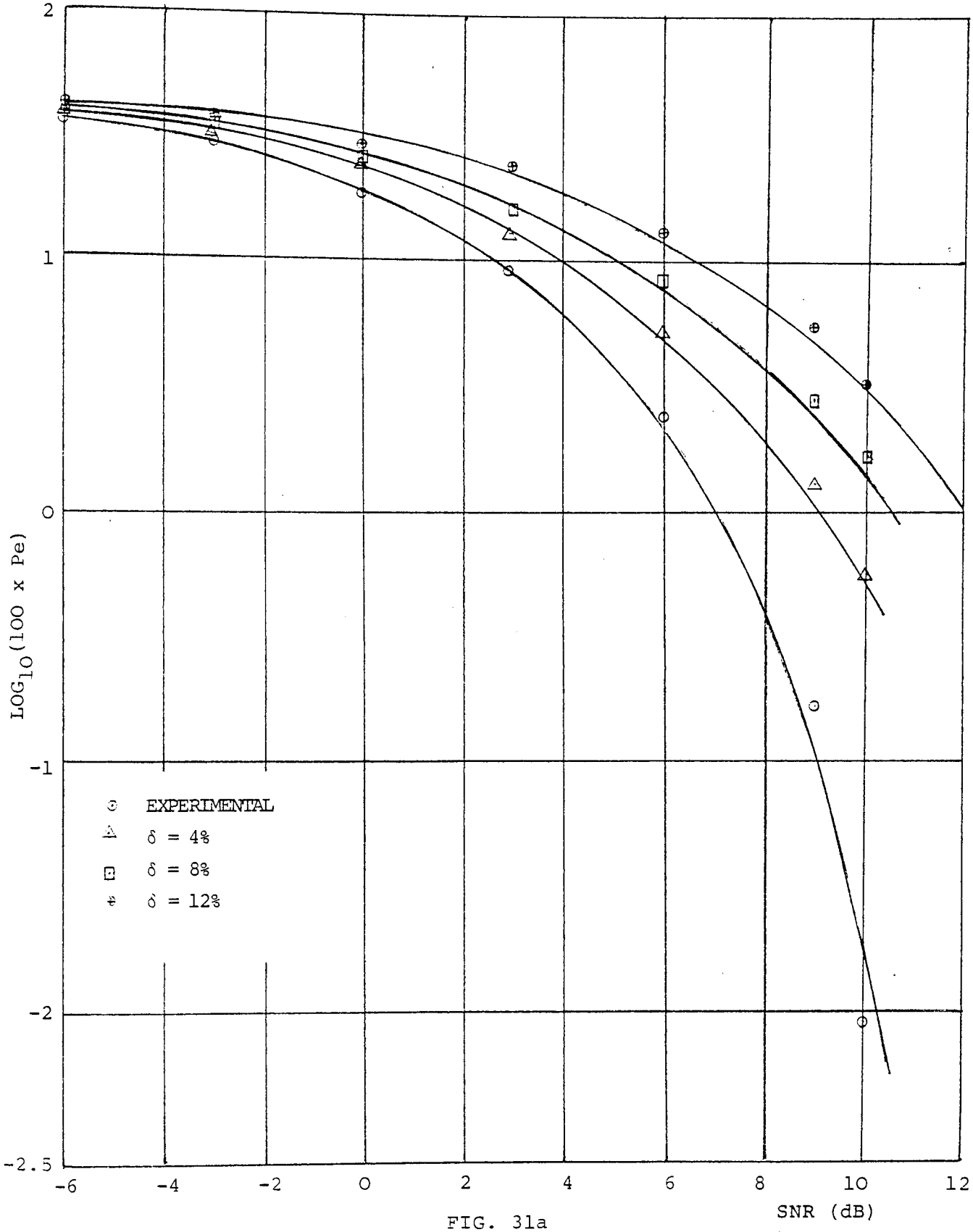

FIG. 31a

ERROR-RATES OF D.P.S.K. DETECTION SCHEME IN THE PRESENCE OF NON-LINEARITY

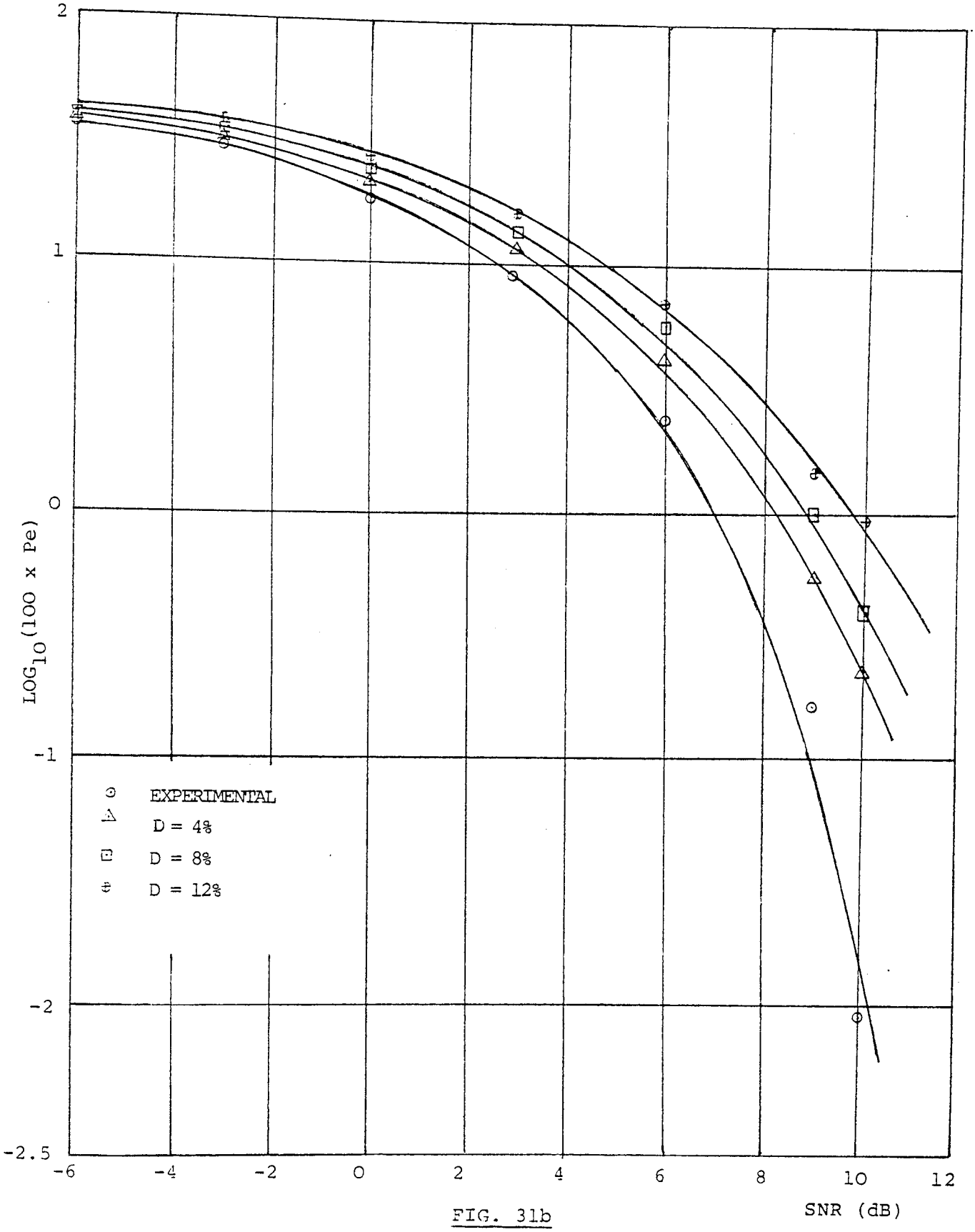

FIG. 31b

ERROR-RATES OF D.P.S.K. DETECTION SCHEME IN THE PRESENCE OF SLOPE MISMATCH

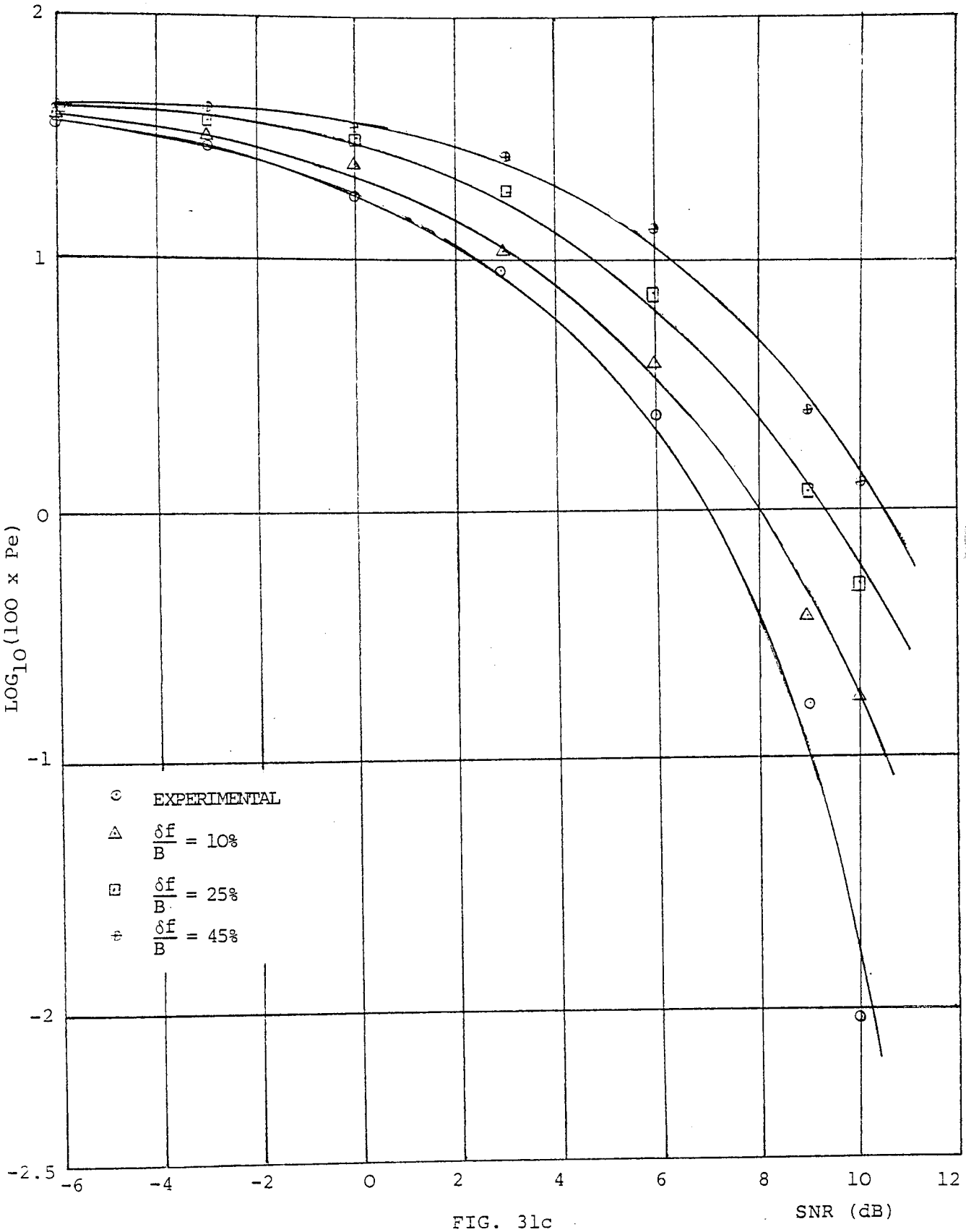

FIG. 31c

ERROR-RATES OF D.P.S.K. DETECTION SCHEME IN THE PRESENCE OF FREQUENCY DRIFT

and A.W.G.N. were conducted for the D.P.S.K. detection scheme. The same values of time delay used in the F.S.K. case are used in this case, to facilitate comparing the performances of both detection schemes in the presence of time delay. The error-rate results obtained are plotted in Fig. 32, together with the performance of the D.P.S.K. detection scheme in A.W.G.N.. At practical probabilities of error and the same amount of time delay, the F.S.K. detection scheme appears to perform better than the D.P.S.K. detection scheme when each scheme is compared with its performance in A.W.G.N. . For example, the degradation in performance of the D.P.S.K. detection scheme due to a delay of 12-samples (i.e. $\Delta = 0.46775T$), at $Pe \leqslant 10^{-2}$ is approximately 2.5 dB. This is 0.5 dB more than the F.S.K. detection scheme suffers at the same time delay, if compared with its performance in A.W.G.N..

4.3.1.3 Carrier Interference

The single carrier interference model of Fig. 20 was used in conjunction with the D.P.S.K. error-rate model to perform error-rate measurements on the D.P.S.K. detection scheme by pulse compression. A constant amplitude sinusoidal signal at the carrier frequency of the D.P.S.K. data signal was digitized and stored in RAM prior to conducting the measurements. Error-rate measurements in the presence of carrier interference

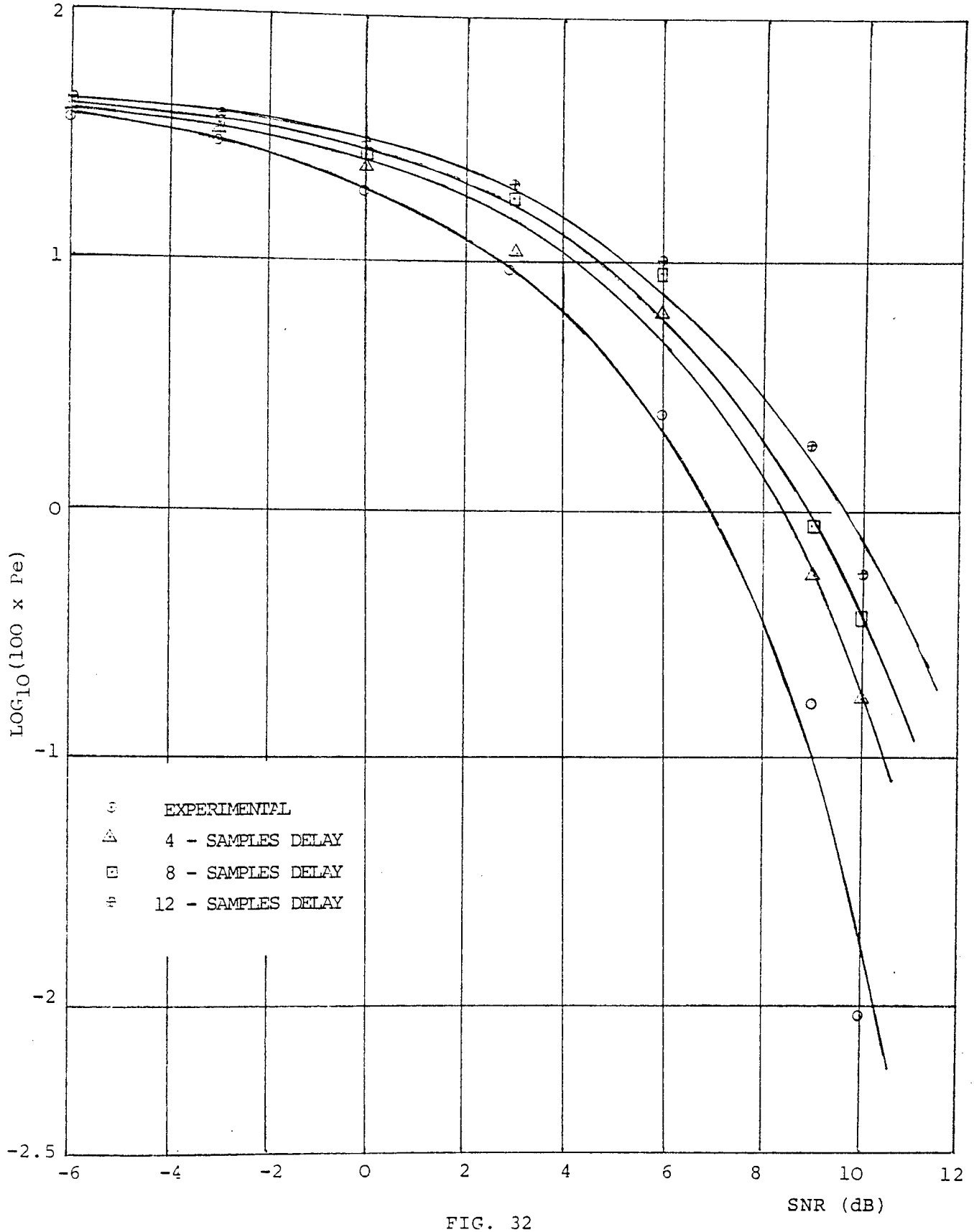

FIG. 32

ERROR-RATES OF D.P.S.K. DETECTION SCHEME IN THE PRESENCE OF TIME DELAY

and A.W.G.N. were conducted for CSR's of - 10 dB and - 15 dB.

The experimental results obtained are plotted in Fig. 33. The theoretical error-rate results obtained by Rosenbaum, A.S.[39], for a conventional D.P.S.K. detector in the presence of an inband, random phase carrier interference, may be used for comparison purposes. The theoretical investigation involved two cases. The first case when the relative phase of two adjacent interfering signals is dependent (i.e. worst case), whereas the second case is when the relative phase is independent (i.e. best case). Error-rate results of both cases[39] for CSR's of - 10 dB and - 15 dB are added to Fig. 33.

The experimental results of the D.P.S.K. detection scheme by pulse compression suffer about 1 dB for CSR = - 10 dB, and slightly more than 1 dB for CSR = - 15 dB, compared with the worst case of the conventional D.P.S.K. detector[39]. It may be expected that the degradation in performance is due to the limited values that the phase of the interfering signal may take (see Section 3.4.3, equation 3.8), as well as the limited range of errors investigated. However, results do establish an experimental performance for the D.P.S.K. detection scheme in the presence of carrier interference. Moreover, it was observed during error-rate measurements that most of the time errors occurred in pairs. This observation of errors occurring in pairs seems to be one of the typical behaviours of a differential phase detector, when

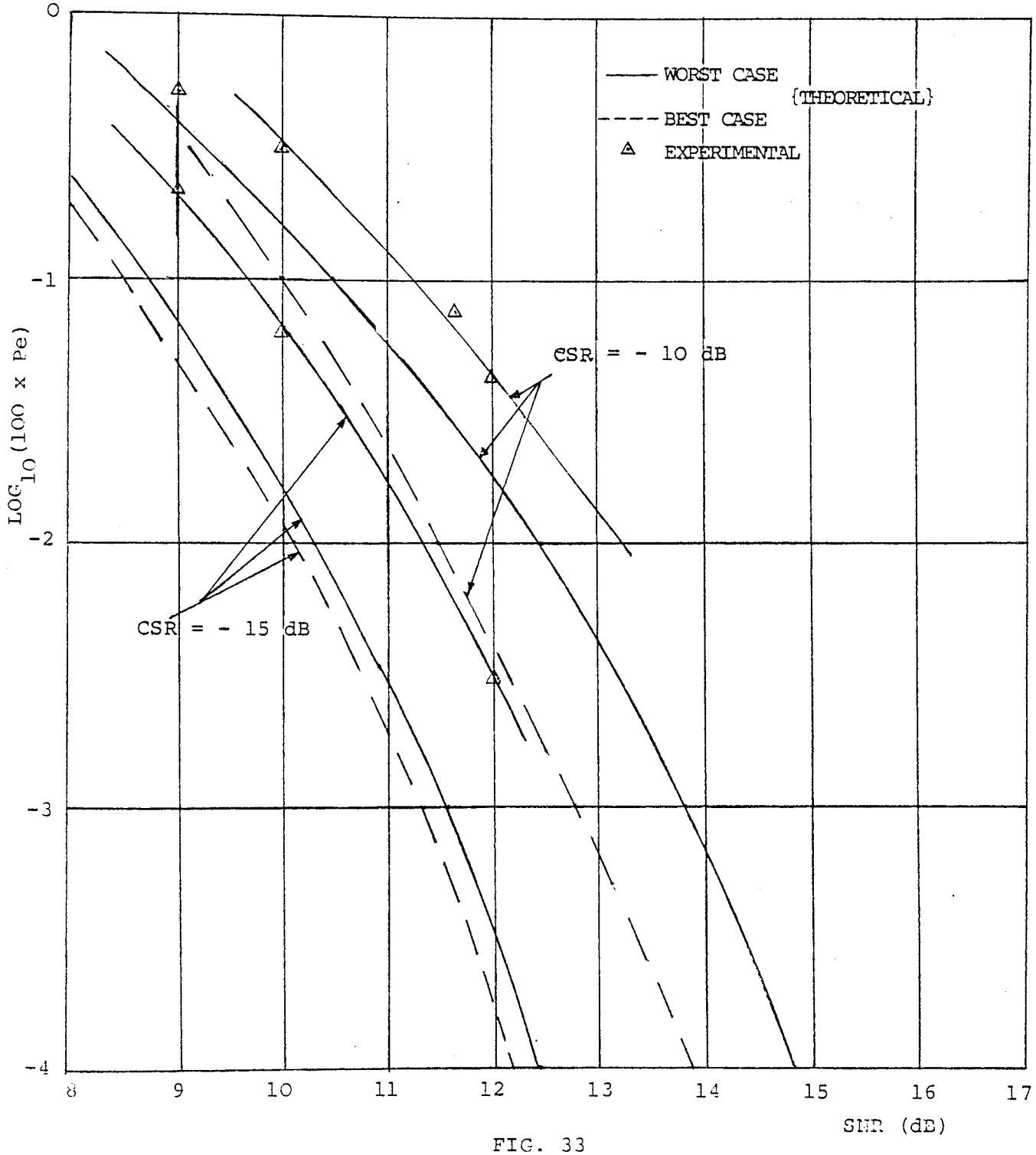

FIG. 33

ERROR-RATES OF D.P.S.K. DETECTION SCHEME IN THE PRESENCE OF CARRIER INTERFERENCE

processing signals corrupted by impulsive interference[51], (e.g. carrier interference).

4.4 DISCUSSION

Comparison of the performances of the F.S.K. and D.P.S.K. detection schemes in the presence of practical imperfections and time delay is valid because both detection schemes incorporate the same mixer-P.C.M.F. compound as their predetector processor. Fig. 34a, and Fig. 34b, show the degradation in performance of each detection scheme due to practical imperfections and time delay when each scheme is compared with its performance in A.W.G.N., at Pe = 10^{-2}. The F.S.K. detection scheme appears to give the superior performance in such a comparison. Moreover, a full assessment of the time delay problem should assume the type and conditions of a given communication channel[52]. Nevertheless, the time delay error-rate results obtained (i.e. Fig. 27 and Fig. 32) do establish the tolerances of each detection scheme to time delay in an A.W.G.N. channel. Furthermore, results show that the F.S.K. detection scheme enjoys better performance than the D.P.S.K. detection scheme in the presence of time delay. However, the good performance that the D.P.S.K. detection scheme enjoys in A.W.G.N., highlights its candidacy as a potential detection scheme for use in digital data transmission.

The performances of both detection schemes in the

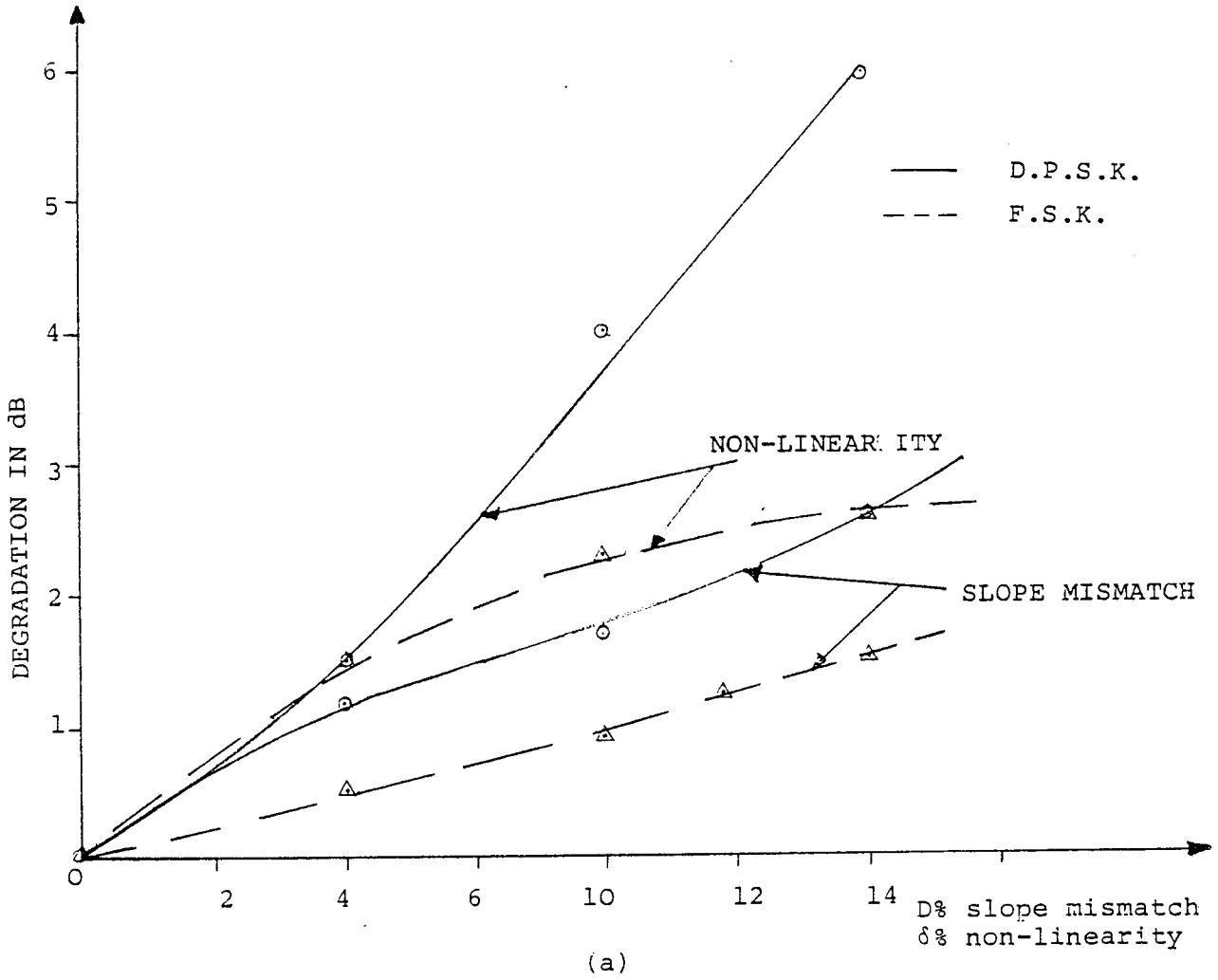

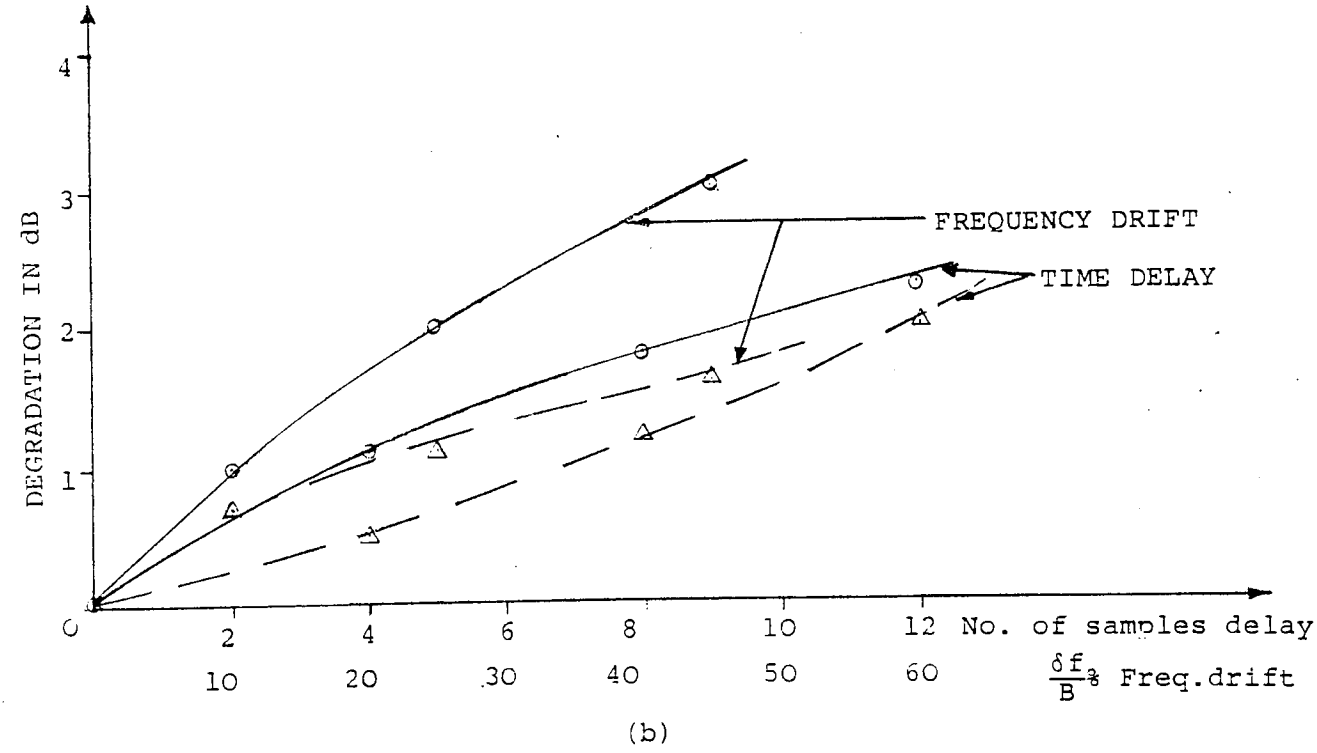

FIG. 34 DEGRADATION IN PERFORMANCE OF F.S.K. AND D.P.S.K. DETECTION SCHEMES AT Pe $= 10^{-2}$ IN THE PRESENCE OF

(a) NON-LINEARITY AND SLOPE MISMATCH
(b) FREQUENCY DRIFT AND TIME DELAY

presence of carrier interference may be compared on the basis of degradation in performance of each detection scheme at a specific level of interference. Fig. 35 shows the experimental error-rates of both schemes at CSR's of - 10 dB and - 15 dB. The F.S.K. detection scheme appears to suffer more than 3 dB at Pe = 10^{-3} for both CSR's considered. This result agrees with the ideal performances of conventional D.P.S.K. and non-coherent F.S.K. detection schemes in the presence of carrier interference and A.W.G.N.[50].

The performance in A.W.G.N. of other D.P.S.K. schemes, which detect D.P.S.K. chirp data signals[31] may be compared with the present D.P.S.K. scheme performance. Fig. 36, which gives experimental error-rates of the present D.P.S.K. detection scheme, together with the D.P.S.K. chirp system, shows that the present D.P.S.K. scheme enjoys an advantage of 1.1 dB in performance over the chirp system. However, since the time-bandwidth product of a chirp signal can be made higher than any unitary data signal (e.g. P.S.K., F.S.K., and A.S.K.), the chirp system would tolerate more carrier interference and fading due to its inherent inband-frequency diversity[5],[37]. The latter fact also applies to the F.S.K. chirp system[21], compared with the present F.S.K. detection scheme. However, both detection schemes investigated can handle F.S.K. and D.P.S.K. data signals of the common type used

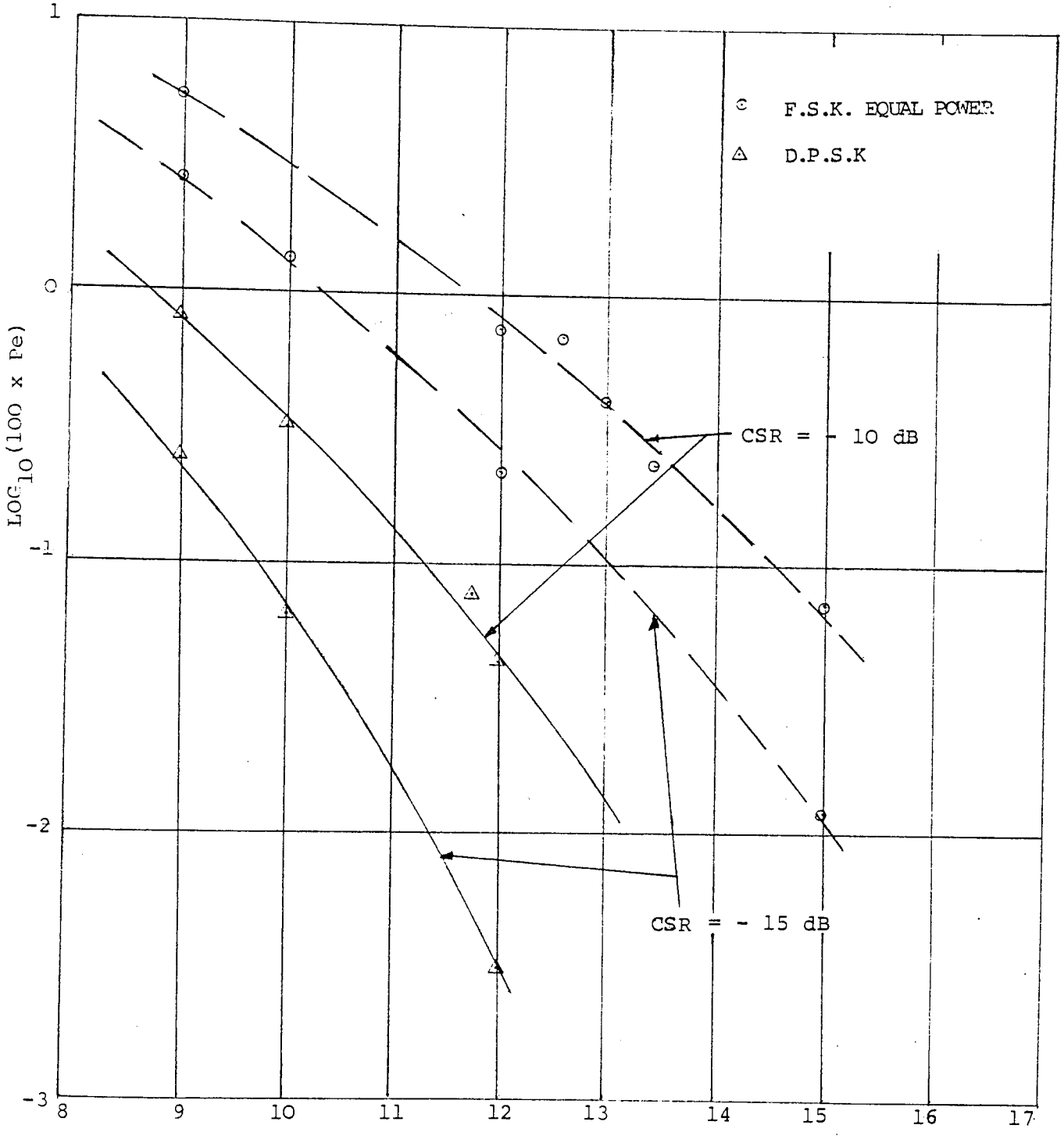

FIG. 35

ERROR-RATES OF F.S.K. AND D.P.S.K. DETECTION SCHEMES IN THE PRESENCE OF CARRIER INTERFERENCE

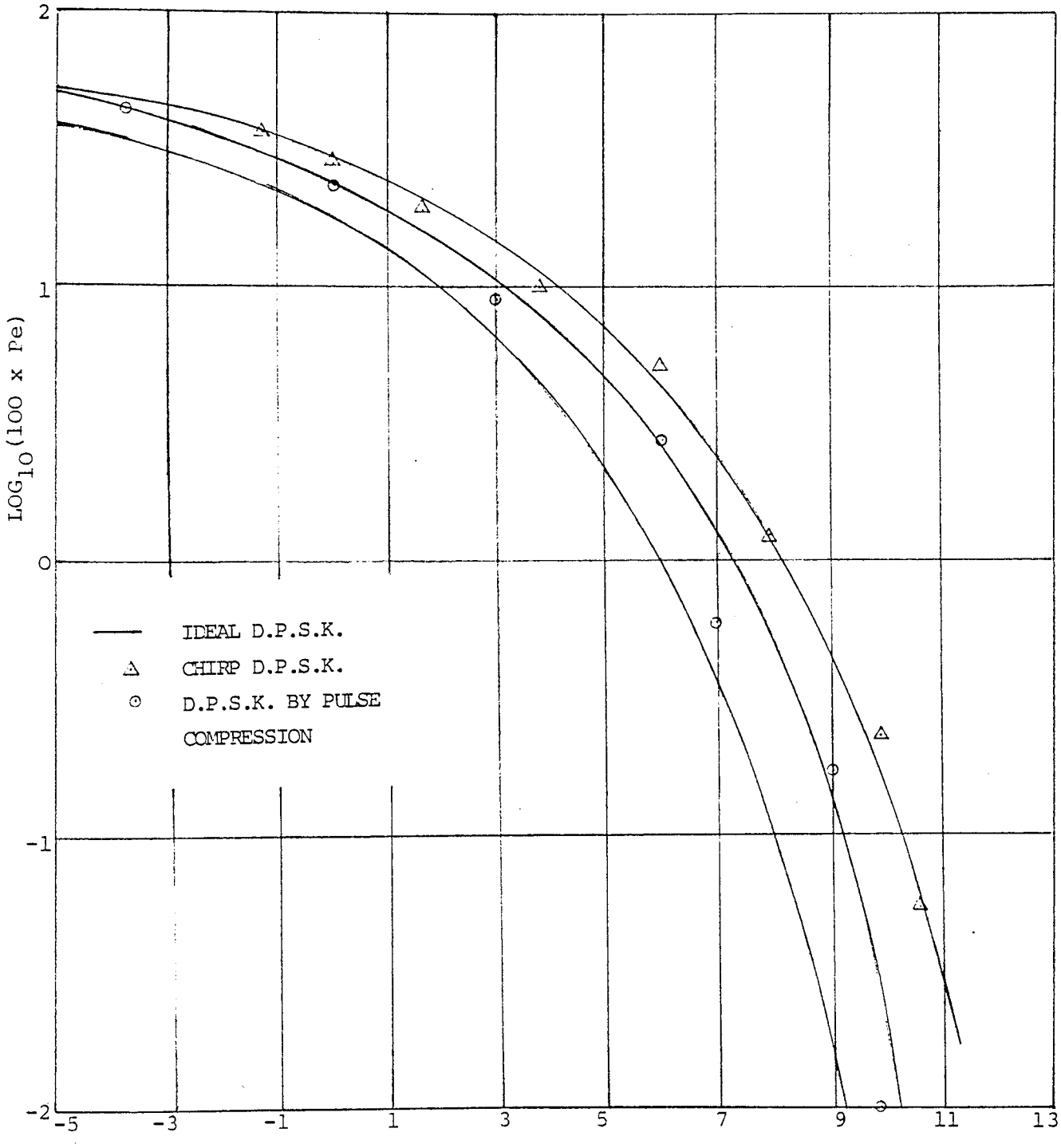

FIG. 36

ERROR-RATES OF D.P.S.K. CHIRP SYSTEM AND D.P.S.K. DETECTION SCHEME BY PULSE COMPRESSION IN THE PRESENCE OF A.W.G.N.

in the communication industry without the need to design new formats for each data signal.

CHAPTER FIVE

CONCLUSIONS

5. CONCLUSIONS

Chirp modulation of the received F.S.K. or P.S.K. data signals, followed by pulse compression facilitates the implementation of the matched filter detector for both data signals. The matched filter may be implemented in the form of the P.C.M.F. utilising C.C.D., SAW devices or digital techniques, which all have reached a high level of maturity that allows the design and construction of a more compact P.C.M.F. with a relatively low cost. Furthermore, both operations performed on the data signal form the mixer-P.C.M.F. compound, which was shown to be capable of maximizing its output SNR at a predetermined instant in time.

A systematic study was carried out on the mechanisms of the mixer-P.C.M.F. compound to find its responses to F.S.K. and P.S.K. data signals. It was determined that in P.S.K. reception, the perfect match state between the P.C.M.F. and its input signal can be achieved, whereas in F.S.K. reception this state cannot be achieved, due to the doppler shift created by the received F.S.K. signal. These two properties of the A.C.F. of the P.C.M.F. made the mixer-P.C.M.F. compound act as an optimum detector for P.S.K. data signals, and near optimum detector for F.S.K. data signals. Moreover, the effects produced by time delay and frequency

drift of the local chirp on the output A.C.F. of the P.C.M.F. were determined. These effects highlighted the deviation of the A.C.F. from the state of perfect match for both F.S.K. and P.S.K. receptions. Expressions for the A.C.F. in the presence of additive carrier interference for both F.S.K. andP.S.K. receptions were found. These expressions may be used to determine the capability of the mixer-P.C.M.F. compound to resolve interfering signals from the wanted signal providing they differ in frequency.

To establish the performance of both detection schemes, an experimental system was implemented. The experimental system was utilized to develop error-rate models for F.S.K. and D.P.S.K. detection schemes, as well as a carrier interference model. Error-rate models were operated under the supervision of a microprocessor system, which offered a high level of versatility for experimental purposes.

Although, the range of errors investigated was limited, the F.S.K. detection scheme performance in A.W.G.N. was 1.5 dB below optimum, whereas the performance of the D.P.S.K. detection scheme was less than 1 dB below optimum. However, in comparison with other detection schemes, the F.S.K. scheme appeared to compare reasonably well with other F.S.K. detection schemes (see Fig. 23). Moreover, the D.P.S.K. detection scheme outperformed the D.P.S.K. chirp system by 1.1 dB.

(see Fig. 36).

The established performances of both detection schemes in the presence of practical imperfections (i.e. non-linearity and slope mismatch of the P.C.M.F., and frequency drift of the local chirp signal), highlighted the need for a linear mixer-P.C.M.F. compound if a good performance with a relatively low SNR is required. Furthermore, it was substantiated that frequency drift of the local chirp signal produces less damaging effects than slope mismatch of the P.C.M.F. on the overall probability of error for both F.S.K. and D.P.S.K. detection schemes (see Fig. 34a and Fig.34b).

Error-rate results concering time delay of the local chirp signal outlined the capabilities of both detection schemes in the presence of constant time delays. It was substantiated that the F.S.K. detection scheme is more tolerant of time delay than the D.P.S.K. detection scheme when each scheme is compared to its performance in an A.W.G.N. channel (see Fig. 34a).

The performances of the F.S.K. detection scheme in the presence of single-carrier interference, two-tone interferers with equal power, and two-tone interferers with 3 dB power difference, were established. These performances compare well with the theoretical performance of a conventional F.S.K. detection scheme (see

Fig. 28a, Fig. 28b, and Fig. 28c). The D.P.S.K. detection scheme appeared to suffer less in the presence of carrier interference compared with the F.S.K. detection scheme, when each scheme is compared to the theoretical performance of its conventional system. However, the established performances of both detection schemes were obtained for relatively low CSR's (i.e. - 10 dB and - 15 dB), with the interfering signal at the same frequency as the transmitted signal. This indicates that both detection schemes may cope adequately with a congested frequency communication channel.

Finally, the author hopefully anticipated that the present work would lead to further development in the design and utilization of both of the investigated detection schemes for the purpose of digital data communication.

5.1 SUGGESTIONS FOR FURTHER WORK

The performances of both F.S.K. and D.P.S.K. detection schemes have been established under conditions of steady-received signals, and additive stationary Gaussian noise, as well as additive carrier interference. However, in many radio applications, the channel characteristics are often strongly non-stationary. These communication channels are known as fading channels[2], [3], [53], [54].

Non-coherent F.S.K. and D.P.S.K. data signals are

widely used over fading channels, since their detection process does not require a phase reference. Except when signal fading is slow, it is possible to derive a suitable phase reference for coherent detectors of F.S.K. and P.S.K. data signals[2],[3]. Thus, it is of practical interest to establish the performances of both F.S.K. and D.P.S.K. detection schemes by pulse compression, under simulated conditions of signal fading. A practical model is the Rayleigh envelope fading and uniform random phase characteristics for the envelope and phase of a single transmitted tone[3]. This model may be implemented utilizing the experimental system described in Chapter 3. However, the search and implementation of other suitable fading models, utilizing the experimental system, are also of practical interest. Moreover, a search for a synchronization scheme would be necessary. The synchronization scheme must be capable of rapidly recovering the timing information after each signal fade to minimize the loss of information due to timing errors.

Nevertheless, the main object of such a research topic would be to establish the utility and practicability of both of the investigated detection schemes for use under fading channel conditions.

APPENDICES

APPENDIX A

AUTOCORRELATION FUNCTION AT THE OUTPUT OF THE P.C.M.F.

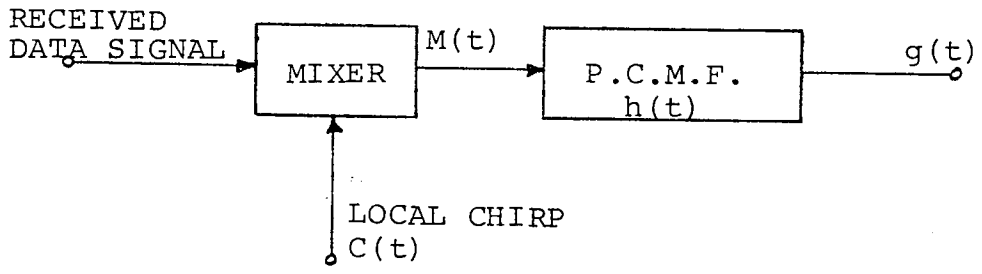

FIG. A1

A.1 THE F.S.K. CASE

Let F.S.K. signal be

$$S(t) = A \exp.j(\omega_a t + \pi RFt), \quad |t| \leq \frac{T}{2} \qquad (A.1)$$

where A is the amplitude

ω_a is the angular centre frequency

R = ± 1 for a mark, or space respectively

F is the bandwidth

Let the modulation index be,

$$h = (f_s - f_m)T = FT \qquad (A.2)$$

where f_s is the space frequency

f_m is the mark frequency

T is the period of one bit.

Let the local chirp signal be

$$C(t) = \exp.j(\omega_o t + \frac{1}{2}\mu t^2), |t| \leq \frac{T}{2} \qquad (A.3)$$

where ω_o is the angular centre frequency

$\mu = \frac{2\pi B}{T}$ is the slope

The output of the mixer may be expressed as

$$M(t) = [S(t)][C(t)]^*$$

Hence, $M(t) = A \exp.j[(\omega_a - \omega_o)t + \pi RFt - \frac{1}{2}\mu t^2], |t| \leq \frac{T}{2}$

(A.4)

let $\omega_c = \omega_a - \omega_o$, and $\omega_d = \pi RF$

The impulse response of the P.C.M.F. is

$$h(t) = \exp.j(\omega_c t + \frac{1}{2}\mu t^2) \quad , \quad |t| \leq \frac{T}{2} \qquad (A.5)$$

The output of the P.C.M.F. is found using the convolution integral as follows

$$g(t) = k \int_{-\infty}^{\infty} M(\tau) h(t-\tau) d\tau \qquad (A.6)$$

substituting for M(t) and h(t) in (A.6) we get

$$g(t) = kA \int_{-\frac{T}{2}}^{T/2} \exp.j[(\omega_c+\omega_d)\tau - \frac{1}{2}\mu\tau^2] \exp.j[\omega_c(t-\tau) + \frac{1}{2}\mu(t-\tau)^2] d\tau$$

Taking the real value of g(t), neglecting second harmonic terms, and simplifying

$$\text{Re.}[g(t)] = kA\int_{-\frac{T}{2}}^{T/2} \text{Cos}\left[\omega_c t + \omega_d \tau + \mu t\tau - \frac{1}{2}\mu t^2\right].d\tau$$

The above integral may be evaluated as follows[16].

$$\text{Let } a = -\frac{T}{2} + t, \quad b = \frac{T}{2}, \text{ for } t > 0 \qquad \text{(A.7a)}$$

$$a = \frac{T}{2}, \quad b = \frac{T}{2} + t, \text{ for } t < 0 \qquad \text{(A.7b)}$$

Hence,

$$\text{Re.}[g(t)] = \frac{kA}{2}\left[\frac{\text{Sin}\left[\omega_c t+\omega_d \tau+\mu t\tau-\frac{1}{2}\mu t^2\right]}{\omega_d+\mu t}\right]_{\tau=a}^{b} \qquad \text{(A.8)}$$

solving (A.8), using (A.7a)

$$\text{Re.}[g(t)] = \frac{kA}{2}\left[\frac{\text{Sin}\left[\omega_c t+\omega_d (t-\frac{T}{2})+\mu t (t-\frac{T}{2})-\frac{1}{2}\mu t^2\right]}{(\omega_d+\mu t)} - \right.$$

$$\left. \frac{\text{Sin}\left[\omega_c t+\omega_d t - \frac{\omega_d}{2}T+ \frac{\mu t}{2}(T-t)\right]}{(\omega_d + \mu t)}\right]$$

add and subtract $\frac{\omega_d}{2}t$ to the argument of the first term in the above equation we get

$$\text{Re.}[g(t)] = \frac{kA}{2}\left[\frac{\text{Sin}\left[(\omega_c+ \frac{\omega_d}{2}) t + \frac{\omega_d+\mu t}{2}(T-t)\right]}{(\omega_d-\mu t)} - \right.$$

$$\left. \frac{\text{Sin}\left[(\omega_c+ \frac{\omega_d}{2}) t - \frac{\omega_d+\mu t}{2}(T-t)\right]}{(\omega_d - \mu t)}\right]$$

Let $\alpha = (\omega_c+ \frac{\omega_d}{2}) t$, and $\beta = \frac{\omega_d+\mu t}{2}(T-t)$, and using the sum and difference of sines the above equation is

simplified to the following for $t > 0$

$$\underset{t > 0}{\text{Re.}[g(t)]} = kA \frac{\text{Sin}\left[\frac{\omega_d+\mu t}{2}(T-t)\right]}{(\omega_d+\mu t)} \text{Cos}(\omega_c+\frac{\omega_d}{2})t \qquad (A.9)$$

Similarly, solving (A.8) using (A.7b); $\text{Re.}[g(t)]$ is found for $t < 0$

$$\underset{t < 0}{\text{Re.}[g(t)]} = kA \frac{\text{Sin}\left[\frac{\omega_d+\mu t}{2}(T+t)\right]}{(\omega_d+\mu t)} \text{Cos}(\omega_c+\frac{\omega_d}{2})t \qquad (A.10)$$

Combining (A.9), (A.10), and substitute for the following

$$h=FT, \omega_d=\pi RF, \quad \mu = \frac{2\pi B}{T}, \quad k = \sqrt{\frac{2\mu}{\pi}}, \text{ and } \frac{\text{Sin}\pi(.)}{\pi(.)} = \text{SinC}\pi(.)$$

$$\underset{t \lesssim 0}{\text{Re.}[g(t)]} = A\sqrt{BT}(1-\frac{|t|}{T})\text{SinC}\pi(Bt+\frac{Rh}{2})(1-\frac{|t|}{T})\text{Cos}(\omega_c+\frac{\pi Rh}{2T}), |t| \leq T \qquad (A.11)$$

Equation (A.11) expresses the output of the P.C.M.F. for a received F.S.K. signal of modulation index h.

A.2 THE P.S.K. CASE

Let the P.S.K. signal be

$$S_i(t) = G \exp.j(\omega_b t+\phi_i), \quad |t| \leq \frac{T}{2} \qquad (A.12)$$

where G is the carrier amplitude

ω_b is the carrier angular frequency

ϕ_i is the phase angle carrying the digital data.

Consider the presence of $S_i(t)$ at the input of the mixer-P.C.M.F. compound of (Fig. A.1). As in the F.S.K. case before the output of the mixer may be found using equation (A.3.)

$$M(t) = G \exp.j(\omega_p t - \frac{1}{2}\mu t^2 + \phi_i), |t| \leq \frac{T}{2} \qquad (A.13)$$

where $\omega_p = \omega_b - \omega_o$

The impulse response of the P.C.M.F. is expressed as

$$h(t) = \exp.j(\omega_p t + \frac{1}{2}\mu t^2), \quad |t| \leq \frac{T}{2} \qquad (A.14)$$

As in the F.S.K. case the output of the P.C.M.F. may be found by substituting (A.14) and (A.13) in (A.6) and integrating to get

$$\text{Re.}[g(t)] = \frac{kG}{2}\left[\frac{\text{Sin}[\omega_p t + \mu t\tau - \frac{1}{2}\mu t^2 + \phi_i]}{\mu t}\right]_{\tau=a}^{b}$$

Substituting for a and b from (A.7a) and (A.7b), and solving for $t \gtrless 0$ as in the F.S.K. case

$$\text{Re.}[g(t)] = kG. \frac{\text{Sin}\left[\frac{\mu t}{2}(T-|t|)\right]}{\mu t}\text{Cos}2\pi(f_p t + \phi_i)$$

Substituting for $k = \sqrt{\frac{2\mu}{\pi}}$, $\mu = \frac{2\pi B}{T}$, and $\frac{\mathrm{Sin}\pi(.)}{\pi(.)} = \mathrm{SinC}\pi(.)$

$$\mathrm{Re.}\left[g(t)\right] = G\sqrt{BT}\left(1-\frac{|t|}{T}\right)\mathrm{SinC}\pi Bt\left(1-\frac{|t|}{T}\right)\mathrm{Cos}(\omega_p t+\phi_i),\ |t| \leq T \qquad \text{(A.15)}$$

which expresses the output of the P.C.M.F. for a received P.S.K. or D.P.S.K. data signal.

APPENDIX B

AUTOCORRELATION FUNCTION IN THE PRESENCE OF CARRIER INTERFERENCE

B.1 THE F.S.K. CASE

Let the carrier interfering signal be

$$I_1(t) = C_1 \exp.j\ (\omega_1 t + \theta_1), \quad |t| \leq \frac{T}{2} \qquad (B.1)$$

If $I_1(t)$ is added to the F.S.K. signal expressed by (A.1), and mixed with the local chirp given by (A.3), the output of the mixer is given by

$$M(t) = A \exp.j(\omega_c t + \pi RFt - \tfrac{1}{2}\mu t^2) + C_1 \exp.j\ (\omega_k t - \tfrac{1}{2}\mu t^2 + \theta_1) \qquad (B.2)$$

where $\omega_c = \omega_a - \omega_o$

$\omega_K = \omega_1 - \omega_o$

The first term in (B.2) resembles to the A.C.F. for the F.S.K. case as in Appendix A. The second term when convolved with the impulse response of the P.C.M.F. (A.5), using (A.6), and then integrated resembles to

$$[g(t)] = \frac{kC_1}{2}\left[\frac{\mathrm{Sin}(\omega_c t + \omega_R \tau + \mu t\tau - \frac{1}{2}\mu t^2 + \theta_1)}{(\omega_R + \mu t)}\right]_{\tau=a}^{b} \qquad (B.3)$$

where $\omega_R = \omega_K - \omega_c$

a, and b are given by (A.7a), and (A.7b) respectively.

Using the same procedure used to solve (A.8) in Appendix A, (B.3) may be reduced to the following

$$Re.[g(t)] = C_1\sqrt{BT}\ (1-\frac{|t|}{T})\,SinC\pi[Bt + (f_K - f_c)T](1-\frac{|t|}{T}).$$

$$Cos(\omega_c t + \frac{\omega_K - \omega_c}{2}t + \theta_1),\ |t| \leq T \qquad (B.4)$$

Hence, the output A.C.F. of the P.C.M.F. for a received F.S.K. signal in the presence of carrier interference is

$$Re.[g(t)] = \sqrt{BT}\ (1-\frac{|t|}{T})\{A\,SinC\pi(Bt+\frac{Rh}{2})(1-\frac{|t|}{T})\,Cos(\omega_c + \frac{\pi Rh}{2T})t$$

$$+ C_1\,SinC\pi[Bt + (f_1 - f_a)T](1-\frac{|t|}{T})\,Cos(\omega_c t + \frac{\omega_1 - \omega_a}{2}t + \theta_1)\} \qquad (B.5)$$

B.2. THE D.P.S.K. CASE

Consider the interfering carrier of (B.1) added to the P.S.K. signal of (A.12)

$$S_i(t) + I_1(t) = G\ exp.j(\omega_b t + \phi_i) + C_1 exp.j(\omega_1 t + \theta_1),\ |t| \leq \frac{T}{2} \qquad (B.6)$$

Since, the A.C.F. of the P.C.M.F. is derived in Appendix A, consider the interference part only to be mixed with the local chirp of (A.3), and then convolved with the impulse response of (A.14).

The mixer output is

$$M(t) = C_1 \exp.j\left[(\omega_1-\omega_o)t-\frac{1}{2}\mu t^2+\theta_1\right], \quad |t| \leq \frac{T}{2} \qquad (B.7)$$

The output of the P.C.M.F. using (A.6), and (A.14) is

$$g(t)= C_1 k \int_{-T/2}^{T/2} \exp.j\left[(\omega_1-\omega_o)\tau-\frac{1}{2}\mu\tau^2+\theta_1\right]\exp.j\left[(\omega_b-\omega_o)(t-\tau) + \frac{1}{2}\mu(t-\tau)^2\right]d\tau$$

Simplifying and taking the real value

$$\text{Re.}\left[g(t)\right]=C_1 k \int_{-T/2}^{T/2} \text{Cos}\left[\omega_p t+\omega_s\tau+\mu t\tau-\frac{1}{2}\mu t^2+\theta_1\right]d\tau \qquad (B.8)$$

where $\omega_p = \omega_b - \omega_o$, $\omega_s = \omega_1 - \omega_o$

integrating (B.8) we get

$$\text{Re.}\left[g(t)\right] = \frac{C_1 k}{2}\left[\frac{\text{Sin}(\omega_p t+\omega_s\tau+\mu t\tau-\frac{1}{2}\mu t^2+\theta_1)}{\omega_s+\mu t}\right]_{\tau=a}^{\tau=b} \qquad (B.9)$$

(B.9) is similar to (A.8), therefore using (A.7a), and (A.7b) for the value of (τ), the interference part reduces to the following for $t \gtrless 0$

$$\text{Re.}\left[g(t)\right] = \frac{C_1 k}{2}\,\frac{\text{Sin}\left[\frac{\omega_s+\mu t}{2}(T-|t|)\right]}{\omega_s+\mu t}\,\text{Cos}\left(\omega_p t+\frac{\omega_s}{2}+\theta_1\right) \qquad (B.10)$$

substituting for k, μ, ω_s and $\frac{\text{Sin}\pi(.)}{\pi(.)} = \text{SinC}(.)$ the output A.C.F. of the P.C.M.F. is

$$\text{Re.}[g(t)] = \sqrt{BT}\left(1-\frac{|t|}{T}\right)\{G\,\text{SinC}\pi Bt\left(1-\frac{|t|}{T}\right)\text{Cos}(\omega_p t + \Phi_i)$$

$$+ C_1\,\text{SinC}\pi\left[Bt+(f_1-f_b)T\right]\left(1-\frac{|t|}{T}\right)\text{Cos}\left(\omega_p t+\frac{\omega_1-\omega_b}{2}t+\theta_1\right)\}$$

APPENDIX C

ENVELOPE OF AUTOCORRELATION FUNCTION IN THE PRESENCE OF TIME DELAY

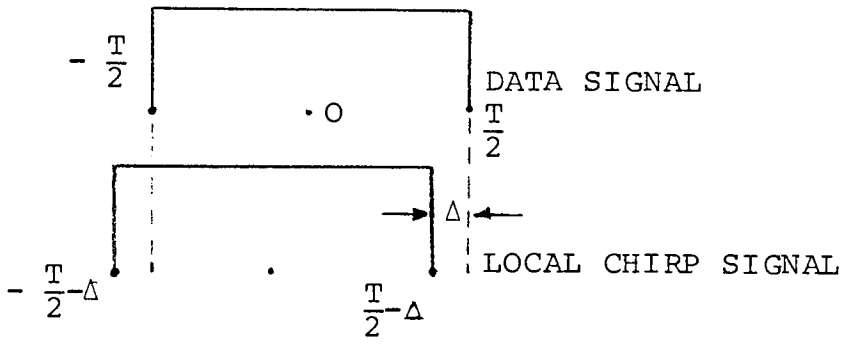

FIG. C1

C.1 THE F.S.K. CASE

The local chirp signal with a time delay (Δ) may be expressed as

$$C(t-\Delta) = \exp.j\left[\omega_o(t-\Delta)+\frac{1}{2}\mu(t-\Delta)^2\right], \quad -\frac{T}{2}\ \Delta \leqslant t \leqslant \frac{T}{2}+\Delta \qquad (C.1)$$

Using the F.S.K. signal expressed by (A.1), the output of the mixer is

$$M(t) = A\exp.j\left[\omega_c t+\pi RFt+\omega_o\Delta-\frac{1}{2}\mu t^2+\mu t\Delta-\frac{1}{2}\mu\Delta^2\right] \qquad (C.2)$$

where $\omega_c = \omega_a-\omega_o$

using (A.5), and (A.6) the output of the P.C.M.F. is

$$g(t) = kA \int_{-T/2}^{\frac{T}{2}-\Delta} \exp.j\left[\omega_c t+\pi RF\tau+\omega_o\Delta+\mu\tau\Delta-\frac{1}{2}\mu\Delta^2+\frac{1}{2}\mu t^2-\mu t\tau\right] d\tau$$

taking the real value of both sides

$$\text{Re.}\left[g(t)\right] = \text{Re.}\left[E(\tau)\exp.j(\omega_c t + \frac{1}{2}\mu t^2+\omega_o\Delta-\frac{1}{2}\mu\Delta^2\right] \qquad (C.3)$$

where, $E(\tau) = kA \int_{-T/2}^{\frac{T}{2}-\Delta} \exp.j(-\mu t+\mu\Delta+\pi RF)\tau \, d\tau$ is the complex envelope.

For perfect time start (i.e. $\Delta = 0$) between the received F.S.K. signal and local chirp signal, the complex envelope $E(\tau)$ resembles to the matched filter A.C.F. evaluated in Appendix A. However, to continue the evaluation of $E(\tau)$ in the presence of time delay, it may be separated to real and imaginary parts, as follows.

$$\text{Re.}\left[E(\tau)\right] = Ak \int_{T/2}^{\frac{T}{2}-\Delta} \text{Cos}(-\mu t+\mu\Delta+\pi RF)\tau \, d\tau$$

$$\text{Img.}\left[E(\tau)\right] = Ak \int_{-T/2}^{\frac{T}{2}-\Delta} \text{Sin}(-\mu t+\mu\Delta+\pi RF)\tau \, d\tau \qquad (C.4)$$

Evaluating the real part

$$\text{Re.}\left[E(\tau)\right] = Ak\left[\frac{\text{Sin}(-\mu t+\mu\Delta+\pi RF)(\frac{T}{2}-\Delta)}{-\mu t+\mu\Delta+\pi RF} - \frac{\text{Sin}(-\mu t+\mu\Delta+\pi RF)(-\frac{T}{2})}{-\mu t+\mu\Delta+\pi RF}\right]$$

Let, $\sigma = -\mu t+\mu\Delta+\pi RF$

$$\text{Re.}\left[E(\tau)\right] = Ak\left[\frac{\text{Sin}\sigma(\frac{T}{2}-\Delta)+\text{Sin}\sigma\frac{T}{2}}{\sigma}\right]$$

Similarly,

$$\text{Img.}\left[E(\tau)\right] = Ak\left[\frac{\text{Cos}\sigma\frac{T}{2} - \text{Cos}\sigma(\frac{T}{2}-\Delta)}{\sigma}\right]$$

If the output of the P.C.M.F. is fed to an envelope detector, the output of the envelope detector is given by

$$\eta = \{\text{Re.}\left[E(\tau)\right]^2 + \text{Img.}\left[E(\tau)\right]^2\}^{\frac{1}{2}} \qquad (C.5)$$

Substituting for real and imaginary in (C.5), and simplifying the output of the envelope detector becomes

$$\eta = \frac{2Ak}{\sigma}\ \text{Sin}\ \frac{\sigma}{2}\ (T-\Delta) \qquad (C.6)$$

substituting for σ, k, μ, h, and $\frac{\text{Sin}\pi(.)}{\pi(.)} = \text{SinC}\pi(.)$

$$\eta = A\sqrt{BT}(1-\frac{\Delta}{T})\ \text{SinC}\pi\left[B(\Delta-t)+\frac{Rh}{2}\right](1-\frac{\Delta}{T}) \qquad (C.7)$$

which is the envelope of the A.C.F. at the output of the envelope detector in the event of a time delay (Δ) between the F.S.K. signal, and the local chirp signal.

C.2 THE D.P.S.K. CASE

Using the D.P.S.K. signal expressed by (A.12), and the

local chirp signal expressed by (C.1), the output of the mixer is given by

$$M(t) = G\exp.j\left[\omega_p t+\phi_i+\omega_o\Delta-\frac{1}{2}\mu t^2+\mu t\Delta-\frac{1}{2}\mu\Delta^2\right] \qquad (C.8)$$

where $\omega_p = \omega_b - \omega_o$

The output of the P.C.M.F., using (A.14), and (A.6), becomes

$$g(t) = Gk\int_{-T/2}^{\frac{T}{2}-\Delta} \exp.j\left[\omega_p t+\omega_o\Delta+\phi_i+\mu\tau\Delta-\frac{1}{2}\mu\Delta^2+\frac{1}{2}\mu t^2-\mu t\tau\right]d\tau \qquad (C.9)$$

taking the real value of both sides of (C.9)

$$\text{Re.}\left[g(t)\right] = \text{Re.}\left\{E_1(\tau)\exp.j\left[\omega_p t+\omega_o\Delta+\phi_i-\frac{1}{2}\mu\Delta^2+\frac{1}{2}\mu t^2\right]\right\}$$

where, $E_1(\tau) = Gk\int_{-T/2}^{\frac{T}{2}-\Delta} \exp.j(-\mu t+\mu\Delta)\tau d\tau$ is the complex envelope.

Hence, $E_1(\tau)$ may be separated into real and imaginary parts to find the envelope similar to the F.S.K. case before. The real and imaginary parts become

$$\text{Re.}\left[E_1(\tau)\right] = kG\frac{\text{Sin}\sigma_1(\frac{T}{2}-\Delta)+\text{Sin}\sigma_1\frac{T}{2}}{\sigma_1} \qquad (C.10)$$

$$\text{Img.}\left[E_1(\tau)\right] = kG\frac{\text{Cos}\sigma_1\frac{T}{2}-\text{Cos}\sigma_1(\frac{T}{2}-\Delta)}{\sigma_1}$$

where $\sigma_1 = -\mu t + \mu\Delta$

Using the same method used for F.S.K. case to find the envelope we arrive at

$$\eta_1 = \frac{2Gk}{\sigma_1}\text{Sin}\ \frac{\sigma_1}{2}(T-\Delta) \qquad (C.11)$$

Substituting for σ_1, k, μ, and $\frac{\text{Sin}\pi(.)}{\pi(.)} = \text{SinC}\pi(.)$

$$\eta_1 = G\sqrt{BT}\ (1-\frac{\Delta}{T})\text{SinC}\pi B(\Delta-t)(1-\frac{\Delta}{T}) \qquad (C.12)$$

which is the envelope of the output A.C.F. in the presence of time delay (Δ) between the received D.P.S.K. signal and the local chirp signal.

REFERENCES

1. Turin, G.B.
An Introduction to Matched Filters
IRE, Trans., on Inf. Theory, IT-6, pp.311-329; June 1960.

2. Stein, S. and Jones, J.J.
Modern Communication Principles
Mc Graw-Hill, New York, 1967.

3. Schwartz, M., Bennett, W.R., and Stein, S.
Communication Systems and Techniques
Mc Graw-Hill, New York, 1966.

4. Viterbi, A.J.
Principles of Coherent Communication
Mc Graw-Hill, New York, 1966.

5. Gott, G.F.
Digital Communication Theory
AGARD Lecture Series, No.58, on Spread Spectrum Communication, June 1973.

6. Schilling, D.L., Hoffman, E., and Nelson, E.A.
Error Rates for Digital Signals Demodulated by an FM-Discriminator
IEEE Trans. on Comm. Technology, Vol. COM-15, No.4, pp.507-517, August 1967.

7. Pardoe, B.H.
Theoretical and Practical Investigation of Error Rates for Digital f.m.

The Radio and Electronic Engineer, vol.46, No.11, pp.549-552; November 1976.

8. Lindsey, W.C., and Simon, M.K.
Detection of Digital FSK and PSK using a First-Order Phase Locked Loop.
IEEE Trans. on Comm., vol. COM-25, No.2, pp. 200-214; February 1977.

9. Wishna, S.
Design of an Advanced Satellite Receiver for a Binary FSK Data Collection System
Proc. NEC (National Electronic Conference), pp. 490-494; December 1969.

10. Carlson, A.B.
Communication Systems (An Introduction to Signals and Noise in Electrical Communication)
Mc Graw-Hill, 2nd edition, 1975

11. Darlington, S.
Demodulation of Wideband Low-power FM-Signals
BSTJ, vol.43, No.1, Part 2, pp. 339-374; January 1964.

12. Murarka, N.P.
Detection of FSK Signals Using Linear-FM Dispersion Method
Proc. IEEE, vol.60, pp. 469-471; April 1972

13. Ramp, H.O. and Wingrove, E.R.
Principles of Pulse Compression

IRE Trans., on Military Electronics, vol. MIL5, pp. 109-116; April 1961

14. Klauder, J.R., Price, A.C., Darlington, S., and Albershem, W.J.
The Theory and Design of Chirp Radars
B.S.T.J, vol. XXXIX, No.4, pp. 745-808; July 1960.

15. Skolnik, M.I.
Introduction to Radar Systems
Mc Graw-Hill, New York, 1962

16. Cook, C.E., and Bernfeld, M.
Radar Signals
Academic Press, New York, 1967

17. Kallmann, H.E.
Transversal Filters
Proc. of IRE, vol.87, pp. 302-310; July 1940

18. Lambrell, A.J.
A Tapped Delay Line Compression Network for Linear-f.m. signals
IEE Conf. pub. (Delay Devices for Pulse-Compression), No.20, pp. 35-47; 1966.

19. Winkler, M.R.
Chirp Signals for Communications
IEEE WESCON, paper 14.2; August 1962

20. Forgan, D.H., and Newsome, J.P.
The Application of Dispersive Networks in Chirp

Signal Data Transmission Receivers.
Proc. IEE, vol. 121, pp.237-244; April 1974.

21.Gott, G.F., and Newsome, J.P.
H.F. Data Transmission Using Chirp Signals
Proc. IEE, vol. 118, No.9, pp. 1162-1166; September 1971.

22.Ash, C.P., and Newsome, J.P.
An Experimental Delta-Modulation Transversal Filter for Compression of Chirp Data-Signals
The Radio and Electronic Engineer, vol.46, No.6, pp. 299-308; June 1976.

23.Hobson, G.S.
Review of CCD
Proc. IEE, vol. 124, No. 11R, pp. 925-945; November 1977

24.Mitchell, R.F.
Acoustic Surface-Wave Filters
Philips Tech. Rev., vol. 32, No. 61718, pp.179-189; 1971.

25.Mistein, L.B., and Pankaj, K.D.
Surface Acoustic Wave Devices
IEEE Magazine, vol.17, No.5, pp. 25-33; September 1979.

26.Mavor, J., and Denyer, P.B.
Design and Development of c.c.d. Programmable Tennsversal Filters

IEE on Electronic Circuits and Systems, vol. 2, No.1, pp. 1-8; January 1978.

27. Roy, D., and Menard P.
High-Performance Digitally Programmable Analogue Transversal Filter
Electronic Letters, vol.14, No.20, pp.671-672; 28th September, 1978.

28. Denyer, P.B., Mavor, J., and Arthur, J.W.
Miniature Programmable Transversal Filter Using CCD/MOS Technology.
Proc. IEEE, vol.67, No. 1, pp. 42-50; January, 1979.

29. Cook, C.E.
General Matched-Filter Analysis of Linear-FM Pulse Compression
Proc. IRE (Correspondence), vol.49, p.831; 1961

30. Dorman, M.I., and Sotnikov, Y.Y.
Phase-Shift Keyed LFM Signals and Their Optimal Processing
Radio Engineer Elect. Phys., vol. 20, No.7, pp. 62-64; July 1975

31. Gott, G.F., and Karia, A.J.
Differential Phase-Shift Keying Applied to Chirp Data Signals
Proc. IEE, vol. 121, No.9, pp. 923-928; September 1974

32. Bennett, W.R., and Davey, J.R.

Data Transmission

Mc Graw Hill, New York, 1965

33. Pelchat, M.G.

The Autocorrelation Function and Power Spectrum of PCM/FM with Random Binary Modulation Waveforms

IEEE Trans. on Space Electronics and Telemetry, vol. SET-10, pp. 39-44; March 1964

34. El-Alem, M.S.Y.

Data Transmission by Pulse Compression

Ph.D. Thesis, University of Aston in Birmingham, 1978

35. Lawton, J.G.

Theoretical Error Rate of "Differentially Coherent" Binary and "Kineplex" Data Transmission Systems

Proc. IRE, vol.47, pp. 333-334; February 1959

36. Doelz, M.L., Heald, E.T., and Martin, D.L.

Binary Data Transmission Techniques for Linear Systems

Proc. IRE, vol.45, pp. 656-566; May 1957

37. Gott, G.F., and Staniforth, M.J.D.

Characteristics of Interfering Signals in Aeronautical H.F. Voice Channels

Proc. IEE, vol. 125, No. 11, pp. 1208-1212; November 1978

38. Shannon, C.E.

Communication in the Presence of Noise

Proc. IRE, vol. 37, pp. 10-21; January 1949.

39. Rosenbaum, A.S.
PSK Error Performance with Gaussian Noise and Interference
BSTJ, vol. 48, pp. 413-442; February 1969.

40. Mancianti, M., Russo, F., and Verrazzani, L.
On the Detection of M-ary FSK Signals by Chirp Technique
Alta Frequenza (Italy), vol.43, No.3, pp. 167-172; March 1974

41. TMS-9900 Microprocessor Data Manual
Texas Instruments, Ltd., March 1977

42. Rowe, M.D.
The Selection of Microprocessors
POEEJ, vol.71, pp. 101-109; 1979

43. 9900 Assembly Language Programmer's Guide
Texas Instruments, Ltd., September 1978

44. Schwartz, M., and Shaw, L.
Signal Processing (Discrete Spectral Analysis, Detection, and Estimation)
Mc Graw-Hill, New York, 1975

45. Gaunt, D.L., and Lamb, R.T.
Microprocessors Peripherals
POEEJ, vol.71, pp.214-220; January 1979

46.Witten, I.H.

Microcomputer Interfaces 1 and 2

Wireless World, pp.67-80 and pp. 77-78; September 1979, October 1979

47.Wang, L.

Error Probability of a Binary Non-Coherent FSK System in the Presence of Two CW Tone Interferers

IEEE Trans. on Comm. (correspondence), vol.22, No.12, pp. 1948-1949; December 1974

48.Hansen, R.D., and Stephenson, R.G.

Commmunication at Megamile Rangers

J.Brit. Inst. Radio Enggrs., vol.22, pp. 329-345; October 1961.

49.Robin, H.K., Bayley, O.B.E.D., Murray, T.L., and Ralphs, J.D.

Multitone Signalling System Employing Quenched Resonators for Use on Noisy Radio-Teleprinter Circuits

Proc. IEE, vol.110, No.9, pp. 1554-1568; September 1963

50.Oetting, J.D.

A Comparison of Modulation Techniques for Digital Radio

IEEE, Trans. on Comm., vol.27, No.12, pp. 1752-1762; December 1979.

51.Salz, J., and Saltzberg, B.R.

Double Error Rates in Differentially Coherent Phase Systems

IEEE Trans. on Comm. Systems, vol. CS-12, pp. 202-205; June 1964.

52. Wintz, P.A., and Hancock, J.C.
An Adaptive Receiver Approach to the Time Synchronization Problem
IEEE Trans. on Comm. Technology, vol. COM-13, No.1, pp. 90-96; March 1965

53. Kennedy, R.S.
Fading Dispersive Communication Channels
John Wiley and Sons, Inc., 1969

54. Monsen, P.
Fading Channel Communications
IEEE Communication Magazine, vol.18, No.1, pp. 16-25; January 1980

LIST OF PRINCIPAL SYMBOLS AND ABBREVIATIONS

A	constant
A/D	analogue-to-digital
A.S.K.	amplitude-shift keying
A.W.G.N.	additive white Gaussian noise
A.C.F.	autocorrelation function
B	bandwidth of chirp signal
C(t)	local chirp signal
C.C.D.	charge coupled device
C.P.U.	central processing unit
CSR	carrier-to-signal ratio
C_1, C_2	constants
D.P.S.K.	differential phase-shift-keying
D/A	digital-to-analogue
D%	$= \frac{\mu-\mu'}{\mu}$ slope mismatch factor
E	constant
e	number of errors
E|.|	mean square value of |.|
F	bandwidth of F.S.K. signal
f	current frequency
FM	frequency modulation
G	constant
g(t)	output of P.C.M.F. (signal part)
h	modulation index of F.S.K. signal
h(t)	impulse response chirp signal

H.F.	high frequency
Hz	Hertz or cycle/second
i,I	integers
$I_1(t), I_2(t)$	interfering signals
Img.[.]	imaginary part of [.]
J,K.	integers
k	matched-filter scaling factor
L	total number of samples
L.S.I.	large scale integration
L.P.F.	low pass filter
m	modulation index
msec.	millisecond
M(t)	output waveform of mixer
M(n)	digital output of mixer
n	integer n = 1, 2, ---, L
n(t)	noise component input to mixer
$n_i(t)$	noise component input to P.C.M.F.
$n_o(t)$	noise component output of P.C.M.F.
N	A.W.G.N. single-sided spectral power density
P	value of noise sample
PAM-FM	pulse amplitude modulation FM
P.C.M.F.	pulse compressor matched filter
P.P.M.	pulse position modulation
PROM	programmable read-only memory
Pe	probability of error
Q	number of samples given by $O \leqslant Q \leqslant U$
r	integer

R	$= \pm 1$ for mark or space transmitted
$Rn(\tau)$	A.C.F. of noise
RAM	random-access-memory
Re.[.]	real value of [.]
s	integer
$S_n(2\pi f)$	power spectral density of noise
S(t)	F.S.K. signal transmitted
$S_i(t)$	P.S.K. or D.P.S.K. signal transmitted
SAW	surface acoustic wave
SNR	signal-to-noise ratio
T	duration of one bit
T_s	sampling interval given by $\frac{nT}{L}$
t	time
t_m, t_s	mark, and space times respectively
U	number of samples/cycle
u	constant
W(t)	time weighted chirp signal
X	number of samples shift
x	total number of transmitted signals
$x_s(n)$	digital sequence input to mixer (signal part)
$x_c(n)$	digital sequence input to mixer (carrier part)
Z	constant
ω	current angular frequency given by $2\pi f$
ω_a	angular centre frequency of F.S.K. signal
ω_b	angular carrier frequency of P.S.K. signal

ω_c	angular centre frequency of P.C.M.F.
ω_o	angular centre frequency of local chirp
ω_1, ω_2	interfering angular frequencies
Δ	time delay
$\delta\%$	non-linearity weighting factor
$\delta\omega$	angular frequency shift
$\delta(\tau)$	delta function
ε	number of quantization levels
η	envelope of A.C.F. in the presence of time delay (F.S.K. case)
η_1	envelope of A.C.F. in the presence of time delay (P.S.K. case)
$\theta(t)$	phase angle of chirp signal
θ_1, θ_2	random phases of interfering carriers
θi	phase shift
λ	time taken by processor to output one sample from RAM (given by equation 4.1)
μ	slope of chirp signal
μ'	departed slope of chirp signal from (μ)
μsec.	microsecond
ρ	signal energy per bit/noise power per unit bandwidth
$\sum$	summation
τ	arbitrary time delay
ϕ_i	initial phase of P.S.K. signal
$\lvert . \rvert$	absolute value of
$[.]^*$	complex conjugate of [.]
$\leqslant$	less than or equal